
Universidad
Carlos III de Madrid

# Non-linear actuators and simulation tools for rehabilitation devices

*Dorin Sabin Copaci*

Ph.D. Thesis

Department of Systems Engineering and Automation
Leganés, Madrid, Spain, November 2017

# Non-linear actuators and simulation tools for rehabilitation devices

Candidate
*Dorin Sabin Copaci*

Advisers
*Dolores Blanco Rojas*
*Luis Moreno Lorente*

Review Committee

President: Eduardo Rocón _____

Secretary: Concepción Monje _____

Vocal: Martin Stoelen _____

Grade:

Leganés, Madrid, Spain, November 2$^{th}$, 2017

*"Îmi displac în egală măsură atât complicarea inutilă a lucrurilor simple, cât şi simplificarea fără rost a celor complexe."*

---

# Preface

Rehabilitation robotics is a field of research that investigates the applications of robotics in motor function therapy for recovering the motor control and motor capability. In general, this type of rehabilitation has been found effective in therapy for persons suffering motor disorders, especially due to stroke or spinal cord injuries. This type of devices generally are well tolerated by the patients also being a motivation in rehabilitation therapy. In the last years the rehabilitation robotics has become more popular, capturing the attention at various research centers. They focused on the development more effective devices in rehabilitation therapy, with a higher acceptance factor of patients tacking into account: the financial cost, weight and comfort of the device.

Among the rehabilitation devices, an important category is represented by the rehabilitation exoskeletons, which in addition to the human skeletons help to protect and support the external human body. This became more popular between the rehabilitation devices due to the easily adapting with the dynamics of human body, possibility to use them such as wearable devices and low weight and dimensions which permit easy transportation.

Nowadays, in the development of any robotic device the simulation tools play an important role due to their capacity to analyse the expected performance of the system designed prior to manufacture. In the development of the rehabilitation devices, the biomechanical software which is capable to simulate the behaviour interaction between the human body and the robotics devices, play an important role. This helps to choose suitable actuators for the rehabilitation device, to evaluate possible mechanical designs, and to analyse the necessary controls algorithms before being tested in real systems.

This thesis presents a research proposing an alternative solution for the current systems of actuation on the exoskeletons for robotic rehabilitation. The proposed solution, has a direct impact, improving issues like device weight, noise, fabrication costs, size an patient comfort. In order to reach the desired results, a biomechanical

software based on Biomechanics of Bodies (BoB) simulator where the behaviour of the human body and the rehabilitation device with his actuators can be analysed, was developed.

In the context of the main objective of this research, a series of actuators have been analysed, including solutions between the non-linear actuation systems. Between these systems, two solutions have been analysed in detail: ultrasonic motors and Shape Memory Alloy material. Due to the force - weight characteristics of each device (in simulation with the human body), the Shape Memory Alloy material was chosen as principal actuator candidate for rehabilitation devices.

The proposed control algorithm for the actuators based on Shape Memory Alloy, was tested over various configurations of actuators design and analysed in terms of energy efficiency, cooling deformation and movement. For the bioinspirated movements, such as the muscular group's biceps-triceps, a control algorithm capable to control two Shape Memory Alloy based actuators in antagonistic movement, has been developed.

A segmented exoskeleton based on Shape Memory Alloy actuators for the upper limb evaluation and rehabilitation therapy was proposed to demosntrate the eligibility of the actuation system. This is divided in individual rehabilitation devices for the shoulder, elbow and wrist. The results of this research was tested and validated in the real elbow exoskeleton with two degrees of freedom developed during this thesis.

# Acknowledgments

Many people deserve to appear in these acknowledgments for both personal and professional reasons.

Firstly, I would like to thank my supervisors for guiding, challenging, and encouraging me during these years. Prof. Dolores Blanco for her patience and guidance which allowed me to grow, both professionally and personally. Prof. Luis Moreno, for his encouragement words and comments during these years, which have contributed to realize and improve this thesis. I have been extreme lucky to have supervisors who cared so much about my work, and who responded to my questions and queries so promptly.

My acknowledgements to Prof. James Shippen who allowed me to be part of his research team during my stage in Coventry University and gave me the possibility to use his simulator BoB. Also, I must to express my gratitude to Prof. Tetsuya Mouri which gave me the incredible opportunity to be a visitor in his laboratory in Gifu University. These experiences I will never forget.

I would like to thanks to the laboratory members, and all the colleges which I met during my research, for their patience and their opinions which always helped me. I cannot forget most sincerely thanks for Ángela Nombela, Fernando San Deogracias, Jose Antonio Campo for their support.

And last, but not least, I want to hugely thanks to my family that has always been so close to me, even though thousands of kilometers separate us... .

Many thanks to all of them...

# Abbreviations

2D - two-dimensional
3D - three-dimensional
ADL - Activity of Daily Life
BOB - Biomechanics of Bodies
CAD - Computer-Aided Design
CVA - Cerebrovascular Accident
DIP - Distal Interphalangeal
BPID - Bilinear PID (controller)
DARPA - Defense Advanced Research Projects Agency's
DOF - Degrees of Freedom
DSTO - Defense Science and Technology Organization
EMS - Electrical Muscle Stimulation
FES - Functional Electrical Stimulation
GH - Glenohumeral (movement)
MCP - Metacarpo-Phalangeal
MR - Magneto-Rheological
MSMS - Musculo-Skeletal Modeling Software
NARX - Nonlinear Autoregressive Exogenous
NMES - Neuromuscular Electrical Stimulation
PID - Proportional-Integral-Derivative (controller)
PIP - Proximal Interphalangeal
PTFE - Polytetrauoroethylene
RBM - Rigid Body Motion
SCI - Spinal Cord Injury
SEA - Series Elastic Actuators
SIMM - Software for Interactive Musculoskeletal Modeling
SMA - Shape Memory Alloy
SPI - Serial Peripheral Interface
ST - Scapulothoracic (movement)
PC - Personal Computer
PWM - Pulse With Modulation

UC3M - Carlos III University of Madrid
USA - United States of America
USB - Universal Serial Bus
USM - Ultrasonic Motors

# Contents

# List of Tables

# List of Figures

# Chapter 1

# Introduction

## 1.1 Motivation

According to the World Health Organization [26], the stroke represent the second leading causes of the death in the world. Approximately 15 million people suffer a stroke worldwide each year. Of these, 6 million die (Fig. 1.1) and another 5 million are permanently disabled. In Europe the average of stroke death is approximately 650 000. Approximately two-thirds of these individuals survive after a stroke and require rehabilitation. The goals of rehabilitation are to help survivors become as independent as possible and to attain the best possible quality of life [27].

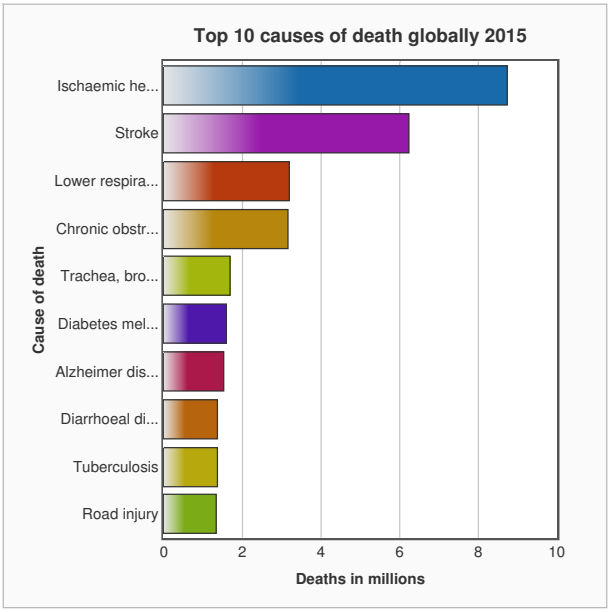


Figure 1.1: Top 10 causes of death globally 2015.

The consequences of this trauma for the survive individuals, end unfortunately, with damage in the brain which affect motor functions, leaving behind paralysis or paresis. The post-stroke rehabilitation helps the stroke survivors to relearn skills that are lost when part of the brain is damaged. Unfortunately this process of rehabilitation needs special care of each patient which implicate a high financial and time cost. The rehabilitation therapy needs one or more therapist during every session, which can be several weeks, for individual patient. For this reason, many research groups investigated in the development of new robotic platforms to support the therapist in repetitive therapy (rehabilitation), in compensation of the force and monitoring the evolution of the patient. They focus the research in development of rehabilitation devices, which improve the rehabilitation treatment.

This thesis is a part of two projects (HYPER Consolider Ingenio 2010 and Robohealth) which aims among other things, a progress in rehabilitation devices for persons with disabilities of motor function as a result of stroke, spinal cord injury or diseases of the motor function.

### 1.1.1 HYPER

The HYPER Project[3] (Fig. 1.2) represent a progress in the research of rehabilitation devices, neurorobotic (NR) and motor neuroprosthetic (MNP) in close cooperation with the human body, both for the rehabilitation and functional compensation of motor disorders in activities of daily living.


Figure 1.2: HYPER Project (Consolider Ingenio 2010) [3].

In this project, the research group from Carlos III University of Madrid, led by Prof. Dr. Luis Moreno and Prof. Dr. Dolores Blanco, was in charge of the objective to develop new actuators based in technologies such Ultrasonic Motors (USM) and Shape Memory Alloy (SMA), which improve the characteristics of the rehabilitation devices, in terms of efficiency in rehabilitation therapy, comfort, weight, noise, fabrication cost and safety.

### 1.1.2 Robohealth

The main objective of the Robohealth project [4] (Fig. 1.3) is the development of assistive and rehabilitation robots for the smart hospitals spaces. The UC3M research group where this thesis is involved has the objective to develop upper-body exoskeletons (for shoulder, elbow, wrist and hand) for the rehabilitation of patients in hospital environments; here the focus will be on over-actuated low-cost systems with novel human-machine interfaces.


Figure 1.3: Robohealth Project [4].

In this project, the thesis proposes a low-cost solution in the control and actuation system presenting a new type of actuator based on Shape Memory Alloy with its control algorithm, a preliminary design of a segmented exoskeleton for the upper limb and the data validation of the actuator over a real developed elbow exoskeleton.

## 1.2 Motor function losses after CVA and SCI

The capacity of realization the manipulation tasks is fundamental for the humans. The activity of the daily life (ADL) [28], such as: eating by a hand, pouring from a bottle, drinking with a cup, combing hair, picking up a phone on a table, etc., require the mobilization and synchronization of various muscles groups which move the articulations of the upper limb. However, a large number of diseases and musculoskeletal and neurological disorders result in the losses of mobility, involving a total or partial disability to perform daily manipulation tasks autonomously. The most common causes of motor function loss are the stroke or the Cerebrovascular Accident (CVA), the Spinal Cord Injury (SCI) lesions and the musculoskeletal and neurological disorders. One part of these disorders, depending on the type, can be recuperate with the aid of the treatment which consist in: medicine administration, occupational therapy, or work with a psychiatrist, therapist, neurologist, or other healthcare professionals. In continuation, the two more common causes for motor function losses are explained.

### 1.2.1 Cerebrovascular Accident

Stroke or CVA consists in a brain part function loss after a blood flow was stopped, either by a blockage or by the rupture of a blood vessel. According to the World Health Organization, 15 million of people suffer this type of accident every year, representing the second cause of death in the world, with approximately 6.7 million of deaths in 2015, of which 1.138 million only in Europe region. These data are even more worrying when we analyze with the last years because the number of cases of stroke is continuously growing.

The two major mechanisms causing the brain damage in stroke are: hemorrhage and ischemia. The ischemia represent about 80% of the causes of stroke and happen when the blood vessel who carrying blood to the brain is blocked by a blood clot (Fig. 1.4), [29]. This causes a bad alimentation with blood and oxygen to the brain, leading to the cells death. In function of the blood clot origin, the ischemia can be of two types: embolic and thrombotic. The embolic stroke happen when the blood clot is formed somewhere in the body, more frequent in the heart and is transported to the brain. When this arrives to the brain, practically blocks the blood fluctuation. The thrombotic stroke happens when the blood clot was formed directly in the brain. When ischemia happen, the affected person suffer disorders of motor function. This

results in one or more limbs paralyzed in one side of the body, this occuring because the contralateral affected area on the brain can no longer function. In case of the upper limb functional motor affection, the rehabilitation therapy is necessary to recuperate this disorders. Also, have been demonstrated that if therapy is done in the first six weeks it is more beneficial with more probability to recovery of motor function [30].

The second type of stroke, hemorrhagic stroke (bleeds), is less common than ischemia and results from a weakened vessel that ruptures and bleeds into the surrounding brain. When this occur,it is most likely that the person will not survive [5].

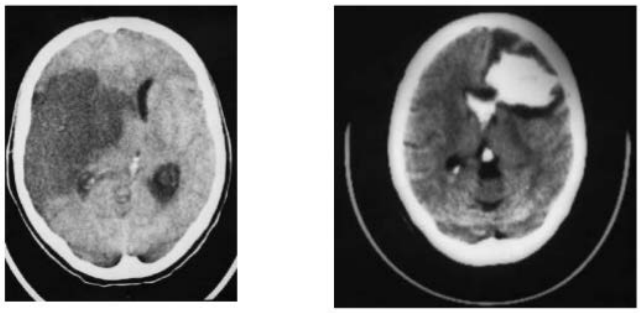

Figure 1.4: Computed tomography scan of two type of stroke: in the right part a ischemia stroke and in the left part hemorrhagic stroke [5].

### 1.2.2 Spinal Cord Injury

The human spine, is a complex structure whose principal functions are to protect the spinal cord and transfer loads from the head to trunk and to the pelvis, while simultaneously allowing movement and providing stability to the trunk [25]. The spinal cord is a long, thin, tubular bundle of nervous tissue and support cells that extends from the brain, down to the space between the first and second lumbar vertebrae, terminating in a fibrous extension known as the *filum terminale* [6]. It consists of 24 articulated vertebrae, separated by intervertebral discs, and 9 fused vertebrae in the sacrum and the coccyx. The spinal cord are divided in five regions: the cervical zone containing 7 vertebrae (C1−C7), thoracic zone with 12 vertebrae (T1−T12), lumbar area with 5 vertebrae (L1−L5), sacral area with 5 vertebrae (S1−S5) and coccyx zone with 4 (3−5) (fused) vertebrae (tailbone), Fig. 1.5.

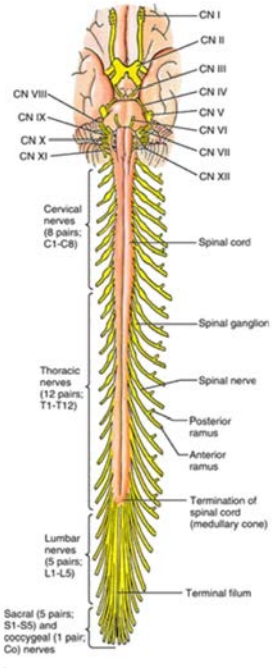


Figure 1.5: Human spinal cord [6].

A cross section of the spinal cord, presents a butterfly shape core a gray matter and surrounded by white matter. Gray matter is made up of neuronal cell bodies, whereas the white matter is composed of bundles of axons, which connect various gray matter areas and carry nerve impulses between neurons. The shape and size of the gray matter varies according to spinal cord level: at the lower levels, the ratio between gray matter and white matter is greater than in higher levels, because the lower levels have less nerve fibres (Fig. 1.6 - Transverse sections of spinal cord at different levels: A. Cervical region, B. Thoracic region, C. Lumbar region, D. Sacral region).

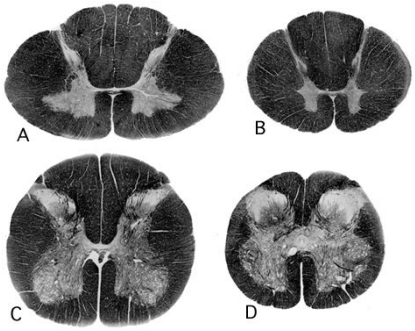


Figure 1.6: Transverse sections of spinal cord at different levels [7].

A spinal nerve is a mixed nerve, which is capable to carry motor sensory and autonomic signals between the spinal cord and the human body. The areas of sensory innervation on the skin for each spinal nerve are represented by the dermatome. Because each segment of the cord innervate a different region of the body, dermatomes can be easy identified and precisely mapped on the body surface. This mapping can be seen in Fig. 1.7.

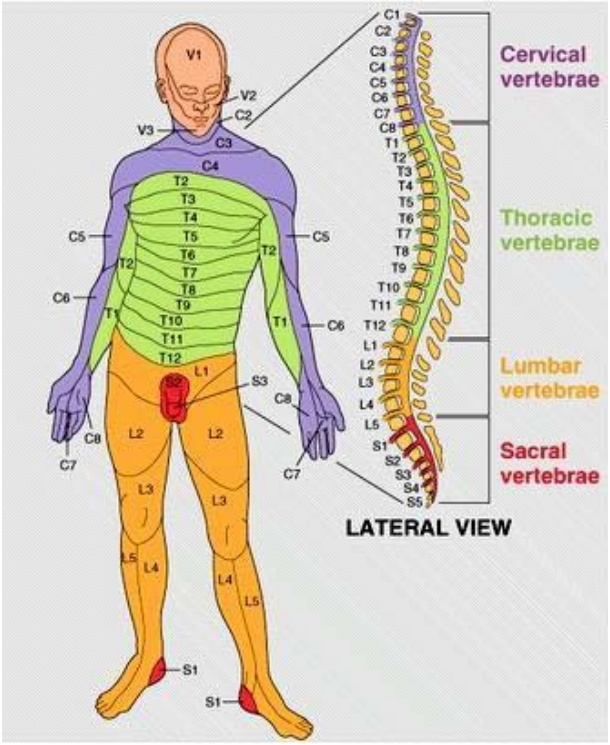


Figure 1.7: Spinal cord dermatome [8].

The spinal cord injury (SCI) can be defined as any injury or alteration of the spinal cord that interrupts the nervous impulse connection between the brain and the periphery and vice versa. The major causes of SCI in the world are represented by the traffic accidents, gunshot injuries, knife injuries, falls and sports injuries. In function of the level where the injury was produced,they cause alteration in the sensory − motor system and autonomous systems under the level at which the lesion is located. The symptoms of SCI depend the location where the spinal cord and nerve roots are damaged. In function of these symptoms, can vary widely, from pain to paralysis and to incontinence. One of the most used classifications are the terms paraplegia, tetraplegia, tetraparesis and paraparesis [31].

*Paraplegia* happen when the injuries or alteration occur in the thoracic, lumbar

or sacral (but not cervical area) segments of the spinal cord. This lesion can cause impairment or loss of motor and/or sensory function under the cervical vertebrae. With paraplegia, the upper limbs still functioning and the affection can appear in the trunk, legs and pelvic organs depending where the level of injury happen. Also, the term is used in referring to cauda equina and conus medullaris injuries, but not to lumbosacral plexus lesions or injury to peripheral nerves outside the neural canal.

*Tetraplegia* occur when the lesion or injuries of the spinal cord occur in the cervical segments. This damage the motor and/or sensory function under the cervical area, including then upper limbs, the trunk, legs and pelvic organs. The tetraplegia is characterized by paralysis in the four extremities. This not included the brachial plexus injuries and injuries to peripheral nerves which happen outside of the neural canal.

*Tetraparesis and paraparesis* use of this terms is discouraged and as they describe incomplete lesions imprecisely and incorrectly imply that tetraplegia and paraplegia should only be used for neurologically complete injuries.

The acute and subacute rehabilitation in SCI begin with the admission of the patient in the hospital and stabilizing the neurological state of this. This period can be between 6 and 12 weeks bed period. The aim of this period is to prevent possible complication that may occur and doing passive exercise for resolve contractures, muscle atrophy and pain. The most important in this period of time is avoid the contractures of joints and stiffness. These exercises should be done in a flaccid period at least once a day and at least 2-3 times a day in the presence of spasticity. In this period, spinal cord shock period, the muscle are flaccid and the exercises can be done more easily. After this period, the flaccidity is replaced with the spasticity and this has negative effects on mobility, daily living activities and transferring. One of the most important point is strengthening of the upper extremities to the maximal level in the acute period of rehabilitation in patients with complete paraplegia. This was characterized from empowering exercises for the muscle, for example rotation of the shoulder proposing for using crutches, swimming, electrical bicycles and walking. In the aid of this type of exercises come the robotics of rehabilitation. This can offer a good rehabilitation but also a good evaluation of the patient.

## 1.3 Rehabilitation engineering

Rehabilitation engineering is the application of science and technology to improve the quality of life for people with disabilities. The rehabilitation therapy is the process that assists a person in recovering from a serious disorders after an injury, illness or surgery. One of the most common rehabilitation consist in the musculoskeletal rehabilitation, who can often improve functional capacity, reduce symptoms, and improve the well-being of the patient. This type of rehabilitation consist in repetitive exercises

realized by the patient with the aid of a therapist. This involves special attention, every patient needs one or more therapist, which implicate a huge consumption of the health care and financial resources. In the aid and support the therapist the robot-aided rehabilitation was proposed. This consists in repetitive movement of the impaired limb through the robot. This type of rehabilitation offers to the patient a more effective and stable therapy, offering interesting measured data from the patient such as velocity, direction, strength of the patient's limb, enabling the therapist to evaluate the evolution of the patient. Among the most promising technologies it is considered that the robotic therapies with exoskeletons are very beneficial for the patient's rehabilitation requiring a repetitive treatment for re-education of lost movements. Robotic rehabilitation devices come in the aid of the therapists, offering a more effective and stable rehabilitation process compared to the traditional rehabilitation sessions effectuated by therapists and reducing the cost of hospitalization.

The main objective of this work is to develop a new prototype of rehabilitation exoskeleton for the upper limb, based on a new type of actuator which contribute to the systems of actuation such as solution with low weight, noiseless operation and low cost of fabrication. For this it is necessary to analyse the new types of actuators, developing a simulation environment: actuator - exoskeleton - human body, and the design of the exoskeleton based on the new actuation system.

In function of the main objective this work is divided in 8 chapters. The first chapter presents an introduction to the actual problem and the main objective of this thesis. The second chapter presents a classification of the actual rehabilitation devices with commercial and research examples. The third chapter presents the actuators used in the present in rehabilitation devices and the proposed actuators for this work. Chapter four presents the proposed actuators, based on USM and SMA , with its proposed controller and first results. The fifth chapter is dedicated to the development of biomechanical software simulation based on BoB where the behaviour of the exoskeleton with its actuator together with the human body is analysed. The preliminary results are analysed in a simulation over the upper limb. The sixth chapter presents the proposed segmented exoskeleton for the upper limb based on the chosen actuator. Chapter seven presents a summary of the elbow SMA exoskeleton with two DOF, the operation modes of its, and results on real persons. To the ending of this thesis the chapter eight is dedicated to the conclusions and future works.

# Chapter 2

# Rehabilitation devices - state of the art

An exoskeleton type system is an external rigid or flexible (soft robotics) mechanical structure actuated or not actuated, that allows the limbs to move and increases the strength and endurance of the human body. In the last decade dozens of companies and research centers have centered the attention on this type of devices, but still a field of research with many challenges. Themes such as the portability and wearability of the devices are closely related with the system actuation and mechanical structure. In this fields, the researchers are looking for new solutions which offer more safety, with a lighter weight and power consummation, noiseless operation, size, low fabrication cost. In function of the final applications, the exoskeletons can be divided in:

- Exoskeletons in rehabilitation therapies. This type of device comes to aid the therapists, offering a more effective and stable rehabilitation process cooperated with the traditional rehabilitation sessions effectuated by therapists.
- Exoskeletons for work and industry. This type of exoskeleton provide a power assistance and increase the human stretch. This can be used at construction, factories, warehouses, surgical rooms etc.
- Military exoskeletons. This type of device aid the soldiers by increasing their strength and providing support to the military equipment, for example collect energy which can be turned into electricity to recharge a battery or directly power a device (such as a communication device).

## 2.1 Exoskeletons in rehabilitation therapies

Exoskeletons and the rehabilitation device is a new way to help the patients to recuperate the motor functions after spinal cord injury, stroke or other condition. This type of rehabilitation is more than an effective therapy, it gives the possibility to the patient to do the therapy more independently, in some cases at home where the attendance of a therapist is not required. There are many ways to classify these types of devices, and here are some of them:

- In function of the human body extremity which needs assistance. Here can be classified: for upper extremity (shoulder, elbow, wrist and hand), lower extremity (hip, knee, and ankle) or full body.
- In function of the actuation system type: actuated (active) and no actuated (passive) exoskeletons. The actuated exoskeletons, can be classified in: with rehabilitation passive tasks (where the exoskeleton executes all the necessary force for the human joint movement) and active tasks (where the exoskeleton

compensates the missing force necessary for the articulation to complete the task).

- In function of the device portability: stationary (cannot be moved easily), mobile (some of them can be moved easy giving the possibility to use them at home), wearable (devices that can be dressed, portables and the most common with autonomy).
- Depending on the stage of development these can be: commercial devices (which can be purchased) and prototype devices which are only used for tests in the research laboratories, hospitals, etc.
- In function of the device rigidity: rigid exoskeletons or soft exoskeletons (exosuits).
- In function of the controller type: not controlled (passive), controlled with the aid of a joystick, controlled with a panel or buttons, controlled in function of the sensors signals (in especially for active tasks execution, for example with BCI, EMG, etc).

In the last decades, different devices have been developed for the upper limb rehabilitation. A broad review of the actual rehabilitation devices (excluding the commercial devices) can be found in [32], [33] and [34]. Some examples of commercial and current rehabilitation devices which are used in the hospitals are presented below:

### 2.1.1 Commercial rehabilitation devices

#### Armeo

Armeo is a product of the Swiss company Hocoma, founded in 1996. They develop innovative therapy solutions working closely with leading clinics and research centers. They offer solution for locomotion and for upper limb rehabilitation and evaluation therapy. For the upper limb, Hocoma has launched in close cooperation with the leading researchers and the Rehabilitation Institute of Chicago (USA) the first product Armeo. The first device was in use the summer of 2007. This is a device for the rehabilitation of the upper extremities after stroke, traumatic brain injury or other neurological disorders. In function of the disorders type this come in three possible versions:

#### Armeo Power®

Armeo Power® is a rehabilitation device used for upper limb therapy in the first period after suffering a injury [9] Fig. 2.1. This is specifically designed for persons

with functional motor disorders or bone-related disorders to assists in the rehabilitation process and assists clinicians in the evaluating process. Optionally have a hand rehabilitation module, ManovoPower®, capable to open and close in reach and grasp movements. The system has 6 DOF, and give the possibility of: shoulder abduction form -169 to 50 degrees, shoulder flexion/extension from 40 to 120 degrees, shoulder internal/external rotation from 0 to 90 degrees, elbow flexion/extension from 0 to 100 degrees, forearm supination/pronation from -60 to 60 degrees and wrist flexion/extension from -60 to 60 degrees. Each DOF is equipated with a motor and two position sensors. The hand grip is capable to measure the grip pressure. Optionally, it can be connected with the $7^{th}$ DOF ManovoPower®.

Figure 2.1: Armeo Power [9].

The software includes a database with an individual account for each patient where data history about the rehabilitation exercises is can be stored. The rehabilitation exercises presents a motivational software game with different degrees of difficulty. The documentation of the patient performances can be consulted and is easy to understand and detailed in an excel format.

The rehabilitation device is designed for patients with a maximum weight of 135 kg, and the length of arm and forearm support can be set in function of the patient. The weight of the whole system is approximately 205 kg and is mounted over a mobile platform.

**Armeo Spring®**

Armeo Spring® is a rehabilitation device used in the second phase of rehabilitation therapy (Fig. 2.2). The rehabilitation device is designed for patients who have lost the

function of or have restricted function in their upper extremities caused by cerebral, neurological, spinal, muscular or bone-related disorders. This is an unactuated device (passive device), with a spring mechanism for adjustable arm weight support. This device has 6 DOF which permit: shoulder abduction, shoulder flexion, horizontal shoulder abduction, shoulder rotation, elbow flexion, forearm pronation, wrist flexion, hand grasp and extension. Moreover this can be connected with ManovoSpring® which has one angle sensor and two DOF for thumb and fingers. ArmeoSpring® has 7 position sensors and one pressure sensor.

Figure 2.2: Armeo Spring [9].

Similar with Armeo Power®, the software includes a database with individual account for each patient where stored rehabilitation history. This has motivation games and rehabilitation exercises. The whole system has a weight of 82 kg and is mounted on a mobile platform.

Armeo Spring®, separately has a version for children's patients rehabilitation therapy (Armeo Spring Pediatric®) with the age between 4-12 years. In terms of technical data this is similar with Armeo Spring® but has a different system of adjustments for the patients.

**Armeo Boom®**

Armeo Boom® is a rehabilitation device designed for upper extremity therapy outside of clinic in the last phase of patient's rehabilitation. This device has a weight compensation mechanism with low inertia, without actuators and only offering a feedback to the user. The design of this device can bee seen in the Fig. 2.3.

The Armeo Boom® for the moment dosen't have an extension for the hand rehabilitation. The device can be mounted on a wheelchair.

Figure 2.3: Armeo Boom [9]

### InMotion Robots

InMotion Robots is a technology in the rehabilitation industry developed by the Bionik Company, born from Newman Laboratory for Biomechanics and Human Rehabilitation from Massachusetts Institute of Technology (MIT).

InMotion Robots come with three available products for upper limb rehabilitation: InMotion ARM®, InMotion WRIST® and InMotion HAND® (Fig. 2.4). All three rehabilitation devices are stationary systems and in terms of mechanics, are end-effector devices, which contact the patient limb only at its most distal part and exoskeleton devices. These are dedicated to persons who have a very limited movement ability after accidents such ACV or SCI but after other trauma e.g. Cerebral Palsy, Multiple Sclerosis (MS) [10].

InMotion ARM® (Fig. 2.4 a), is an interactive therapy system, being the clinical version from the MIT Manus exoskeleton. This is a end-effector device, with two active DOF which permit the elbow flexion/extension, shoulder protraction/retraction

and shoulder internal/external rotation. This is mounted on a mobile platform and offers an easy access to patients with a wheelchair. The software of this system consists in programs which permit the evaluation of the patient and therapeutic exercise games for motor planning, eye-hand coordination, attention, visual field deficits/neglect and massed practice.

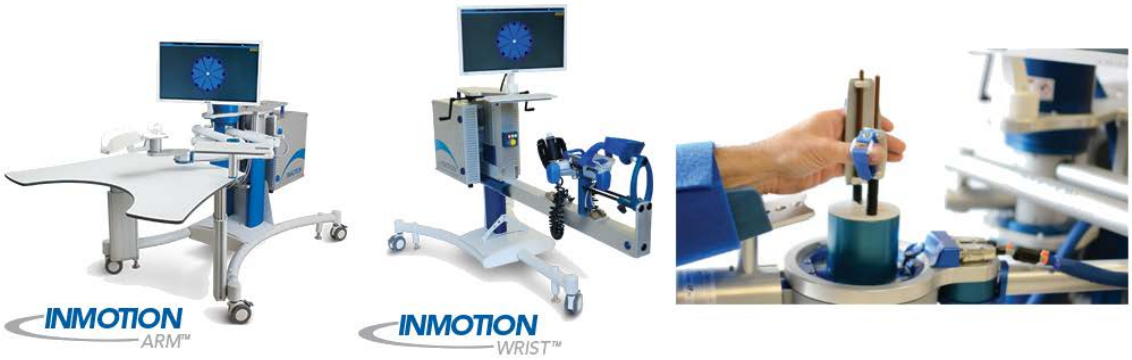


Figure 2.4: InMotion Robots for rehabilitation therapy. a) InMotion ARM®, b) InMotion WRIST® and c) InMotion HAND® [10].

InMotion WRIST® (Fig. 2.4 b), is an exoskeleton based device which can replicate the wrist movement in the ADL: flexion/extension 60/60 degrees, abduction/adduction 30/45 degrees and pronation/supination 70/70 degrees. This device has three DOF and similar with the InMotion ARM®, its software permits the clinicians to evaluate the patients, and motivate the therapy with 25 therapeutic exercises games.

InMotion HAND® (Fig. 2.4 c)), is a module which can be used with the InMotion ARM. This device has *assist-as-needed* grasp and release training with flexible positioning.

### Wearable Robotics - KINETEK

Wearable Robotics is a spin-off company of the Scuola Superiore Sant'Anna of Pisa-Italy. They produce and develop wearable robotic systems for rehabilitation, assistance and human-power augmentation. For the upper limb, the company produces two rehabilitation devices: ALEx and Track-Hold exoskeletons [11].

**ALEx**

Arm Lightweight Exoskeleton (ALEx) is a exoskeleton for the upper limb rehabilitation with six DOF where four are actuated and two are passive (Fig. 2.5). The exoskeleton has sensorized and actuated joints, that permit movements such as: shoulder abduction and adduction, shoulder rotation, shoulder flexion-extension and flexo-extension of the elbow joint. The two passive DOF are sensorized and permit the prono-supination movement of the forearm and the wrist flexion-extension. With this configuration, the exoskeleton covers 90% of the human arm workspace. This can be controlled in torque or motion movement, and is capable to detect the intention of movement. It is indicated for usage in both, acute and chronic phases of stroke for upper limb rehabilitation.

Figure 2.5: ALEx exoskeleton from Wearable Robotics - KINETEK® [11].

The exoskeleton consists of a backpack and four implemented robotic limbs which give the possibility to follow the complex movement of the human body. The actuation of this device consist in a combination between electrical motors and elastic elements, which permit the reduction of electrically consumption. The actuators was placed in the backpack and the transmission force is made using cables.

The rehabilitation therapy software permits the patient evaluation. In a passive mode and in active mode stimulate the patients with therapeutic exercise games and virtual reality.

**Track-Hold**

It is the second rehabilitation device of the Wearable Robotics-KINETEK® company (Fig. 2.6). This is a rehabilitation device for upper limb passive training with support of gravity in spatial movements. The device passive and the setting of the gravity support is made with the physical weights is can be easily replaced. This

connected with the PC via USB port and the rehabilitation exercises are in Virtual Reality.

Figure 2.6: Track-Hold exoskeleton from Wearable Robotics - KINETEK [11].

### Instead Technologies

Instead Technologies, Ltd. is a Spain company that designs, develops and manufactures products for neurorehabilitation as well as intelligent robotic-assisted tools to help disabled people. This company has two products in the field of rehabilitation: Robo Therapist 2D and Robo Therapist 3D [35].

#### Robo Therapist 2D

This is a planar rehabilitation device with two DOF for persons who suffered ACV. The device consists of one robotic arm, a monitor and the support for the patient's arm. With this configuration the rehabilitation device offer a complete workspace for the two arms rehabilitation. For the patient's motivation, the exoskeleton has a software with an interactive game. All data, the amplitude movement and force, are individually stored.

#### Robo Therapist 3D

It is a modular device that allows the adaptation of the patient to the necessary therapy by doing some activities programmed in its software. This consists in two robotic arms, actuated with the pneumatic actuators, which replicate the therapist grasping (one arm catches the hand of the patient and the other one holds him by the arm). Compared with the Robo Therapist 2D, this operate in 3D plan and the motivation of the patients is based in virtual reality.

### Tyromotion

Tyromotion GmbH® is one of the world-wide leading manufacturers and distributors of robot- and computer-assisted therapy units for the rehabilitation sector. This company offers software and robotic solutions for the rehabilitation therapy. Among more commune solutions we find products like Amadeo® for fingers rehabilitation, Diego® for the arm rehabilitation, Myro® an interactive therapy surface, Pablo® for hand and arm rehabilitation, Tymo® a sensor-based rehabilitation device for static and dynamic assessment- and therapy applications [12].

#### Amadeo®

This is a system for the hand and fingers rehabilitation, capable to operate in various modes: passive, assistive, active and interactive (Fig. 2.7). The device presents five actuated lanes one for each finger. It is a stationary device with the end-factor configuration connecting with the distal phalanges of each finger. This configuration permits the flexion/extension of the fingers joints.

Figure 2.7: Amadeo [12].

For the passive finger rehabilitation training, the device offers feedback for proportionately active movement requirement including external focus.

In the assistive mode the patient can work actively with all the fingers or individual fingers. The Amadeo system helps the patient to complete the activity it is not completely performed and offer bio-feedback and external focus.

In the active therapy the system targets repetitive movements with one finger, motivating the patient with a visual and acoustic feedback. In function of the patient motivation mode the therapy can be single movement: where the patient's strength

or mobility range is trained in function of visual shapes, memory: where the patient needs to memorize and copy the movement or interactive: where the therapy motivation is done with the games.

**Diego**

Diego is a stationary device, for upper limb rehabilitation: shoulder and elbow joints (Fig. 2.8).

Figure 2.8: Diego [12].

The idea of this system is similar with the Armeo Boom®. A stationary device, with mobile cables which connects vertically the arm and forearm. Combining the individual actuation of each cable results in individual actuation of the upper limb joints. Is designed for all phases of rehabilitation, and is similar with Amadeo, it has three functional modes: active, assistive and passive therapy. Compared with Armeo Boom® this permits the rehabilitation of both arms simultaneously. The therapy is motivated with virtual reality games.

**Pablo**

Pablo system (Fig. 2.9) is a rehabilitation device for patients with motor deficits of the hands or arms. This is a no actuated system used by the patients in the last phase of rehabilitation treatment. It consist of three devices: Sensorgriff with

position sensors, Multiball for supination and pronation of forearm, flexo-extension of the wrist, and Multiboard for rehabilitation of various joints of the upper extremity. Similar with other products of this company, the system can be connected with a PC via USB and can be used with the interactive software which return data such as force, position, reaction of the patient etc..

Figure 2.9: Pablo [12].

### KINARM Exoskeleton Lab®

The KINARM Exoskeleton Lab® (Fig. 2.10) is a stationary device placed over a mobile platform with an exoskeleton based structure. With a complex linkage to permit planar movements of the arm in the horizontal plane involving flexion and extension movements at the shoulder and elbow joints. This can work with two upper limbs in the same time, the rehabilitation device having two robots arms (Kinarm®). Each Kinarm® can actuate independently in the shoulder and elbow permitting loads to be applied to the shoulder and/or elbow joints (or hand-based loads). The device can be acquired with two Kinarms® or only unilateral. Moreover, the system has a chair, similar to a wheelchair style, a visual display and software for patient's motivation and data acquisition. Separately, it offers the possibility to acquire the Simulink library tools for control customization program of device [13].

Figure 2.10: KINARM Exoskeleton® robot for upper limb rehabilitation [13].

The KINARM Exoskeleton Lab is particularly suitable for subjects with stroke, spinal cord injury or cerebral palsy as the Exoskeleton design provides gravity support of the subject's upper limbs. The set-up process only takes 5-10 minutes, which is quick from a medical point of view.

### HAL®(Hybrid Assistive Limb)

CYBERDYNE Inc. is a venture firm which is established by Dr. Yoshiyuki Sankai, University of Tsukuba, Japan, in order to materialize his idea to utilize Robot Suit HAL for the benefits of humankind in the field of medicine, caregiving, welfare, labor, heavy works, entertainment and so on [14]. Although the company initially centered its products such as non-medical products, in the last two years, it has been planed to expand the product line with rehabilitation devices. Between Suit HAL products, more near of our objective, namely rehabilitation we find: bilateral leg support (HAL-BL), single-leg model of HAL (HAL-SL) and single-joint HAL (HAL-SJ) for elbow and knee joint therapy (Fig. 2.11).


Figure 2.11: HAL®- SJ [14].

The HAL-SJ is used as rehabilitation device for the upper limb, elbow joint with the patients with acute stroke. A rehabilitation study realized in the hospital with various patients demonstrated the beneficial therapy with the Suit HAL, including HAL-SJ [36]. HAL-SJ, which it is the only candidate product of this company for the upper limb rehabilitation, is a small and light device (1,5 kg without electronics and batteries) with an autonomy of approximately 120 minutes. The control loop uses signals based on Interactive bio-feedback (iBF) it is unique in terms that the robot strengthens the residual voluntary movements by an interaction between the robot and patient. This makes the patient to regain lost abilities completely.

### ORTE-Robotic System for Upper Limb Rehabilitation

ORTE device is a robotic rehabilitation platform for the upper limb rehabilitation, focused on restoring mobility to the shoulder and elbow joints developed by Aura Innovative Robotics S.L., Madrid, Spain, spin-off of the Polytechnic University of Madrid [15]. ORTE has an intelligent control system, which allows it to self-adapt as rehabilitation progresses: diagnostic phase, movement assistance phase, recovery phase and opposition phase. At the same time it offers real-time data about the lesion evolution. ORTE is composed of: 1) a computerized musculoskeletal model that allows to study the biomechanical behavior of the upper limb through simulations and animations, and analyse the behaviour of the actuators together with the human body [37], [38]; 2) an exoskeleton that has a space of work with the amplitude necessary to undertake a great amount of activities of the daily life [39] and 3) two human machine interfaces, one for the patient and one for the rehabilitation team.

Currently, the company has a Alpha version of the exoskeleton (non-commercial), with 4 DOF: shoulder flexion-extension, rotation and abduction-adduction and elbow flexion-extension. The actuation system of this version is based on the Dynamixel

MX-64 and RX-64 of Robotics servomotors. A first version of this device can be seen in Fig. 2.12.


Figure 2.12: 3D printed ORTE Alpha [15].

The company work on a commercial version, ORTE Beta with 6 DOF (in addition of the ORTE Alpha this device presents pronation-supination of the forearm and scapula elevation). In this version the manufacturing material consist in aluminium and in terms of electrical, electronic and mechanical is developed in order to be able to overcome all preclinical tests (laboratory tests) and clinical trials (actual tests of technology validation).

### 2.1.2 Exoskeletons in laboratories

In the last decade, various researchers has centered their work in the rehabilitation devices, trying to resolve the actual challenges in this field. More than 50 research laboratory, currently have exoskeletons prototypes for upper limb rehabilitation. A systematic review of this devices can be found in [32], [33], [34]. In continuation some prototypes of this type of devices are presented.

#### RUPERT

RUPERT is an upper limb exoskeleton (Fig. 2.13) for repetitive therapy with four actuated DOF: the shoulder joint with flexion between 15 to 85 degrees, the elbow

joint with flexion between 0 and 125 degrees, 45 degrees of supination, 45 degrees for pronation and 60 degrees for hand flexion and 30 for hand extension [16]. The system actuation is based on pneumatic muscles (PMs) which give the possibility to reduce the total weight of the device, including in the category of the portable exoskeletons. The structure of the exoskeleton in the last version, without electronics and actuators, has a weight of 0.624 kg. In terms of sensors it is equipped with position and force sensors for quantitative evaluation of the task performances. In addition an inertial sensor, is also used to provide the body position.

Figure 2.13: Latest version of RUPERT using carbon fibre composites [16].

The exoskeleton was tested with real patients and was successful evaluated, by the patients and the therapists. The six patients completed the modified Wolf Motor test, used to quantify motor function in stroke and traumatic brain injury patients.

**NEUROExos**

NEUROBOTICS Elbow Exoskeleton (NEUROExos) is a exoskeleton prototype proposed by the BioRobotics Institute, Scuola Superiore Sant'Anna, Italy, for the elbow joint rehabilitation [17]. This exoskeleton is based on three solutions: the first of them presents a double-shelled links for the ergonomic physical human-robot interface and comfortable interaction, the second one presents four passive DOF in the elbow joint, a unique mechanism which permits the rotation of the axes and translation in this

joint, and the last one is represented by the variable impedance antagonist actuation. The exoskeleton structure can been seen in Fig. 2.14.

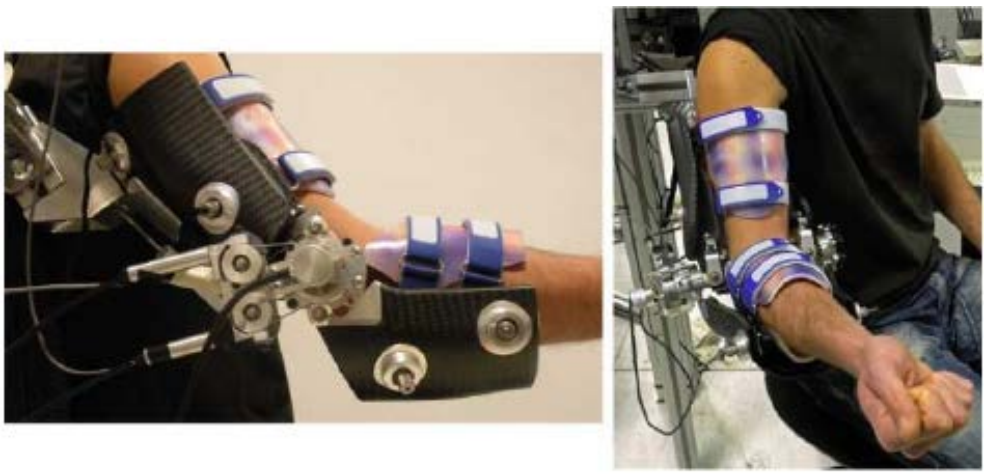

Figure 2.14: NEUROExos [17].

In terms of sensors this is equipped with a position sensor in the elbow joint and force sensors. The system of actuation of this exoskeleton was based on the hydraulic actuators combined with the elastic series elastic actuators. The entire structure, is placed in a stationary support and the force transmission is based on the Bowden cables. The maximum force of the actuators generate in the elbow joint a torque of approximately 15 Nm. The control of the exoskeleton can be chosen between passive compliance control, and torque control. The weight of the NEUROExos is 1,65 kg for the arm and 0,65 kg for the forearm.

### Hybrid Elbow Orthosis - Pylatiuk

Pylatiuk *et all* [18] presents a hybrid elbow orthesis based on electromyographic (EMG) control, functional electrical stimulation (FES), and the use of miniaturized flexible fluidic actuators (FFA). This is actuated by the two fluidic actuators in parallel each of them with a diameter of 20 mm producing a maximum torque of 3 Nm. The reference pattern for the control scheme, is represented by the EMG signals which generate the desired position or directly by the desired position itself. It is a portable exoskeleton (Fig. 2.15) with a low weight, the exoskeleton with the actuators and electronics have a weight of 0.7 kg.

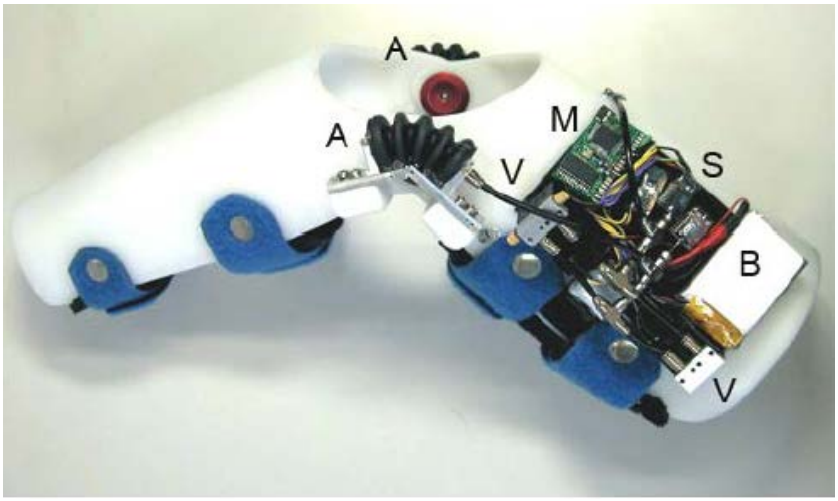


Figure 2.15: Components of a fluidically driven elbow training system prototype. A= flexible actuator, M=microcontroller and drivers, V=valves, B=Battery, S= pressure sensors [18].

### Robot-Aided ArmTraining - Song

In Song *et al.*[40] was described an assistive control system using myoelectric signals for a robot aided arm training, dedicated to the patients after having suffered a stroke. The proposed robot was developed to assist elbow training in flexion-extension movement in a horizontal plane. This is a stationary system based on an active orthesis actuated with a brushless AC servo motor. The system is composed of a personal computer (PC), the mechanical part and the EMG amplifier. In the articulation a torque sensor is placed, and for measurement of the position/velocity an incremental encoder is used. Total torque which can operate in the elbow articulation was limited at 5Nm. The pattern of reference for this system is represented by the desired torque, and is based on a myoelectric signals. Here the authors propose an assistive torque, which can be chosen by the operator proportional with the myoelectric signal. The system was tested successfully with real patients.

### Biomimetic Orthosis for the Neurorehabilitation of the Elbow and Shoulder (BONES)

BONES, developed by the Department of Mechanical and Aerospace Engineering, University of California, is a pneumatic exoskeleton for rehabilitation therapy of the shoulder, elbow, forearm and wrist. This is a stationary exoskeleton controlled in angular position and force (cylinder pressure), with six DOF and is dedicated to persons which have suffered a stroke. Ref [41] presents a study that evaluates the

functional outcomes of two different types of robotic movement training in chronic stroke survivors using the arm exoskeleton BONES. Here is highlighted that the multi-joint exoskeleton is not decisively superior to the single joint robotic training but the functionally-orientated games are during training a key element to improving behaviour outcomes.

### Muscle Suit

A wearable device which initially was centered for manual workers after for non-healthy people, was presented in [19]. This is composed of an armoured type frame actuated with artificial muscles (McKibben). This is capable to do the movements of flexion-extension, abduction-adduction, outer-inner rotation of the shoulder and the flexion of the elbow joint. The mechanical system and the position actuators can be seen in Fig. 2.16.The device was tested with 5 healthy persons and put in evidence measuring with the EMG circuit the force contribution by the wearable device.

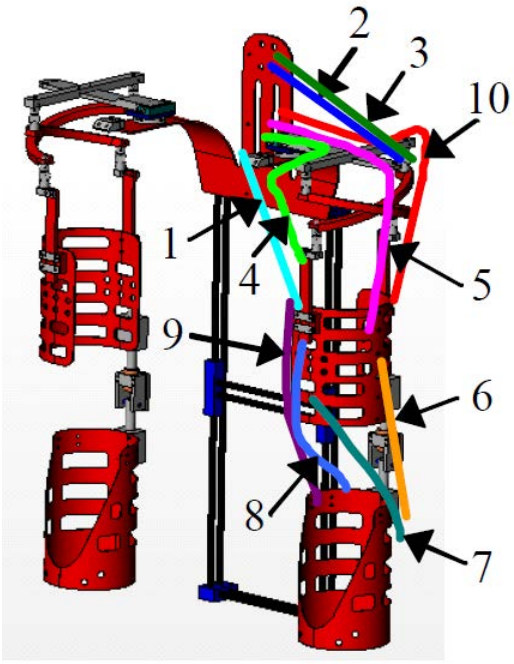


Figure 2.16: Muscle suit exoskeleton where: 2,3,4 was used for shoulder flexion, 10 for shoulder extension, 2,3,5 for shoulder abduction, 1,4 for shoulder adduction, 8 for outer rotation, 7 for inner rotation and 6,7,8,9 for cubital joint flexion [19].

**Five DOF Upper Limb Rehabilitation Robot System**

In Li *et al.*[42] was presented a wearable exoskeleton for rehabilitation, with five DOF which are: shoulder joint abduction-adduction, flexion-extension, elbow joint flexion-extension, wrist flexion-extension, and pronation-supination. This is made from rigid duralumin with two-side structure, and actuated with different servomotors. The shoulder and elbow joints are actuated with Panasonic AC servo motor for a big torque, and the wrist with two maxon DC servo motors. In the joints where placed optical encoders a measure the angles. The control algorithm uses such a reference pattern the angle position provided by the sEMG signals. This placing the electrode along the muscle fibres and on the mid-line of the belly of the muscle, considering there are the sEMG signals with the greatest amplitude. For angle estimation from the sEMG signal, after a preprocessing the sEMG signal they use a nonlinear AR (Auto-regression) model to describe the signal, and an artificial neural network with three layers for recognition of six upper limb rehabilitation motions. The exoskeleton is not tested with real patients.

## 2.2 Exoskeletons for work and industry

The exoskeletons for work and industry is not very common as rehabilitation exoskeletons where dozens of companies with years of experience already exists, but is becoming a field of exoskeleton research which is growing very fast. The exoskeletons dedicated to industry and workplace, offer advantages such as: reducing the fatigue of the worker, reducing related work injuries, keeping the quality and experience of the worker past their physical prime in the work force longer. In function of final application and the human body part it assists, it can be divided in:

- Tool Holding Exoskeletons. This type of exoskeletons assist the upper extremity of the human body and connect with the lower body exoskeleton and a counterweight. Generally it are spring loaded passive exoskeletons but can be prototypes actuated with motors, especially in the legs. Some examples can be Ekso Works by Ekso Bionics, Fortis by Lockheed Martin, Rabo-Mate by EU, RoboShipbuilder by DSME, ShoulderX by SuitX etc.

- Chairless Chairs. This type of device reduce the fatigue of workers that stay in the same position for an extended period of time. Here we can find: Noonee Chairless Chair Wearable Ergonomic Device, Body Weight Assist Device by Honda and Archelis by Wearable Chair.

- Back Support. This type of devices maintain the correct posture of the back while bending down to perform a lift. Here examples are: V-22 Ergoskeleton

by StrongArm Technologies, Laevo by Laevo, MAX by SuitX (formally US Bionics), Hip Auxiliary Muscle Suit by Innophys, Hal for Labor Support Lumber by CYBERDYNE and AWN-03 by Panasonic by ActiveLink.

- Powered Gloves, to assist in the grasping tasks. Examples are: SEM Glove by Bioservo Technologies and Pneumatic Power Assist Glove by Daiya Industries.
- Full Body Power Suits. This category of exoskeletons was slowly abandoned (for the complexity of the device) and the company centered in the specialized exoskeletons. Some examples of this devices are: HULC by Lockheed Martin and Ekso Bionics and XOS 2 by Sarcos / Raytheon, etc.

## 2.3 Military exoskeletons

Another industry field of the exoskeletons is represented by the wearable robotics for the military. In the last decade centers of research from the U.S., China, Canada, South Korea, Great Britain, Russia, Australia and other ones which are still secret, develop and test exoskeletons devices to increase the military potential. Although it is not the topic of this thesis, because rehabilitation exoskeletons have certain similarities in the development of these devices and have common challenges. Firstly the exoskeleton needs to be comfortable and easy to integrate with the already established equipment. On the other hand the exoskeleton need to be reliable and very durable. One of the differences with the rehabilitation exoskeletons is the position of the actuators. In exoskeletons for the rehabilitation the actuators are placed in the lateral limb (exterior part). For example in the military exoskeletons the actuators are positioned in the front or the back of the user.

Military exoskeletons can be divided in four groups:

- Full body military exoskeletons. In this category can be found HULC (Human Universal Load Carrier) developed by Ekso Bionics and Lockheed Martin and XOS2 Sarcos/Raytheon. These two projects remain in the stage of prototype. They are large with many actuators and have a difficult power control. In addition, the power consumption and the autonomy (need to work several hours without recharging) is an issue still unsolved.
- Lower Body Powered Military Exoskeletons. This category of exoskeletons provide assistance to the lower extremities, legs or just one leg. Here various centers of research and companies work in development of this types of exoskeletons: Ekso Bionics and Defense Advanced Research Projects Agency's Warrior Web (DARPA) develop a compliant universal knee exosuit, ExoAtlet® by ExoAtlet, Hercule® by RB3D, Kinetic Operations Suit by B-Temia with Revision Military, etc.

- Passive Military Exoskeletons. The passive exoskeletons for military field don't have any actuator, batteries or electronics. In this category we find the exoskeletons developed by the 20KTS+: Marine Moko® which is developed to absorb the shock and vibrations for military personal on small, fast patrol boats and Terra Mojo®. Australia's Defense Science and Technology Organization (DSTO) developed Operations Exoskeleton which a exoskeleton based in Bowden cables system designed to transfer a percentage of the weight of a soldier's heavy backpack directly into the ground.

- Energy Scavenging Military Exoskeletons.

  This is a group of unactuated exoskeletons which collect energy from the user (soldiers) to charge the batteries or directly offer the power supply for the electronic devices (for example the communications devices). This comes in the aid of the soldiers which need to charge the batteries for the electronics devices during several hours. With this solution, the amount of batteries and in the same time the total weight of the load can be reduced. Some examples of this type of exoskeletons are: PowerWalk® by Bionic Power and SPaRK® by SpringActive.

## 2.4 Conclusions

In this Chapter has been presented the most popular commercial rehabilitation devices actually used in hospitals and rehabilitation centers, and some examples of laboratory exoskeletons which somewhat resemble (in terms of type and dimensions) the proposed device in this thesis.

Most rehabilitation devices for the upper limb that are currently marketed, present a stationary structure or a mobile one, but cannot be transported and installed easily. These configurations due to the weight and installation complexity, are placed in rehabilitation centers and force the patient to move to which implicates time and financial costs. Moreover, this devices presented an elevated cost, which hinders their acquisition by rehabilitation centers.

The rehabilitation devices which are currently laboratory prototypes, present a more compact structure, the majority of such exoskeletons, integrate new sensors to improve the rehabilitation therapy. Nevertheless, in terms of total weight and financial cost of fabrication they can be improved.

Both in commercial and laboratory devices, the total weight of the device and the financial cost of fabrication depend largely on the actuator. The proposed rehabilitation device in this thesis - thanks to the actuation system - is an alternative solution to the current rehabilitation devices (both commercial and laboratory types). The offered device demonstrate a low weight, low fabrication cost and noiseless operation.

# Chapter 3

# Actuators used in rehabilitation devices

The most important aspects for the exoskeleton devices are: to comply the necessary requirements for an efficient therapy and be accepted by the patient. These aspects comply with requirements that need to be considered in the exoskeleton design: patient needs, the weight of the device, price, comfort and less significant, the size. This requirements have a strong connection with the actuation system. The actuator must provide the necessary force for articulation mobilization, have a light weight, noiseless operation, needs to be efficient in terms of energy consumption and have a small dimension. Among the most used systems of actuation for the exoskeletons are: the electromagnetic motors, hydraulic actuators, pneumatic actuators, series elastic actuators and less common functional electrical stimulation (FES) in combination with other type of actuators (hybrid systems). This Chapter 3, presents a brief description of the current actuation systems used in the exoskeletons and the actuation systems, non-linear actuators, proposed in this work to integrate in the rehabilitation devices. Particularly, will be analysed two types of actuators based on USM and SMA, which represent one of the objectives of this thesis.

## 3.1 Current actuators in rehabilitation devices

One of the most important part of the rehabilitation devices is represented by the actuation system. In the current rehabilitation devices, the following actuators can be found the electromagnetic motors, hydraulic actuators, pneumatic actuators, series elastic actuators and functional electrical stimulation which will be described below.

### 3.1.1 Electromagnetic motors

The electric motor is an electromechanical device that transforms the electrical energy in a mechanical energy. The majority of this type of motors works based on the electromagnetic forces which act over one conductor through of electric current in magnetic field. This type of motors are constructed using a stator and a rotor where the stator is the fixed part and the rotor is a mobile part of the motor. Depending on the type of electric current which passes through them, the electrical motors can be divided in DC motors and AC motors.

#### DC motors

These types of motors are very popular and where used successfully in various applications. In the exoskeletons, still the most used actuator, due to the verity, easy to integrate and its characteristics such as size, weight and price. Nevertheless, the principal inconvenience of this type of actuator still is the necessity to decrease the speed through the use of gearboxes, which augments the total weight of the actuator.

Moreover, they are nosily and the driver of this type of actuators most times has remarkable dimensions.

In the rehabilitation devices this type of actuator was used for mobilization of different joints such as: the wrist and elbow using DC servomotors [42], the finger, using DC linear motors [43], the elbow and shoulder [44]. ArmeoPower presented in 2.1.1, or MyoPro [20] (Fig.3.1), are commercial systems which use DC motors in its structure for articulation movement.

Figure 3.1: Myoelectric Arm Orthosis designed to support a weak or deformed arm [20].

#### AC motors

The AC motor is an electric motor that works directly powered from AC power sources. This type of motor can be built in two functional variants:

- Motors operating in asynchronous mode (more common)
- Motors operating in synchronous mode

In the rehabilitation devices, this type of actuation system can be find in: Song *et al.* [40], Sulzer *et. al* [45], Ju *et al.*[46].

### 3.1.2 Hydraulic actuators

A hydraulic motor is a mechanical actuator that convert the hydraulic pressure and flow in the mechanical movement, such as linear or angular displacement. This type of actuators presents characteristic such as low-medium speed with a medium-high torque. One disadvantage, in terms of rehabilitation devices, is the total weight of the actuator. However, this was used in some rehabilitation systems, such in Vitiello *et al.* [17] and Pylatiuk *et al.* [18]. In this applications the actuator is placed in a stationary structure and the force is transmitted by the Bowden cables to the joint.

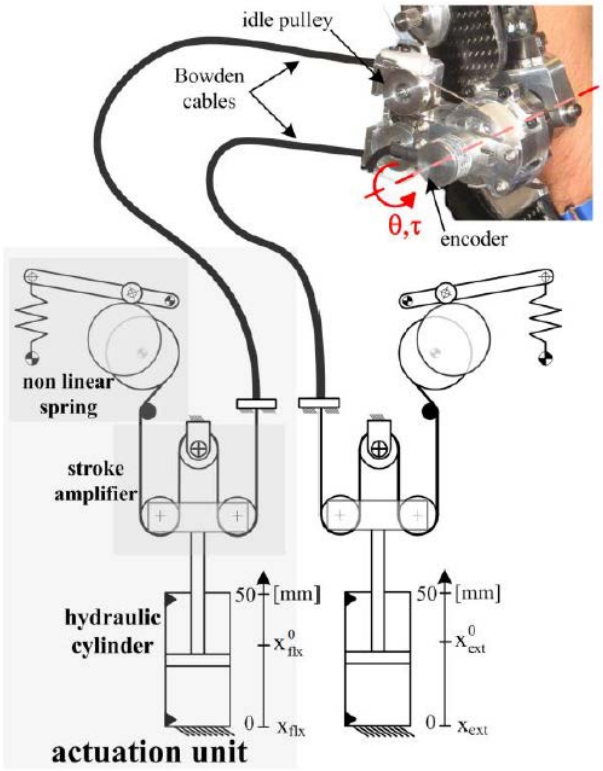


Figure 3.2: Schematic drawing of the antagonistic tendon-driven compliant actuation and sensory system of the NEUROExos [17].

### 3.1.3 Pneumatic actuators

The mechanism to convert the compressed air energy in mechanical motion is the pneumatic actuator. The mechanism of this type of actuator is similar (to a certain extent) with the hydraulic actuators. This can be found in different configurations such a cylinders with simple effect or double effect, rotary actuators, grippers etc. In the last years a special attention goes to the pneumatic artificial muscles (Fig. 3.3). This type of actuators is based on a simple principle as in human muscles. The relation between weight and force of this type of actuator, consider it a good candidate for the system actuation in rehabilitation devices. Nevertheless, currently this is still limited by the pressure generator for the compressed air, which have a remarkable weight and produce noise. This type of actuators was successfully used in rehabilitation devices proposed by Kobayashi *et al.* [19], Milot *et. al* [41] and Rupert exoskeleton [16].

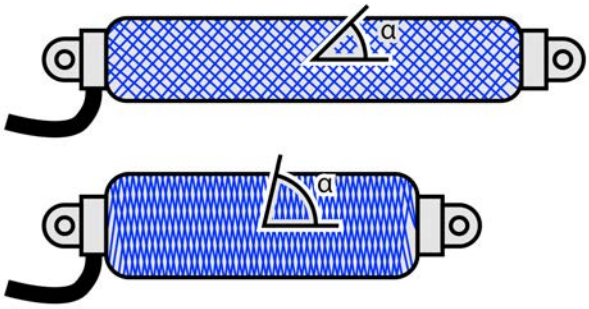


Figure 3.3: Pneumatic muscle actuator

### 3.1.4 Series Elastic Actuators

The Series Elastic Actuators (SEA) are practically composed of an electric motor in series with a spring component. This type of actuator has been used in various robots, particularly in walking humanoid robots. In the rehabilitation devices they are more used in the lower part of the body, but can also be found in the upper limb rehabilitation. A system based on SEA for the elbow rehabilitation was used in [47].

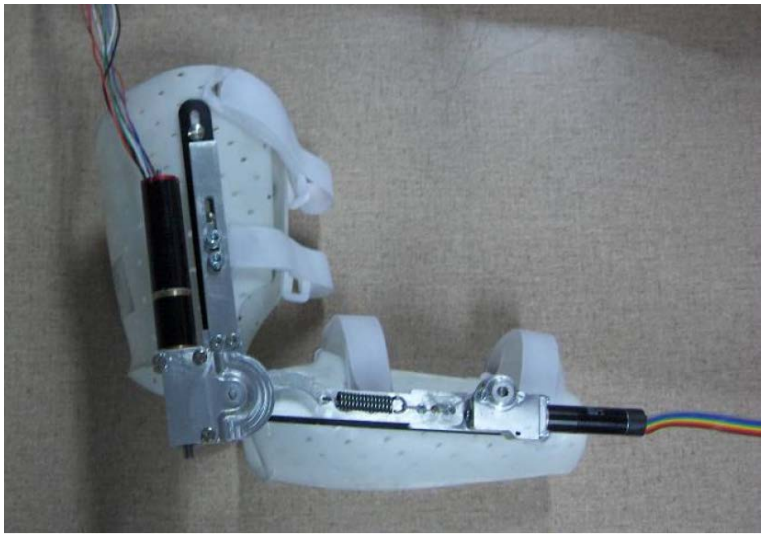

Figure 3.4: Elbow orthosis prototype actuated with SEA

### 3.1.5 Functional electrical stimulation

Functional electrical stimulation (FES) (Fig. 3.5) or also known as electrical muscle stimulation (EMS) or neuromuscular electrical stimulation (NMES), is a technique

that uses low energy electrical pulses over muscle to artificially generate muscle contractions which lead to body movements. In the rehabilitation field, this is applied in individuals which present a disorder of motor function, presenting a total or partial paralysis. It was used in the development of neuroprostheses, most for the lower limbs, due to the minimum necessary distance to the heart, actuated independently or in combination with another type of actuator. Nevertheless, it is difficult to achieve a precise and repeatable movement with this technique, and it may be painful for the patient. An important factor to be taken into account when using this technique in rehabilitation, is also the muscular fatigue. After some cycles of FES application the muscle presents a big fatigue and does not longer respond before recuperation [48].

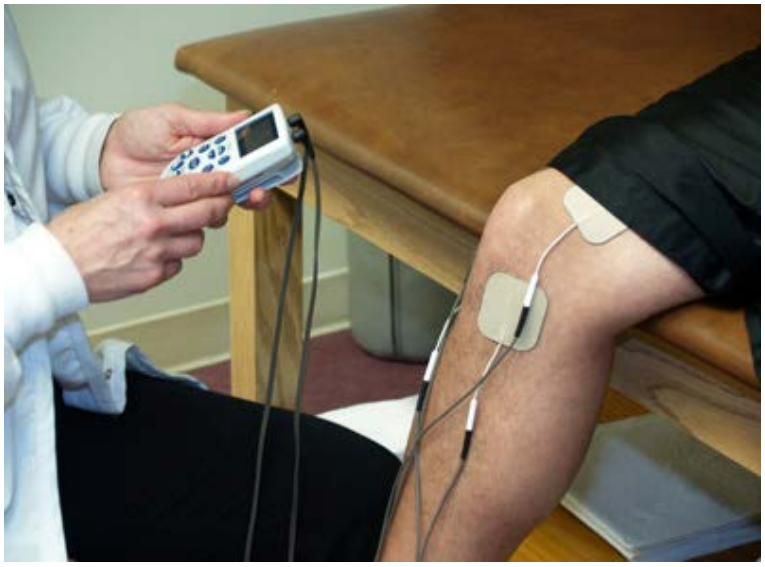

Figure 3.5: Functional electrical stimulation (E-stim)

## 3.2 Ultrasonic motors

Ultrasonic motors (USMs) are actuators that use a high frequency power source which is used to vibrate an element made from a piezoelectric material. The USM uses an ultrasonic level mechanical vibration as a driving source. This type of actuators is characterized by a good relation torque-velocity, presents a high torque with a low velocity which cancels the need to use gears. This results in a device with smaller dimensions. Other good characteristics of this type of motors are the silent operation, they are not affected by the electromagnetic field, don't emit electromagnetic noises and have a very good response with position controlled. Between the disadvantages of this type of motors we found the necessity of the high frequency power source,

reduced life span and slight oscillation of its controlled speed [21].

In Fig. 3.6 is presented a cross section of the USM from the company Shinsei. The stator is composed of a piezoelectric ceramic and elastic element. The rotor in this case is composed of a bronze material pressured over the stator.

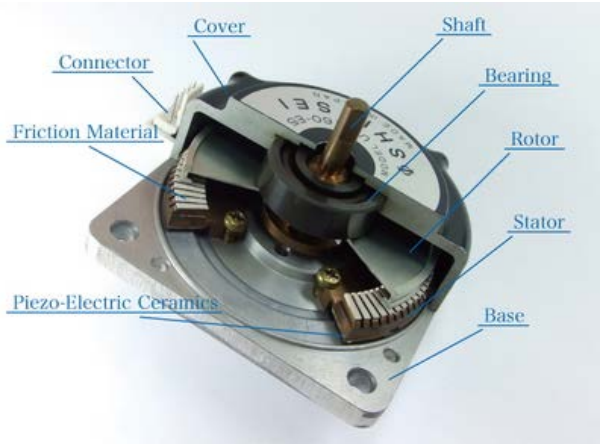


Figure 3.6: Section of the USR60 [21].

In the Fig. 3.7 the principle of operating of this type of actuator can be seen. When the traveling wave propagates to the right part, then the motion path in the stator is elliptical and anti-clockwise. The rotor is permanently in contact with the stator by means of the pressure preload, then the peak of the traveling wave of the stator pushes the rotor to the left. The rotor has a movement opposite to the traveling wave.

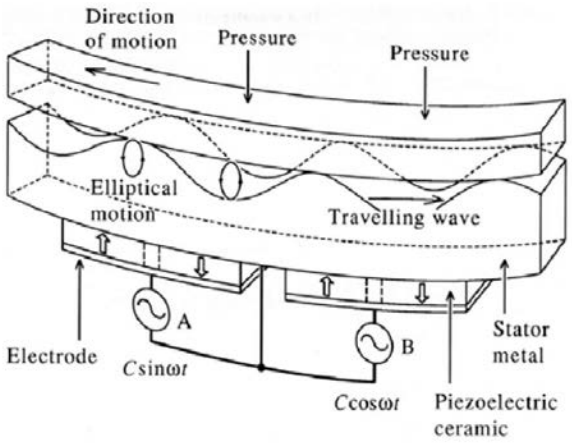


Figure 3.7: Principle of operation of a USM [21].

In the Fig. 3.7 the two piezoelectric ceramics elements are positioned very close to each other. The element $A$ generates a vibration over a relation 3.1:

$$Csin\omega t \tag{3.1}$$

And the element $B$ generates a vibration over the relation 3.2:

$$Ccos\omega t \tag{3.2}$$

where $C$ is the amplitude of the vibration and $\omega$ is the angular frequency. With this configuration, the traveling wave is propagated towards right part. If the element $B$ generates the vibration over the relation 3.3:

$$-Ccos\omega t \tag{3.3}$$

the direction of the traveling wave changes the sense towards the left part.

### 3.2.1 USMs characteristics

- Silent operation. Compared with the conventional electromagnetic motors the USMs have a silent operation. In this moment, the majority of the systems generate an acoustic pollution. In some environments such as: offices, hospitals, hotels, theatres, etc. we need a noiseless systems. There a good candidate are the USMs.

- It has a fast response, a good stop, and a wide speed range that produces excellent control with accurate positioning. As the rotor and stator are tightened together, the torque at the motor stops as a brake when the motor is turned off. The motor has low inertia, with a response time of less than 1ms. In other words it seems easy to control. The speed and position of the USM can be controlled by the amplitude, frequency and phase difference of voltages. Usually the USM is controlled by the frequency method.

- A very simple structure with small dimensions - Its structure is simple, the rotor is only formed by a piezoelectric ring. For this reason it is quite small in size. This characteristics makes it easy to manufacture. Its reduced dimensions allow to expand the area of applications of the motors.

- High torque for reduced speed - this feature allows gearless operation. Presents a torque that can be between 10 and 100 times bigger in comparison with a normal motor of the same size. On the other hand in the conventional motors the use of reductores diminishes the performance of the system and increases the angular pitch.

- Is not affected by the external magnetic fields and doesn't generate them.
- Great power ratio per unit of weight and moderate efficiency.
- Can be easily miniaturized.
- Low life time due to the friction between stator and rotor.
- Over time we need to take into account the torque drop and speed increase.
- Velocity output has small repetitive velocity oscillations around an average value.
- The USM needs a high frequency power supply.

These characteristics of this kind of actuator makes it a good candidate to be used in the rehabilitation devices. The USM in the last years has been used in various fields such a robotics, medicine, various devices for high position control, space, etc. In the rehabilitation and prosthesis robotics this was used for the first time in the project MANUS in prosthetic hand [49] and the trembling reduction device [50].

### 3.2.2 Commercial USMs

In the market we found a variety of this type of actuator. In function of the operation type this actuator can be classified in:

- Linear ultrasonic motors. This is the most common category found in the market from the companies such as: PI, Piezo Motor, Squiggle, Nanomotion, etc. The range of force of these commercial actuators can be found from $2N$ to $600N$.
- Rotary ultrasonic motors. This type of actuators can be found in companies such DTI, Jiangsu TransUSM, Shinsei Corporation, Piezotech, etc. The torque range which this motors can produce is between $0.002Nm$ to $16Nm$.
- Spherical ultrasonic motors. This type of actuator was proposed by the Toyama laboratory from Tokyo University of Agriculture y Technology.

### 3.2.3 Comparison with electromagnetic motors

Compared with the traditional motors, the ultrasonic motors have: a flexible compact and lightweight structure, fast response, are noiseless, high torque at low speed, good control, power lock, a good precision of movement, does not interact with magnetic

fields, etc., also work at low temperature, and adapt to the characteristics of the space environment.

In the Fig. 3.8 (taken and adapted from [51]) is presented a graphic comparison between the DC, Brushless and Piezoelectric motors in function of the velocity and torque range.

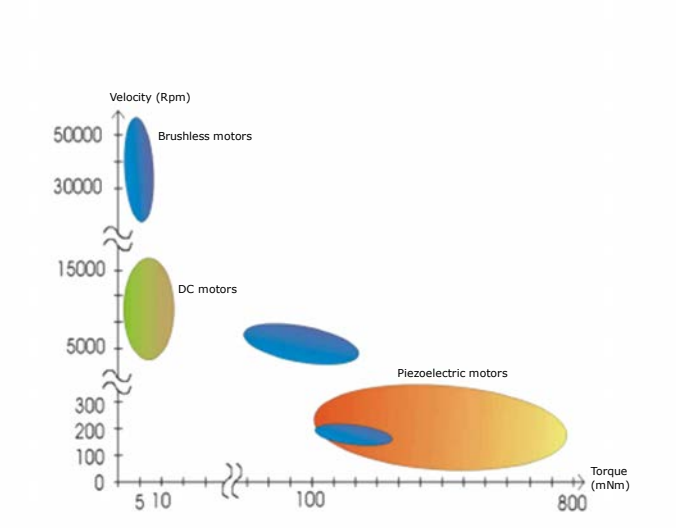


Figure 3.8: Comparison between the DC, Brushless and Piezoelectric motors

To evaluate the characteristics of ultrasonic motors versus electromagnetic motors of similar performance, in the table 3.1 are presented various electromagnetic motors from different companies and an ultrasonic motor, USR60, made from Shinsei Corporation. This proves evidence the characteristics of the conventional electromagnetic motors, without gearbox, comparing with an ultrasonic motor. The actuators with a similar velocity are compared in function of the weight and output torque. For example, a similar velocity with the USR60 have the Crouzet motor. If we compare the weight, this motor weights 1.3 kg, a five times more heavy than the ultrasonic motor USR60.

Comparing with motors with similar output torque, we can compare the USM with the SmartAutomation, D-8630-C-1 Moog, Crouzet, Harmonic Drive and Maxon EC-4pole-CW. The first three motors have a weight dimensions much higher than the USR60. The Harmonic Drive and Maxon motor is more similar to the ultrasonic motor characteristics, but the Maxon has the disadvantage to be only unidirectional and the Harmonic Drive still has a higher weight.

Table 3.1: Comparison between USR60 and conventional motors

| Model name | Max. Torque [Nm] | Weight [kg] | Max. Velocity[rpm] | Power[W] | Dimensions[mm] |
|---|---|---|---|---|---|
| Crouzet | 1.2 | 1.3 | 83 | 30 | 2114.5x91.9x57.1 |
| Maxon EC−4pole-CW | 0.96 | 0.86 | 6420 | 480 | $\phi$ 32x162 |
| D-8630-C-1 Moog | 1.21 | 1.04 | | | $\phi$28.57x11.049 |
| SmartAutomation | 1 | 2.3 | 3000 | 315 | $\phi$ 73x887 |
| Harmonic Drive | 1.8 | 0.4 | 200 | | 50x50x48 |
| USR60 | 1 | 0.25 | 150 | 5 | 67x67x45 |

These types of actuators was used in robotics: robotics hands [52] and [53], prosthetic hand [54], in space [55] and on the automation and medical industry [51].

## 3.3 Shape Memory Alloy

Shape Memory Alloy (SMA) is a metallic alloy that has the property to recover to the original shape (the "memorized" shape) after its deformation above transformation temperature between martensite phase (at low temperature) and austenite phase (at high temperature) [23]. In this transformation the material has the property to reduce the total length between 3%-5% (Fig. 3.9).

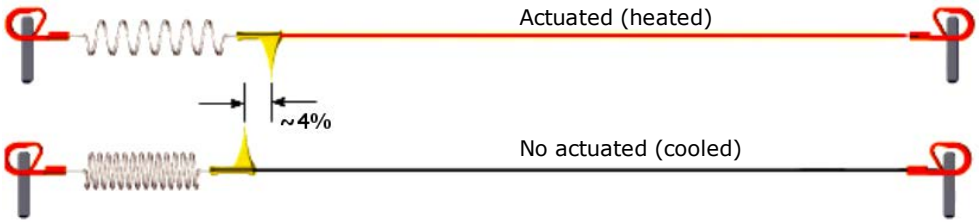


Figure 3.9: SMA actuation.

In the last decade, this type of material has sparked the interest of many researchers through its characteristics such as: very good relation force-weight, simplicity, low weight and small size, making them ideal to replace pneumatic, hydraulic or solenoid actuators. The most common SMA is Nickel- Titanium or Nitinol, but alloys based on Nitinol with other metals can also be found:copper-zinc-aluminum-nickel, copper-aluminium-nickel, etc.. However, the working principle of these types of actuators is based on the heated effect. Nitinol alloys are cheaper to produce, easier and safer to handle, and have better mechanical properties compared to other existing SMAs [22]. Thanks to its characteristics, in this work the Nitinol is used. This is heated by means of the Joule effect, taking place the transformation process: in the first stage the electrical energy is transformed in thermal energy, thanks to the Joule effect in the second stage the thermal energy is transformed in mechanical work. During its transformation two stages can be highlighted: the first one is when the phenomenon is completed which is called austenite. The second one, is when the NiTi is cooled, called martensite . As the Fig. 3.10 represents in the austenite phase As is the temperature where the austenite starts and respectively Af the temperature where austenite finishes. Similarly, in the martensite phase, Ms the temperature where the martensite phase starts and Mf is the temperature where the temperature finishes. During its transformation, the SMA suffers a shape change effect, which

are called SME and pseudoelasticity (or superelasticity), this can be categorised into three shape memory characteristics as follows:

- One-way shape memory alloy effect, is the ability of the shape memory alloy to recover the initial shape upon heating above transformation temperature.
- Two-way shape memory alloy or reversible, in addition to one-way effect the shape memory alloy recovers the shape upon cooling during the transformation temperature.
- Superelasticity or pseudoelasticity, refers to the ability of NiTi to return to its original shape upon unloading after a substantial deformation.

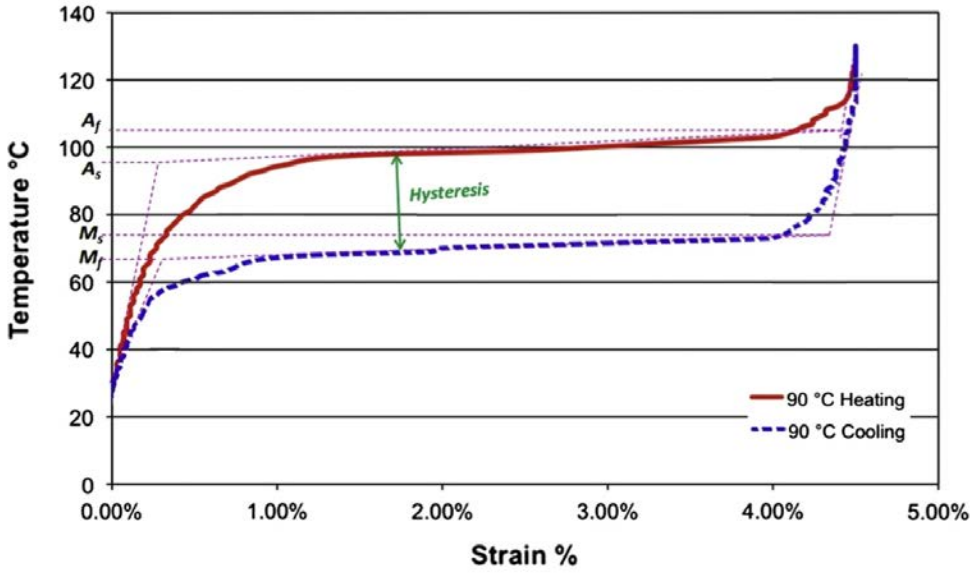


Figure 3.10: Flexinol NiTi SMA (HT) phase transformation [22].

In function of the shape and the alloy type, the SMA can exert a certain force, for example in the wire shape with the diameter of 0.51mm can exert from 35.6N [1] to 118N [56]. With this diameter 1m of SMA wire produces a displacement (contraction) between the two extremities during deformation of approximately 0.04m, and the total weight of this does not exceed 20g (density 6450-6500 kg/m$^3$). Thanks to this good force-weight relation, this alloy is an ideal actuator for low-weight devices and in particular for wearable devices.

### 3.3.1 SMA characteristics

The SMA actuators presents many advantages compared with the conventional actuators presented in the precedent sections. This can be highlighted in function of its characteristics:

- Low weight. The SMA actuators can be found with different dimensions and shapes such as: springs, wires, tubes or ribbons. Due to the forces of actuation and the cooling time, in this work we focused on wires acting as actuators. This can be found with different diameters from 0.001 to 0.020 inches. With these diameters the weight of the wire 1m is not more than 20g which can be considered negligible.

- Good force - weight relation. One wire with a diameter of 0.001 inch can do more than 0.89N force and a wire of 0.02 inch more than 35,6N force. A comparison in function of the force -weight relation between the conventional motors and SMAs can be seen in the Fig.3.11.

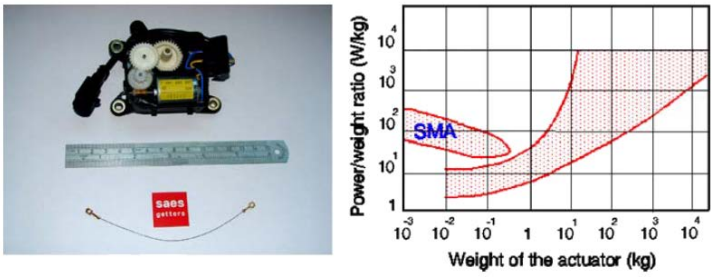


Figure 3.11: Comparison between traditional and shape memory actuators [23]

- Noiseless. Not noise producing during actuation.

- Simple. Presents a simple structure, an alloy wire composed by Ni and Ti in different percentages.

- Long life. To demonstrate the large cycles of life of this type of actuator the publication [23] presents a study about the fatigue of smartflex 76 wire, which work over one million of cycles. This directly depend of the wire stress. A graphic with the life cycles in function of the stress wire can bee seen in Fig. 3.12.

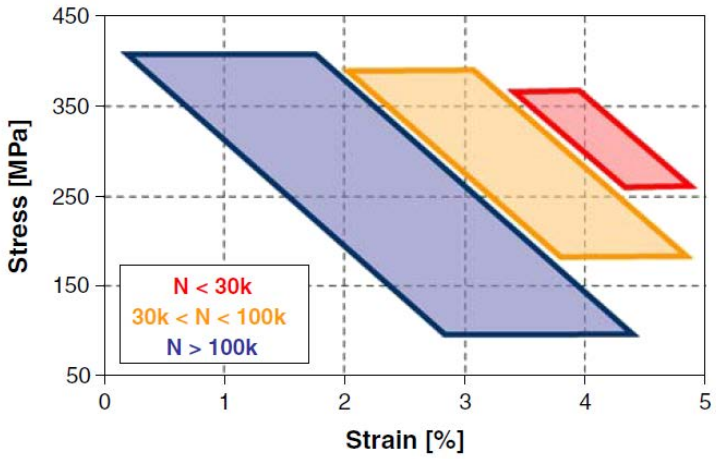


Figure 3.12: Fatigue lifetime for Smartflex 76 under different stress-strain conditions [23].

- Biocompatibility. With a high nickel content in a NiTi, it is possible that, under certain conditions, nickel may dissolve from the material due to corrosion and cause unfavorable effects, but a lot of research has demonstrated a good biocompatibility of the NiTi, showing a good corrosion resistance and advantageous biocompatibility [57].

On the other hand, between the disadvantages of this type of actuator can be found:

- Elevate hysteresis (Fig. 3.10). Hysteresis is a measure of the difference in the transition temperatures between heating and cooling (i.e. $\Delta T = Af - Ms$), which is generally defined between the temperatures at which the material is in 50% transformed to austenite upon heating and in 50% transformed to martensite upon cooling [23]. The NiTi wire presents a big hysteresis which influences the actuation time. The hysteresis of the NiTi depend of the alloy percentage combination. For a good response and for control simplification materials with minimum hysteresis has been chosen.

- Low actuation frequency. After contraction, the initial shape recuperation depends of the cooling process, which directly depends on the ambient temperature, the wire diameter and the recuperation force. If for fine wires this process is less than 1 second for the wires with big diameters this can take some dozens of seconds. Some cooling methods and the ratio of actuation speed improvement is shown in the table 3.2.

Table 3.2: Relative Effects of Cooling Methods [1]

| Method | Improvement in Speed |
|---|---|
| Increasing Stress | 1.2:1 |
| Using Higher Temperature Wire | 2:1 |
| Using Solid Heat Sink materials | 2:1 |
| Forced Air | 4:1 |
| Heat Conductive Grease | 10:1 |
| Oil Immersion | 25:1 |
| Water with Glycol | 100:1 |

- Non-linear model. Thanks to the hysteresis and other properties, this type of actuator presents a non-linear model which to leads to research in non-linear methods for its control.

- Low energy efficiency. Actuated directly with the Joule effect presents a high electrical power consumption.

### 3.3.2 Applications

In the last years, this type of actuator has been used in various types of applications, from biomedical field to robotics and automation. This is reflected by the publications and the patents from the last years, Fig. 3.13:

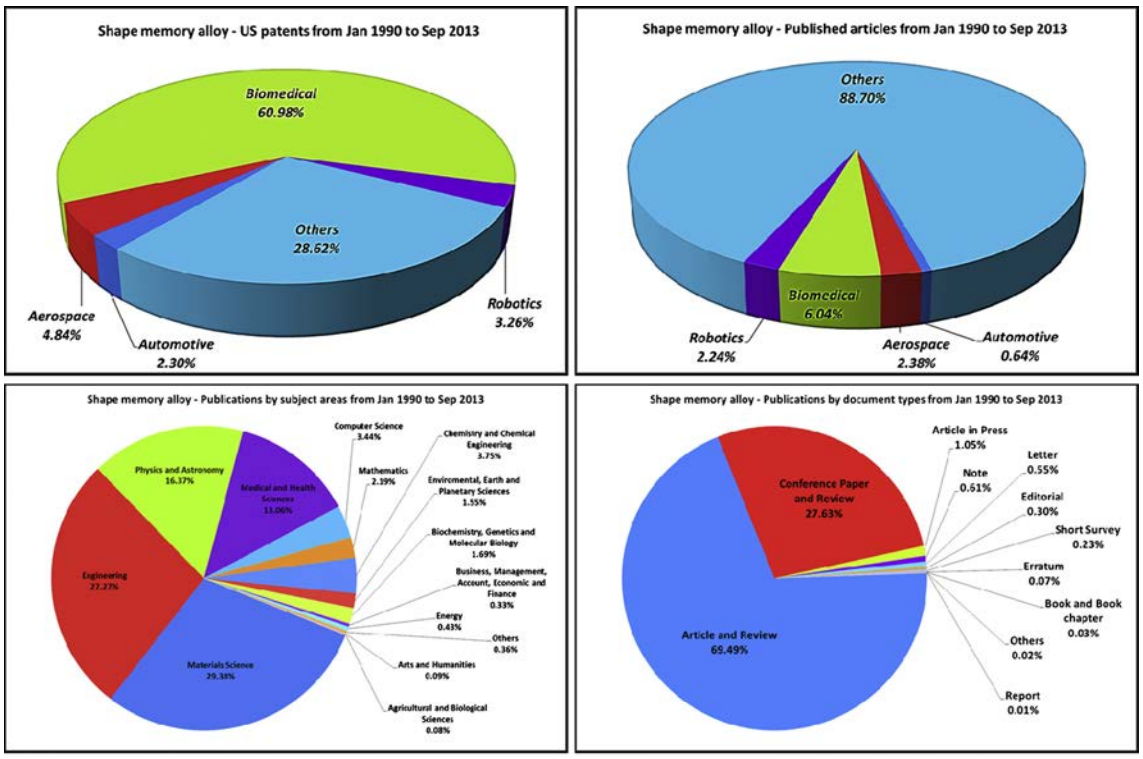


Figure 3.13: SMA publications and US patents from January 1990 to June 2013 [22].

- In automotive industry the safety and comfort represents the principal objective. This leads to an increment in the number of sensors and actuators used in cars. In this field the SMA represents a good candidate to replace the conventional motors. This was used in: rear-view mirror folding, climate control flaps adjustment, lock/latch controls, engine temperature control, carburation and engine lubrication and powertrain clutches [58], [59] and [60].

- In aerospace applications we can find the SMA (especially for the weight and noiseless characteristics) such a actuators, structural connectors, vibration dampers, sealer, release or deployment mechanisms, inflatable structures, manipulators and the pathfinder application [61], [62] and [63].

- Since the 1980s, SMAs have been used in a diverse range of commercial robotic systems, especially as micro-actuators or artificial muscles. Some examples of SMA in robotic applications can be found in humanoids robots, micro-gripper, flying robots such BATMAV and Bat Robot, etc. [64], [65] and [66].

- The SMAs are used in medical equipment and devices in many fields including orthopaedics, neurology, cardiology and intervention radiology, and other medical applications which can include: endodontics, stents, medical tweezers, sutures, anchors for attaching tendon to bone, implants, aneurysm treatments, eyeglass frames and guide wires [67] and [68].

## 3.4 Conclusions

In this Chapter have been analysed the currently actuators solutions implemented in the rehabilitation devices and the characteristics of USM and SMA materials. In function of these characteristics it was decided to conduct detailed study of the USM and SMA materials, such as possible actuators for rehabilitation exoskeletons of upper limb.

# Chapter 4

# USM and SMA actuators proposed for rehabilitation devices

In the Chapter 3 were presented the actual actuators used in rehabilitation devices and the candidate non-linear actuators that are be analysed in this work with the objective to integrate them in rehabilitation devices. In this Chapter, particularly are presented two possible types of actuators based on USM and SMA, to be used in rehabilitation devices, focusing on rehabilitation exoskeletons for the upper limb and analysing the viability of the proposed solution in function of the required torque condition. Here are described, the proposed actuators with their control algorithm, the test benches used for test the actuators and their control algorithms, and the preliminary results.

## 4.1 USM based actuator

This section presents the USM based actuator proposed in this work to be used in rehabilitation devices. In function of the USMs characteristics presented in Section 3.2.1 and considering the elbow joint as the principal articulation for testing the actuators in this work, the proposed actuator is based on an ultrasonic motor USR60-E3NT, a planetary gear (with a ratio of 4.3:1 and 0.25 kg weight), and a magnetorheological clutch. On the other hand, to test the performances of proposed actuator, a test bench capable to simulate (in parameters of weight and length) the elbow joint for a person with 70 kg weight and 1.70 height was developed. This section is based on the publications [69] and [70].

### 4.1.1 Test bench for elbow joint simulation

The elbow is a complex articulation composed by the humeroulnar and humeroradial joints (for the flexion-extension movement) and the proximal radioulnar articulation (for the pronation-supination movement). The flexion-extension movement, in the majority of the cases, has an angular range of movement between 0 and 150 degrees, but in the ADL the functional range is estimated between 30 and 120 degrees. In the pronation-supination movement, the averages are 71 degrees of pronation and 81 degrees of supination (Fig. 4.1). In this study we propose to simulate the weight and movement of the forearm with the aid of a test bench, representing the elbow joint like a simple joint with 1 DOF (degree of freedom). In function of the biomechanical model of the human elbow joint the test bench can be moved from 0 to 150 degrees [25], [71].

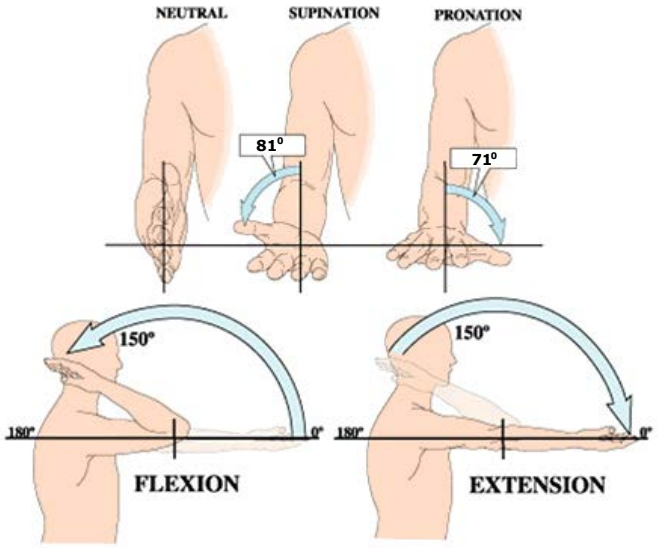


Figure 4.1: Normal range of motion for the elbow joint.

The arm and the forearm weight can be calculated for a person with 70kg weight and 1.70m height. Knowing that the arm segment has the 2.6% of the total mass, forearm has the 1.6% and the hand is the 0.7% [71], can be calculated that the arm has a weight of 1.82kg, and the forearm with the hand, has a weight of 1.61 kg (1.12 kg and 0.49 kg). The sizes were calculated according to individual height, representing the 18.6% for the arm, the 14.6% for the forearm and the 10.8% for the hand. Using these parameters the test bench (Fig. 4.2) is able to simulate the inertia of the segments. According to the test bench characteristics, the torque in the elbow joint can be calculated depending on the centre of gravity of forearm segment with the equation 4.1:

$$M = w_{forearm} * g * r_{forearm} + w_{forearm} * g * (r_{forearm} + r_{hand}) \tag{4.1}$$

where $M$ is the force moment for the elbow joint, $w_{forearm}$ is the forearm weight respectively $w_{hand}$ is the arm weight, $g$ is the gravity acceleration, and $r_{forearm}$ and $r_{hand}$ the radius from the joint to the centre of gravity of the forearm and hand segment. In function of the equation 4.1, the total necessary torque is around 1.6843Nm. This was calculated without taking into account the inertia. In function of the rehabilitation therapy, taking in account the inertia and possibility of additional charge (such a water glass) the necessary torque of the actuator need to be more than 3.5Nm. This necessary moment of force is detailed in Chapter 5.

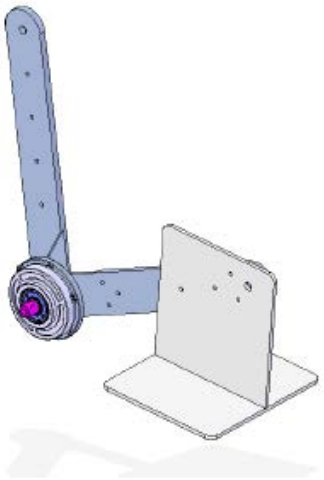

Figure 4.2: Test bench for the elbow joint simulation

**Test bench - software simulation**

The test bench was designed using a Solidworks® program which also permit to export the CAD model to Matlab®, Simmechanics®. The model of the actuator and its control have been developed in Matlab® the test bench model was exported with Simmechanics link and imported in Matlab® Simmechanics®. Thus, all the models are in the same environment for a possible assembly simulation. After the export in function of the material type, set in the CAD program, the Simmechanics® model has set the weight parameters and inertia. The Simmechanics® model is simple joint segment model, where the joint input data, in this case, was set such a torque input. The structure result in addition with the actuator model can be seen in the Fig. 4.3. The environment of simulation permits to connect with new Simulink models and dispose of a graphic interface where the model can be seen.

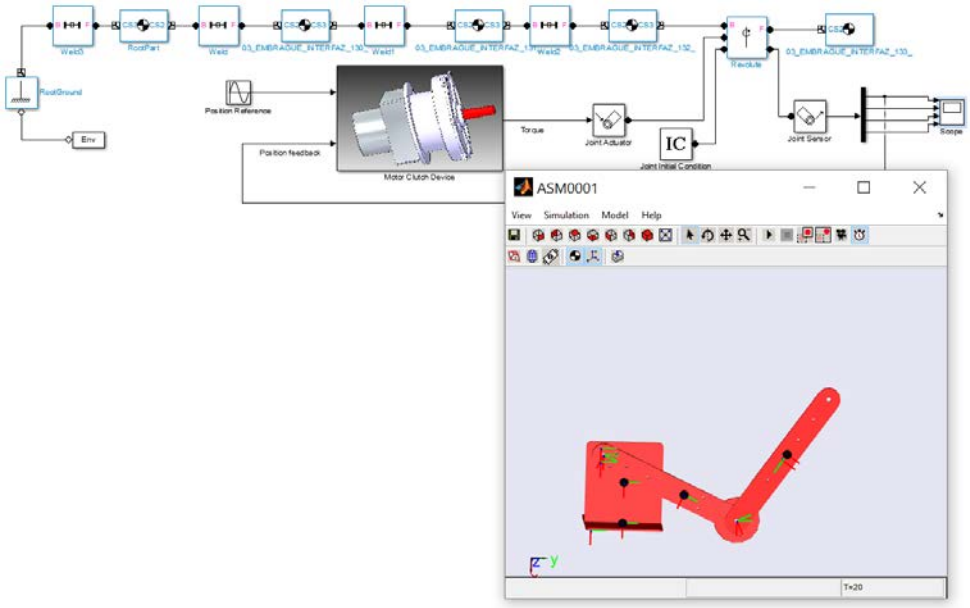


Figure 4.3: Test bench model in Simmechanics

### 4.1.2 USR60-E3NT

In function of the requirements, such as necessary total torque in the elbow joint (from equation 4.1,[72] and [73] ), velocity, the size and weight of the actuator a USM USR60-E3NT from the Shinsei Company was chosen. The characteristics of this actuator are presented in the table 4.1. Additional a planetary gear with the ratio of 4.3:1, was used to increase the total output torque to 4Nm. This ensemble is able to raise the forearm segment, with a maximum velocity of the 37.5rpm (225 degrees/sec). The actuator torque and the maximum velocity of this device, is classified between actuators for rehabilitation of elbow joint in flexion/extension.

The actuator incorporates a Avago incremental encoder with a resolution of 1024 counts per revolution and additionally in the output shaft was placed an absolute Hall effect encoder (as5045) with a resolution of 0.0879 degrees from Austrian microsystem Company. The driver of the USM is the original given by the manufacturer, named D6060/24V.

One of the characteristics of this type of motor is the holding torque with 1Nm without the planetary gear and 4Nm with the planetary gear. This becomes a problem when involuntary muscle contraction or spasms appear during rehabilitation sessions.

Table 4.1: USR60-E3NT [2]

| | |
|---|---|
| Drive Frequency | 40 [KHz] - 45 [KHz] |
| Drive Voltage | 130 [Vrms] |
| Rated Output | 5.0 [W] |
| Maximum Output | 10.0 [W] |
| Rated Speed | 100 [rpm] |
| Maximum Speed | 150 [rpm] |
| Rated Torque | 0,5 [Nm] (5,0[kgcm]) |
| Maximum Torque | 1,0 [Nm] (10,0 [kgcm]) |
| Holding Torque | 1,0 [Nm] (10,0 [kgcm]) |
| Response | Less than 1 [ms] (No-load) |
| Direction of Rotation | CW, CCW |
| Operational Temperature Range | -10 [°C] - +55 [°C] |
| Temperature Limit | Surface of Stator 70 [°C], Surface of Case 60 [°C] |
| Operational Humidity Range | 0 +45 [%] (without condensation) |
| Endurance Time | 1,000 [Hours] (Sum of the time when the motor actually moved) |
| Weight | 272 [g] |
| Resolution of Encoder | 1,000 [p/r] |

### 4.1.3 Magnetorheological clutch

The system must be able to release the elbow joint instantly when involuntary muscle contraction happen. For this reason a magnetorheological clutch was developed. The clutch design consists of a cylinder representing the housing part of the clutch, which is connected to the input shaft. Inside, there is a central disc close to the wall part (housing part), and connected to the output shaft. The space between the disk and the housing is filled with magnetorheological fluid (MR), formed by many micrometer-sized particles, which can be polarized in order to change the viscosity of the whole fluid depending on the intensity of the magnetic field they are exposed to. The proposed design of the clutch is shown in Fig. 4.4. The torque on the output shaft is obtained from the movement of the input shaft and transmitted by the fluid.

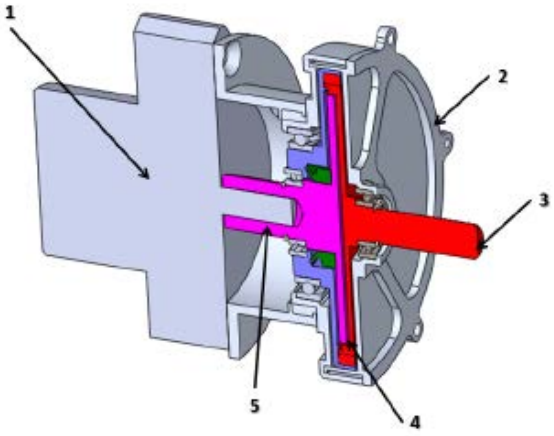


Figure 4.4: Crossection of the proposed actuator. 1. Motor and planetary gear 2. Clutch housing 3. The output shaft 4. Free space for magnetorheological fluid 5. Input shaft.

The transmitted torque on the output shaft, for a variable number of inner disks (n-disk) is calculated using the equations (4.2)-(4.4). This n-disk property is the main difference with the one presented in [74].

In order to simplify the calculations, some modifications are done considering that approximately 95% of the inner disk area is effective in terms of the transmitted torque on the output shaft.

$$\frac{T_d}{n-1} = \frac{\pi\eta \cdot |\Delta\omega|}{h_d}(R_2^4 - R_1^4) + \frac{4}{3}\pi(R_2^3 - R_1^3)\tau_B \tag{4.2}$$

$$T_h = \frac{\pi\eta \cdot |\Delta\omega|}{h_h} \cdot R_2^4 + \frac{4}{3}\pi \cdot R_2^3 \cdot \tau_B \tag{4.3}$$

$$T_{tot} = T_d + T_h \tag{4.4}$$

In equations (4.2)-(4.4), the calculation is divided in two parts.

1. $T_d$ is the term corresponding to the transmitted torque due to the inner disks, and $T_h$ is refers to the housing part. The total sum depends also on the number of inner disks $n$.

   In the expressions above, $\eta$ is the fluid viscosity with no magnetic field applied, and it is assumed to be a constant value of $0.3Pa \cdot s$.

2. $|\Delta\omega|$ is the relative rotational speed between both, input and output shafts.

3. $h_d$ is the separation between two consecutive inner disks, and $h_h$ is the separation between the closer inner disk to the housing part.

4. $R_2$ is the inner disk radio, while $R_1$ is the shaft radio that connects them.

5. $\tau_B$ is the yield stress of the fluid, for the applied magnetic field. This variable parameter in function of the magnetic field offers the possibility to control the transmitted torque or the fully release of the elbow joint in the necessary case. From now on, it is assumed that the fluid, when magnetized, is always at the same level. Therefore this value is approximated to a constant, that for the rest of the calculations is assumed to be $5 \cdot 10^4 Pa$ (Fig. 4.5).

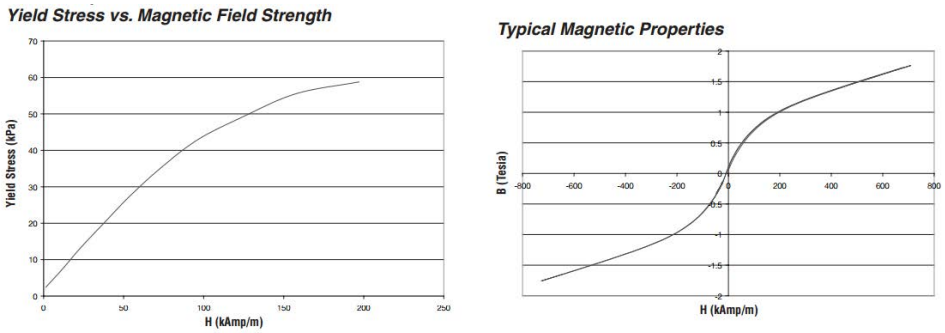


Figure 4.5: Cross-section of the proposed actuator

In function of the equations (4.2)-(4.4), and the required torque in the elbow joint (approximately 3.5 Nm), the proposed clutch was calculated to transmit a maximum torque of 8Nm.

## 4.2 USM USR60-E3NT model

To overcome the drawbacks of the behaviour of the USMs, the design of specific control algorithms that try to improve their performance will be required. The first step in developing these control algorithms is to have a good system model that allows us to reliably simulate their behaviour.

In the first place, it must be taken into account that the behaviour of the USM is highly non-linear so it is necessary to resort to techniques of identification of non-linear systems. Due to the complexity of the mathematical model of this type of motors, most of the controllers have been made based on the acquisition of input/output data, in most cases with a black box model.

As a function of the system behaviour and the simplicity of the method, in the work presented here has chosen a non-linear parametric model of Hammerstein-Wiener type black box [24]. This model is based on a combination of a linear system and non-linear systems with a transparent relationship between them, which makes it easier to implement than other non-linear methods such as neural network or Volterra series.

The Hammerstein-Wiener models have been used in model identification of electro-mechanical systems and components of radio frequency, audio and voice processing and predictive control of chemical processes. They are popular because of their representation in the form of blocks, their transparent relationship with linear systems and the ease of implementing them in comparison with other non-linear models (such as neural networks or Volterra models).

For the identification process a Matlab toolbox called "System Identification" was used. This powerful tool gives the possibility to check various models very fast and easy. The basic structure of this process can be seen in the figure 4.6.

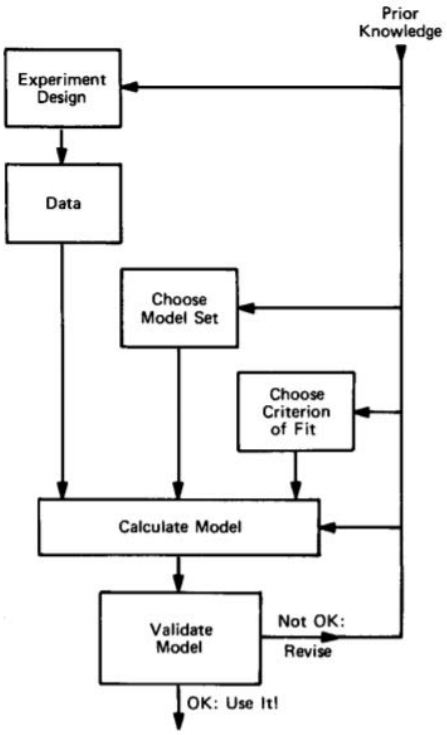


Figure 4.6: The system identification loop [24]

### 4.2.1 Structure of Hammerstein-Wiener model

The block structure of the Hammerstein-Wiener model can be seen in Fig. 4.7


Figure 4.7: Structure of Hammerstein-Wiener model

where [75]:

- $w(t) = f(u(t))$ is a non-linear function transforming input data $u(t)$. $w(t)$ has the same dimension as $u(t)$.
- $x(t) = (B = F)w(t)$ is a linear transfer function. $x(t)$ has the same dimension as $y(t)$. $B$ and $F$ are similar to polynomials in the linear Output-Error model.
- $y(t) = h(x(t))$ is a non-linear function that maps the output of the linear block to the system output.

The structure of the Hammerstein Wiener model is composed of two nonlinear models and one linear model. The first one, $w(t) = f(u(t))$, is computed from the input data. This term represents an input non-linearity, a static function, where the value given in time $t$ depends on the input value in time $t$. The second block represents a linear transfer function $x(t) = (B = F)w(t)$. In this case, the transfer function $(B = F)$ can be configured specifying the order of the numerator B as well as the order of the denominator F. The non-linear output block is represented using a non-linear function $y(t) = h(x(t))$. Similar to the input non-linear function, the output non-linear function is a static function.

The USM model has been obtained in function of the input signal represented by the voltage (control signal) and the output signal the velocity of the engine.

### 4.2.2 Data acquisition hardware

The hardware used in the data acquisition consist of the USM and its driver presented in the subsection 4.1.2, the relative encoder AVAGO heds-5540 with a resolution of 1024 counts per revolution which measures the velocity of the motor and the absolute encoder with 12 bits resolution for the position measurement.

In this work a control hardware is based on a 32 bits microcontroller STM32F4 from STMicroelectronics® which can be fully programmed with Matlab/Simulink® [76].

### 4.2.3 Data acquisition software

The input signal for the system has been chosen based on the method of identification and the behaviour of the USM. Depending on the method of identification, a discrete signal with a sampling time of 0.5 ms and a stepped form is required. The sampling time chosen, allows greater precision of the output signal due to the greater acquisition of data per unit of time. On the other hand, in function of the behaviour of the USM the input signal should be able to reach all possible speed levels and be able to identify the hysteresis phenomenon that appears through the friction between the stator and rotor. Based on these requirements, the following signal has been proposed (Fig. 4.8):

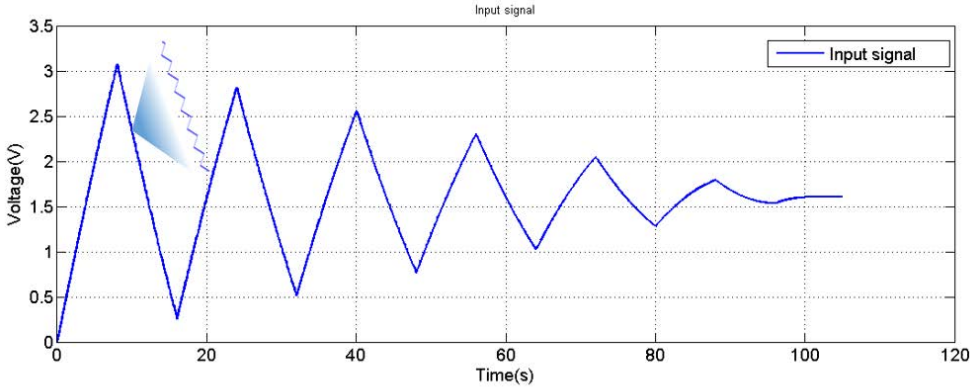


Figure 4.8: Input signal for USM identification.

The input signal (represented by the control signal from the driver between 0 and 3.2V), is capable to generate the entire range of velocity for the USM. This includes the controlled velocity, specified by the maker between 90 and 900 degrees per seconds with the control signal between 0.25 to 2.7V. With a voltage of 1.6V the motor is forced to maintain a constant velocity where can be detected small oscillations around an average value. In addition, in Fig. 4.8, is presented a zoom of the input signal, which is composed of the little steps which represent a specific signals for systems identification.

The data acquisition program using the hardware described in subsection 4.2.2, was entire build in two programs. The first one runs on the microcontroller and the other one runs on PC to connect with the microcontroller and saves the necessary data.

In Fig. 4.9 is represented the Simulink program which run in the microcontroller. Here were configured the microcontroller architecture (Setup System block), the periphery ports ( SPI master and Incremental Quadrature blocks for absolute encoder respectively relative encoder), the necessary signals for the control driver (analog and

digital ports) and receive and send data blocks to the PC. The sampling time was set at 0.5 ms.

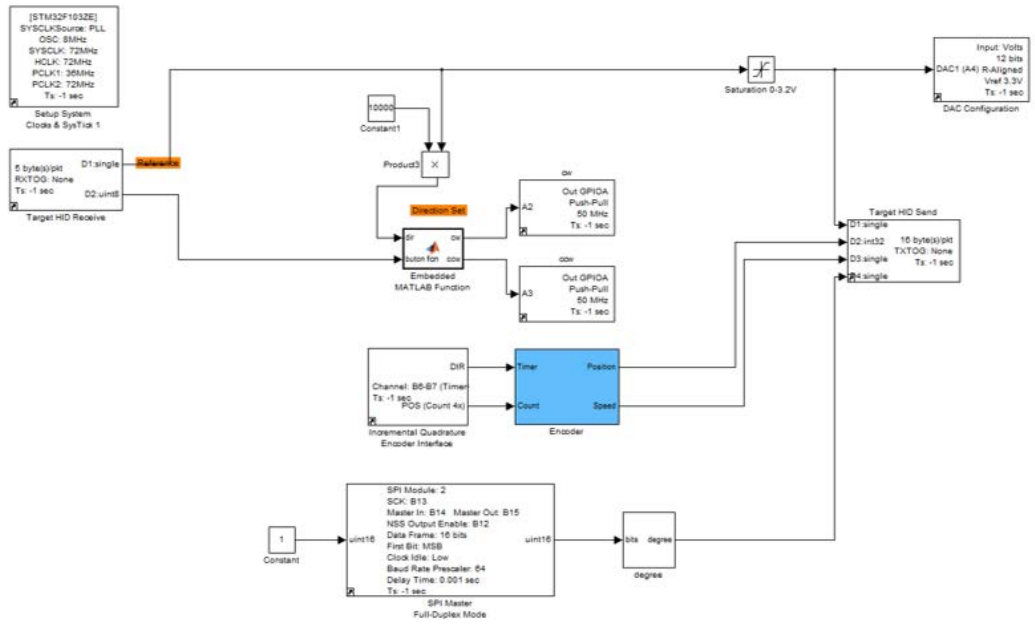


Figure 4.9: Microcontroller Simulink® program.

In Fig, 4.10 is represented the program which runs on the PC and receives the data from the microcontroller. This program generates the input signal for the USM and saves the input (control signal) and output data (position and velocity of the motor).

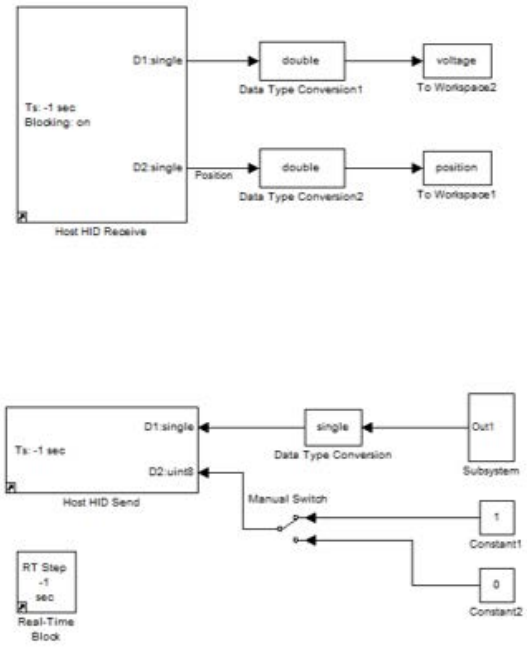


Figure 4.10: PC Simulink® program.

The experimental data used in the motor identification was the input signal represented by the control signal and the output signal represented by the velocity of the motor. The output signal, before used in the identification process was filtered with a low pass filter, eliminating the trends and the means of the signal. Also, the encoder noise was reduced using this filter.

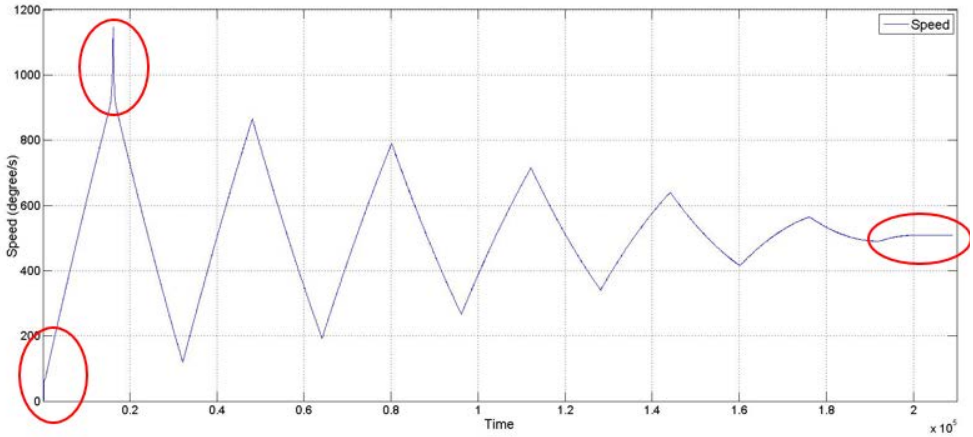


Figure 4.11: Motor velocity

In Fig. 4.11 is represented the velocity of the motor in front of the input signal. Between 0-90 degrees/second and between 900-1200 degrees/second (circled area in Figure) the USM has a different behaviour compared with the range 90-900 degrees/second. In function of this behavior, for a better identification of the model, has been proposed an identification by regions. The first region between 0 to 90 degrees/second, another from 90 to 900 degrees/second and the last one from 900 to 1200 degrees/second. The final model is a black box consisting of these three models.

For a better identification of the intervals 0-90 and 900-1200 degrees/second, a separate identification with stepped signals has been done. The input/output signal used in identification can be seen in the Fig. 4.12. Here are presented the four types of input signals which were used in the identification: two signals with low voltage level for the interval 0-90 degrees/second identification (one for identification and another one for validation) and others two for the interval 900-1200 degrees/second.

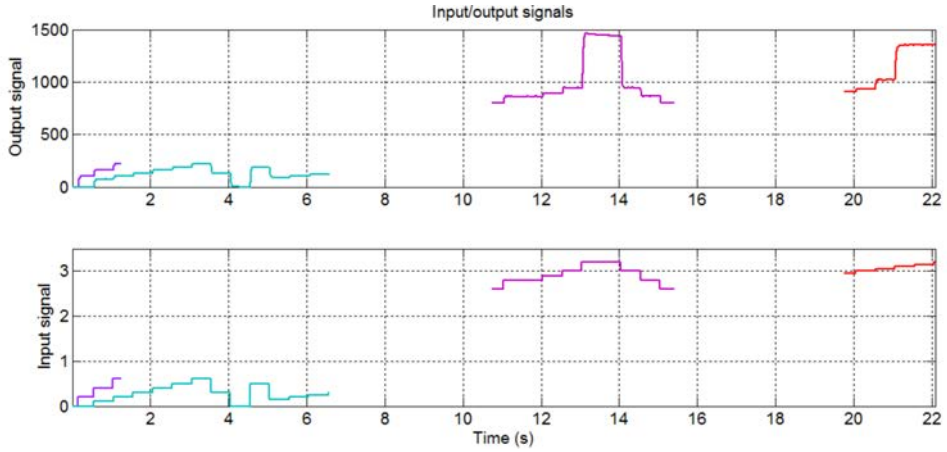


Figure 4.12: Input/output signals

The identification was based on the Hammerstein Wiener model. For the interval 90-900 degrees/second, have been used a non-lineal estimator based on the wavenet model with 28 units. The lineal block is a three order transfer function. The last non-lineal estimator is represented by a pwlinear with 10 units. The selection of this configuration has been done in function of the input/output signal and the priori knowledge.

Comparison between real output data (velocity of the USM) and the estimated output data (estimation velocity output) can be seen in the Figure 4.13. The precision of the resulted model was approximately $91,78\%$.

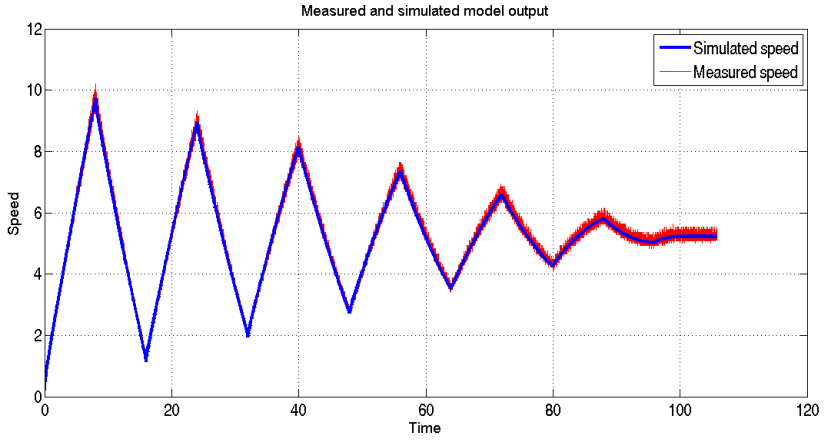


Figure 4.13: Measured and simulated velocity of the USM

## 4.3 USM control algorithm

In the last decade, various publications demonstrate that the USM can be controlled with: PI control models in speed, position or torque [77] [78], fuzzy models [79], [80], models based on neural networks, or a combination thereof.

In this work, a cascade control model was designed, with two control loops for angular velocity, and angular position, each one with its own PI controller in function of the equation 4.5. The primary loop is represented by the position controller (master) and the second loop (intern) is composed from a feed forward controller in parallel with the secondary controller in velocity. Using this type of control, has the possibility to control the actuator in position and velocity at the same time. This condition to control the actuator in position and velocity are primordial in rehabilitation therapies. For this reason a cascade control is the more adequate choice to control independently position and velocity (limiting the velocity) for the USM.

$$Y = k_p e(k) + k_i \int_0^k e(\tau) d\tau \tag{4.5}$$

where $Y$ is the controller output signal (velocity respectively voltage ) , $k_p$ is the proportional gain, $k_i$ is the integral gain and $e(k)$ is the error between the reference and the output. The parameters of the PI controllers are presented in the Table 4.2. These parameters are obtained over simulation model with the aid of PID tuning tool of Matlab/Simulink®.

The cascade control systems are more complex than single-measurement controllers, requiring twice as much tuning. Then again, the tuning procedure is fairly straightforward: tune the secondary controller first and after the primary controller

Table 4.2: Cascade PI Controllers gains

| Gain | Kp | Ki |
|---|---|---|
| Velocity controller value | 0.02 | 0.0001 |
| Position controller value | 1.5 | 0.001 |

using the same tuning tools applicable to single-measurement controllers. The feed forward controller is based on the USM voltage-rotational speed characteristics presented in [2].

The proposed control scheme consists of a relatively simple algorithm that meets the objectives, with an error in the position angle of 0.08 degrees and a low computational power use. The control scheme is shown in Figure 4.14. The control algorithm was developed in Matlab/Simulink® and has been calibrated with the necessary PID gains in the simulation, and tested in the test bench.

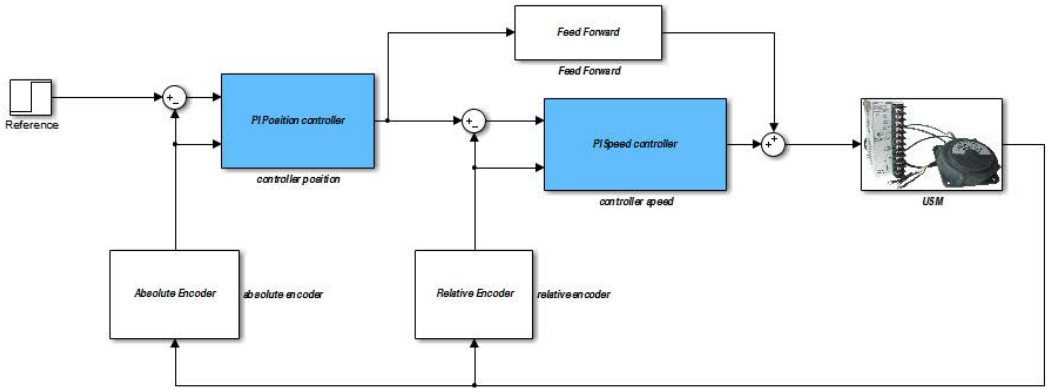


Figure 4.14: Control algorithm for USM based actuator

The control scheme uses the signals of two encoders: a relative encoder, positioned on the shaft of the motor to measure the actual speed of the actuator and one absolute encoder positioned on the shaft of the gear, to operate at lower speed and to calculate the real arm position.

### 4.3.1 USM based actuator control results

The operation of the USM is analysed with several experiments to check the correct performance of the prototype. Firstly, the actuator control algorithm was calibrated

and tested in the simulation environment and after that was implemented in the real plant. The real and the simulation model of the system it can be seen in Figure 4.15.

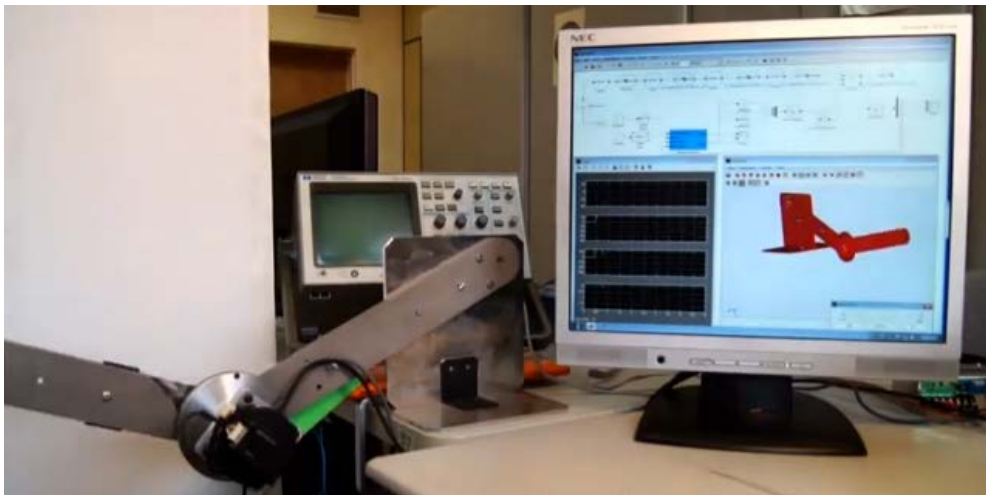

Figure 4.15: Real system and simulation environment

The USM answer in the test bench can be seen in Figure 4.16. The structure of the first device actuator tested is composed of the USM and the planetary gear. Due to the planetary gear tolerance, the error of control in position increases up to 0.7 degrees. In this case, the motor must follow the reference signal in position with a constant speed.

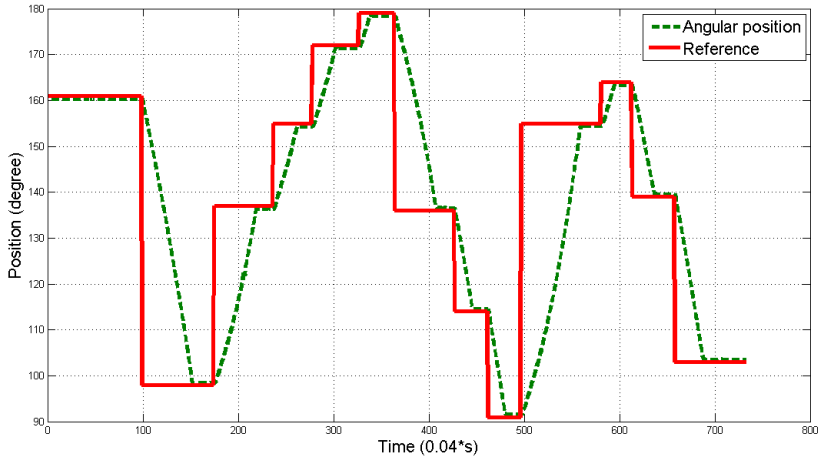


Figure 4.16: USM response in simulation

The objective of the actuator is to move an elbow rehabilitation device, exoskeleton where its movement ( in flexion and extension) needs to have a good response to the input signal, in position with one adequate speed. In this case, the proposed algorithm is able to maintain a constant speed despite of inertia and mass of the arm. Figure 4.16 highlights the output signal, from cascade control with the reference signal in position.

The first tests of the proposed actuator in the test bench were made by magnetization of the magnetorhelogical clutch with Neodymium magnet, allowing transmitting the necessary torque 1:1 (the torque of output shaft clutch is equal with the torque of the motor). In this case, the clutch is subjected to a magnetic induction of approximately 0.8T. In the future, the necessary magnetic field will be produced by an electromagnet which will be able to provide independent control for the torque transmitted by the clutch just by changing the viscosity of the fluid.

Fig. 4.17 shows the response of the proposed actuator controlled in position when the magnetorhelogical fluid is magnetized, giving the possibility to transmit more than 5Nm. In this case, the USM has a constant speed of 200 degrees/second.

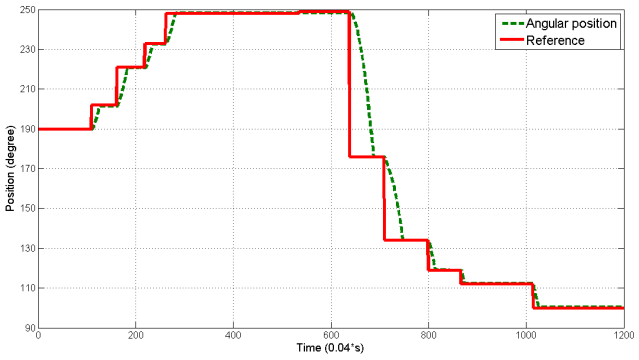


Figure 4.17: USM response with magnetized clutch

As can be observed in Fig.4.17, the clutch doesn't change the performance of the control algorithm, the skating effect doesn't appear for the inner disk.

Fig. 4.18 shows the actuator's response to a step input reference where the clutch is not subjected to a magnetic field. In this case, the inner disk of the clutch skates leaving the output shaft of the actuator free. Then, the torque transmitted is close to $0Nm$. This test highlights the capacity of the actuator to leave free the forearm when the clutch is not subjected to any magnetic field.

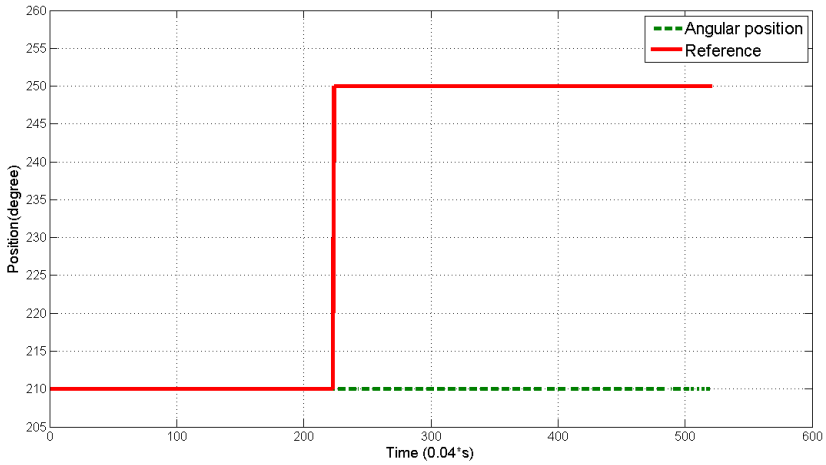


Figure 4.18: USM response without magnetized clutch

The results validate the USM based actuator to be used in the rehabilitation device where less than 4Nm torque is needed. However, it should be taken into account that for the elbow joint the actuator, has the necessary torque to mobilize the joint with little forces of perturbation, such a water glass, but not forces over 10N in the hand where the weight of rehabilitation device is included.

The proposed actuator has a lower weight than the conventional actuators, and together with the magnetorhelogical clutch, compared with the current solution, it offers the possibility to release the joint free in milliseconds.

## 4.4 SMA based actuator

The structure of the SMA based actuator, initialy was proposed by Villoslada *et al.*[81]. In this work a modified version of this actuator is presented. Based on this, various tests argue choosing an appropriate configuration of this actuator which can be used in rehabilitation devices. Similar to the case of the USM based actuator, a test bench where the control algorithms and the actuator is tested is needed.

### 4.4.1 SMA actuator test bench

For the SMA based actuator identification, to tests the control algorithms and different configuration of the actuator a test bench was built. The test bench allows multiple configurations for testing the SMA actuators: the SMA wire with a hanging mass attached to the non-fixed end, the SMA wire with a bias spring attached to the non-fixed end and an agonistic-antagonistic actuation with two SMA actuators.

Moreover, different devices can be installed in the test bench in order to drive them with different SMA actuators, as can be seen in Fig. 4.19. To test the developed control algorithm and for the identification process of the SMA actuator, the movable end of the actuator has been attached to a hanging mass whose weight provides the necessary force to "recuperate" the total length of the SMA wire.

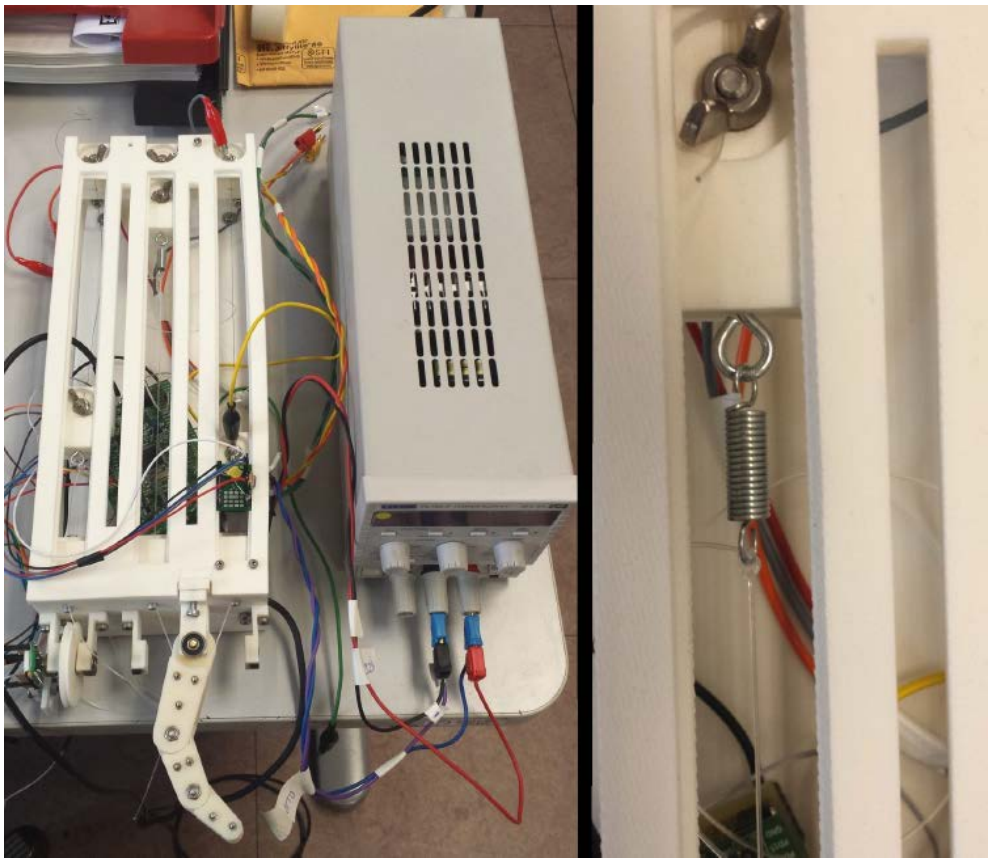

Figure 4.19: Test bench for SMA actuators (left) and detail of a restoring bias spring (right).

The test bench controller is based on a 32-bit ARM microcontroller, which is capable to provide enough computational capabilities and input/output resources to control up to 12 SMA actuators. To measure the contraction of the wire, the test bench has a magnetic linear position sensor (NSE5310 from Austriamicrosystems). One of the ends of the SMA wire is fixed to the structure of the work bench.The non fixed end is crimped to a movable part with a magnetic strip on its top. When the wire contracts the movable part is displaced and the position sensor measures the displacement of the magnetic strip. The resolution of the magnetic sensor is $0.488\mu m$.

In order to heat the SMA wire, which is necessary to activate its shape memory effect and thus contract it, a controlled electric current is passed through the wire. This electric current is provided by a high fidelity commutation circuitry, driving an extremely low on resistance with a MOSFET transistor activated with a pulse width modulated (PWM) signal from the microcontroller. The power electronic hardware is optocoupled from the control unit, providing enhanced security for the user and for all connected equipment. Power is supplied by a simple AC/DC converter or by dry cell batteries.

### 4.4.2 SMA actuator model

Given the peculiarity of these SMA-based actuators, a modelling procedure that provides consistent results is to model the actuator in two parts or stages, the contraction stage and the recovery stage. This division has been done in function of the characteristics of the material, in the contraction stage the actuator requires the input signal, represented by the power supply, and in the recuperation stage the actuator doesn't present the input signal and depends on the recuperation force, diameter of the wires and ambient temperature [82].

The estimated model of the SMA actuator has been done in function of the input/output signals, using non-linear models based on Hammerstein Wiener (presented in the Section 4.2.1) and nonlinear autoregressive exogenous models (NARX) [24]. The NARX model is a dynamic recurrent neural network (the static network doesn't present feedback and delays) with feedback connections that enclose several layers of the network. Such a model can be stated algebraically as:

$$y(t) = f(y_{(t-1)}, ..., y_{(t-n)}; u_{(t-1)}, ..., u_{(t-n)}) + \epsilon_{t_{(1)}} \tag{4.6}$$

Where the output $y(t)$ is regressive to previous values of the output signal and previous values of the input signal. It is frequent to add to the NARX model an error signal, denoted in equation 4.6 by $\epsilon_t$, which is a term that can represent a necessary error or deviation so that the time series ($y(t)$ and $u(t)$) can more accurately predict the desired output for the plant being modelled.

The Fig. 4.20 shows the neural networks NARX scheme [83].

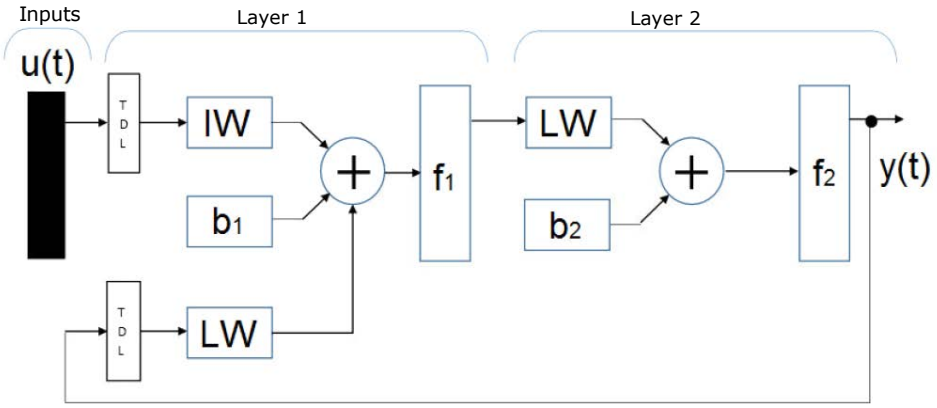


Figure 4.20: NARX, two-layer feedforward network

The identification of the SMA actuator based on these two models, require the input/output signals. In this regard, the stimulus such as an input signal was introduced to the physical systems and the behaviour of this, the output signal, was saved. The input signal, was represented by steps whose amplitude and longevity in time causes the actuator to reach about 4% of its contraction, a value that represents the maximum commonly recommended when working with this type of SMA wires. In Fig. 4.21 is represented the input and output signals over each one model is estimated. The result is presented in the right part of the same figure. The total approximation between the identified model and the real model is about 99.28%.

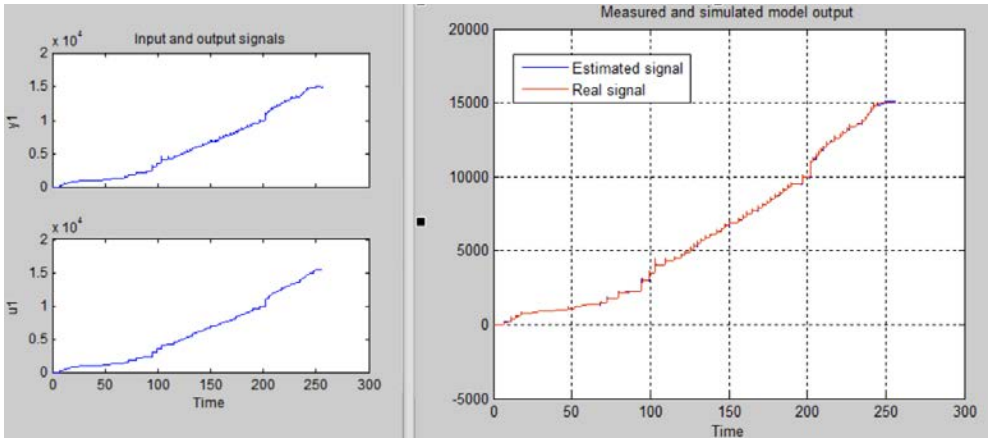


Figure 4.21: Input/output signals and estimated model

For the contraction movement of SMA, the estimation was done with different wires diameters (0,15 and 0,5 mm) and different forces of recuperation. The ambient

temperature for all the models was 19°C and the length of the actuator 23cm. The activation temperature of the used material, Nitinol, is 90°C. For each combination force - diameter of the wire and in function of the datasheet characteristics, a model was estimated, based on Hammerstein Wiener or NARX model. The final model is practically composed of a concatenation of these models.

The principal problem of this type of actuators is represented by the cooling stage, where the SMA material recuperates the initial shape. The input data in this case is missing and the actuator recovering the initial shape with the temperature changes and the and necessary force for shape recuperation, and only the output data is saved. In function of this data (without input data) its impossible to estimate a model with Hammerstein Wiener or NARX. In this case the model was estimated with the aid of the Curve fitting toolbox of Matlab. The number of the recuperation movement models estimated coincide with the number of contraction movement models.

### 4.4.3 Performance and results

With the identified model developed in the simulation program Matlab/Simulink, it is very easy to integrate it into other Matlab/Simulink programs for complex simulation. This permits to develop control algorithms based on SMA actuators for rehabilitation device and test them in simulation before testing them in the real devices, an example can be seen in Section 7.1.5.

The final SMA actuator model, implemented in MATLAB/Simulink can be seen in Fig. 4.22. This model includes a preload function which imports the black box models of the SMA actuator with different identification characteristics. The model block, which simulates the behaviour of the SMA, has a mask where the user can choose the weight necessary for the initial shape recuperation, and the diameter of the SMA wire. For this model, two SMA wires with a diameter of 0.15mm and 0.51mm respectively, with the activation temperature of 90°C, from Dynalloy [1], have been identified.

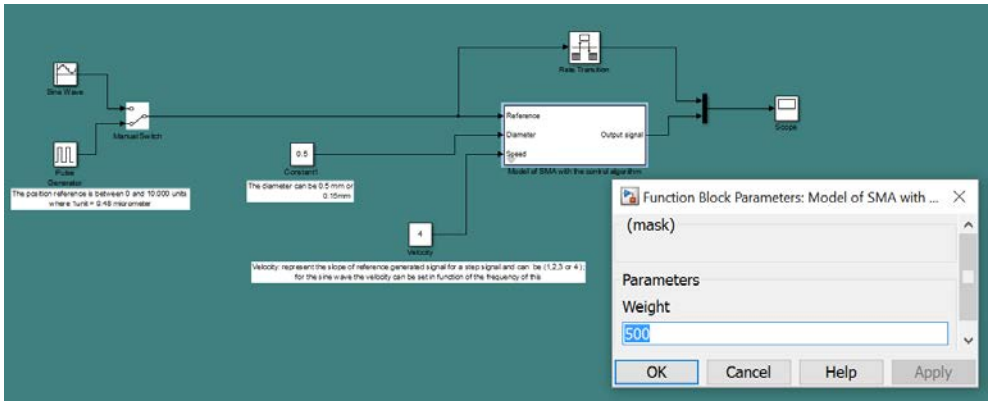


Figure 4.22: SMA model interface in Matlab/Simulink

The recovery weight (necessary force for initial position recovering) can be chosen depending on the diameter of the SMA wire between 0.1 kg and the maximum weight accepted by the wire. For example, for a wire with a diameter of 0.15mm, the value of the recovery weight goes from 0.1 kg to 0.5 kg. The results comparing the response of the simulated model and the real model can be seen in Fig. 4.23 The main parameters of the SMA tested wire are:

- Diameter: $D = 0.15mm$.
- Length: $L = 230mm$.
- Recovery mass: $m = 0.48kg$.

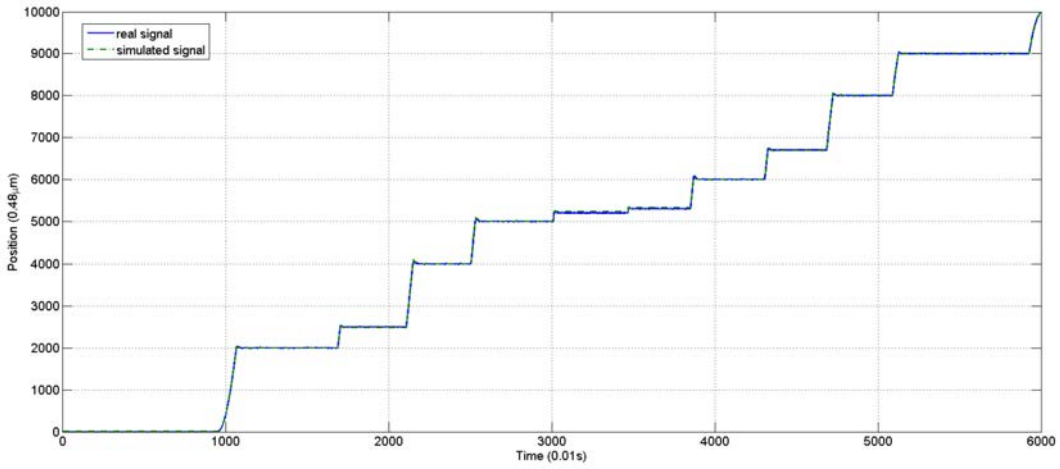


Figure 4.23: Response of SMA actuator model compared with the real response of the SMA actuator

As can be seen, the simulated model has a very similar behaviour compared to the real model, with a minimum error. The differences between the simulated model and the real model are caused mostly by friction between movable parts of the mechanical structure of the test bench. Moreover, in the cooling stage where the model is estimated due to the problem of the missing input signal, and due to the low frequency movement signal of the actuator, the simulated model is very similar with the real model response.

A second test has been performed, comparing the response of the SMA actuator model with the response of the real actuator using a SMA wire with a diameter of $D = 0.51mm$ and a recovery mass of 1 kg. The results of this test are shown in Fig. 4.24.

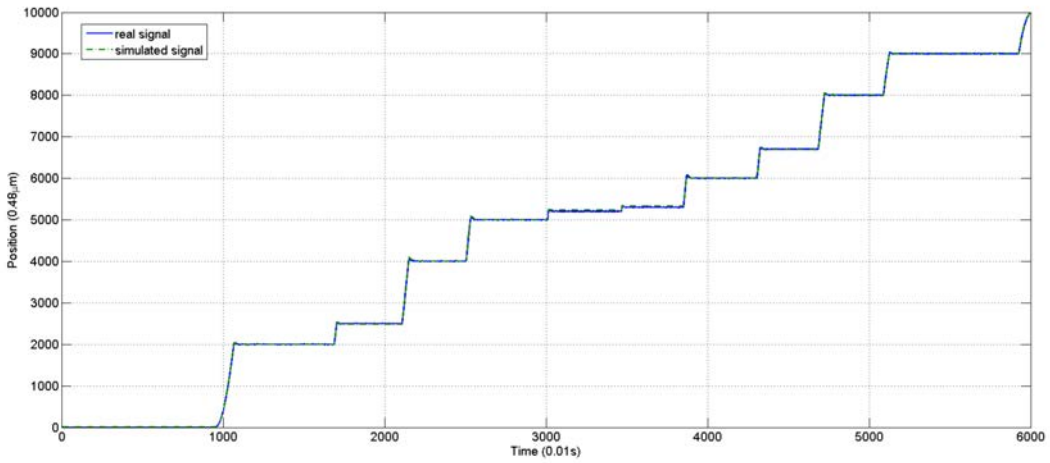


Figure 4.24: Response of the simulated SMA actuator compared with the real response of a SMA wire with $D = 0.51mm$ and a recovery force of 10N

For this second test, the error between the simulated model and the real model can be seen in Fig. 4.25. Most of the time the error does not exceed $10\mu m$. The square error for this test has been $3.59\mu m$.

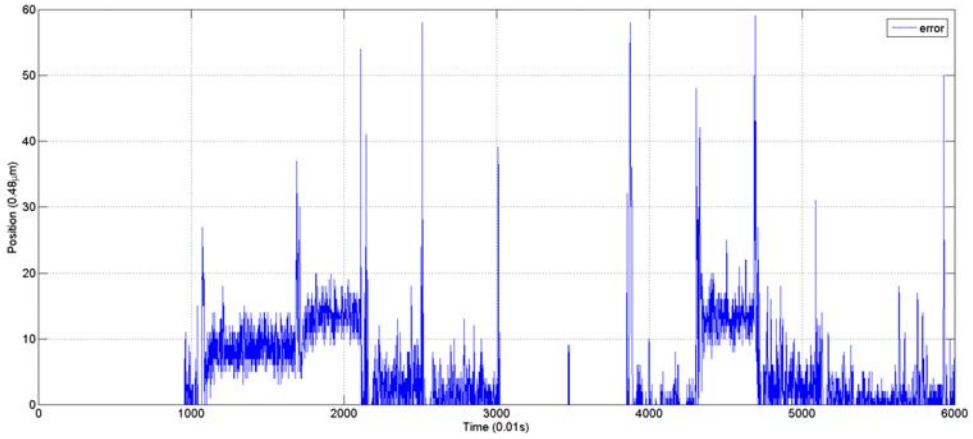


Figure 4.25: Error between the simulated model and real model

In Fig. 4.26, the response of the SMA actuator model when tracking a step position reference can be seen. When maintaining a fixed position, the behaviour of the Shape Memory Alloy presents small oscillations around the reference. This behaviour that occurs to a lesser extent in the real actuators, is exaggerated in the identified model. The closest behaviour between the identified model and the real actuator has been obtained with a 5mm reference using a SMA wire with a diameter of 0.51mm and a weight of 1 kg and a wire with a diameter of 0.15mm and a weight of 0.5 kg.

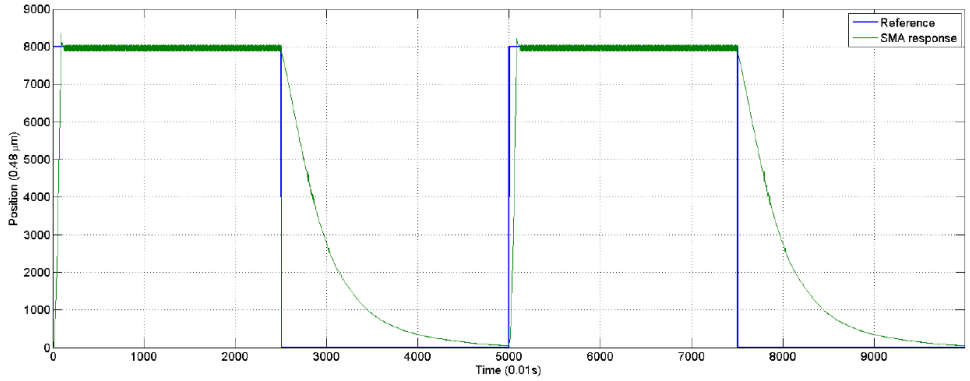


Figure 4.26: Simulated SMA response following step reference

The response of the modelled SMA actuator tracking a sine wave reference is shown in Fig. 4.27.

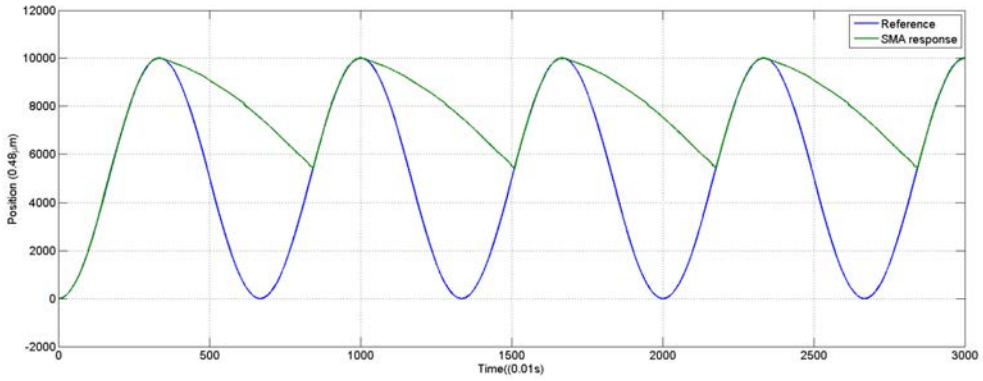


Figure 4.27: Simulated SMA response tracking a sine reference

## 4.5 Actuator design

In this work, the proposed actuator (presented and adapted from [81]) is formed by one or more SMA wires, Bowden cable, a Polytetrafluoroethylene (PTFE) tube, and the terminal parts (Fig. 4.28):

- The Bowden cable is a mechanical flexible cable which consists of a flexible inner cable that forms a metal spiral and a flexible outer nylon sheath. This type of wire can guide the SMA actuators and transmit the force. In addition, the metal has the property of dissipating the heat, which is an interesting advantage during the recovering of the initial position phase.

- The PTFE tube can work with high temperatures, more than 250°C, it is electrically isolated, and it does not cause frictions.

- The terminal units are used in one end to connect the actuator to the actuated system and, in the other one, to fix the SMA wires to the Bowden cable. They also serve as connectors for power supply (using the control signal). These units are formed by two pieces that can be screwed to each other to set the tension force of the SMA wires. The total screwed displacement of these pieces is 0.01 m.

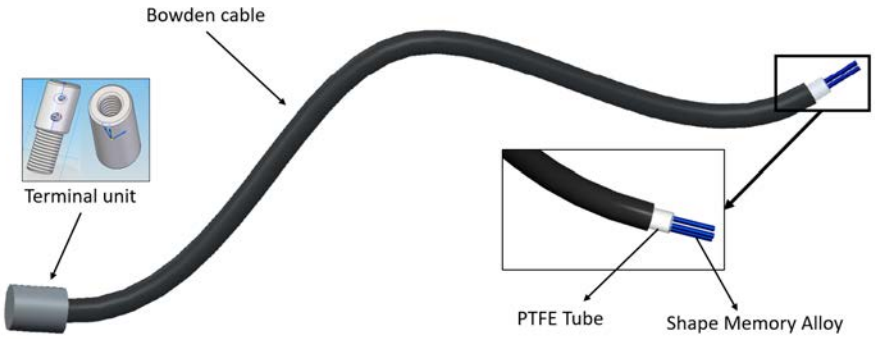


Figure 4.28: Flexible SMA based actuator.

## 4.6 Control algorithm

The main difficulty when controlling SMA - based materials is their saturated hysteretic behaviour, which appears during martensite-austenite and austenite-martensite transformations. This introduces in the system nonlinear behaviors, which makes it difficult to develop control algorithms for this type of actuator. In this work it has been chosen to ignore the effect of the large hysteresis [84].Due to this large hysteresis area a control approach based on sensorless [85] or impedance self-sensing technologies has great difficulties for precise position control (in terms of $\mu meters$) of relatively large SMA wires.

There are multiple examples of relatively simple control approaches in the literature like a PD controller [86], [87], PI controller [88], PID controller or only P controller [89]. But almost all these controllers introduce notable undesirable overshoot to the position control and/or cannot track the reference in a smooth way. Also there are developments that makes use of sofisticated control techniques ([90], [91], [92]). These control methods need a large amount of design rules and computational power in order to reach success.

Moreover, the problem is more complicated when several SMA wires are mounted in parallel and need to be controlled. In this case, various SMA wires can be mounted in parallel in the same Bowden cable or separately. They are fixed with the aid of the terminal units, which do not guarantee the same tension in each wire. Instead of controlling one wire, a sum of non-linear models with different force tensions is controlled with a single controller in this case. Different force tensions between cables cause that one SMA wire will support more force (when compared to the others),

especially at the beginning when the actuators are in their initial positions. If the difference between them is significant, the breaking of the wire is likely.

In [93], a four-term Bilinear PID (BPID) control strategy was successfully applied to control a single SMA wire. Based on this work, a PID controller with a bilinear compensator is proposed to control SMA actuators. The BPID controller is a combination of a standard linear PID controller cascaded with a bilinear compensator. The control scheme is shown in Fig. 4.29. The architecture relies on the structure proposed by Martineau *et al.* [94].

The nonlinearities of the plant limit the performance of the control loop and, applying this type of control architecture, an important advantage was obtained. In this cascaded structure, the secondary loop (bilinear term) is capable of compensating the dominant perturbation of the system. This control strategy is proposed for the control of actuators which will be presented in the next sections. The reference signal is the desired position ($y_{ref\_flex}(k)$) and the system feedback is represented by the position sensor signal ($y_{flex}(k)$), which is the real angular position of the exoskeleton.

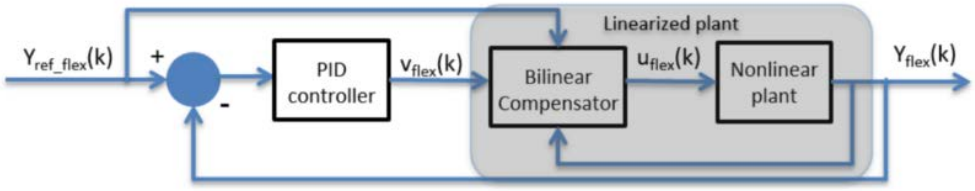


Figure 4.29: BPID control scheme.

In Fig.4.29 is presented the BPID control scheme [93] (taken and adapted from [94]). Where $y_{ref\_flex}(k)$ is the desired position, $y_{flex}(k)$ is the position sensor signal, $v_{flex}(k)$ is the control signal generated by the PID controller and the $u_{flex}(k)$ is the control signal rectified by the bilinear term.

The gains of the BPID controller were experimentally set by changing the gain values and observing the actuator response (trial and error method). The gains of the BPID are shown in Table 4.3.

The state-space representation of a continuous single-input single output (SISO) bilinear system is given by:

$$\dot{x}(t) = Ax(t) + bu(t) + u(t)Nx(t), \tag{4.7}$$

$$y(t) = Cx(t), \tag{4.8}$$

where $x \in \Re^n$ is the state vector, $u(t)$ is the input, $A$ is a $n \times n$ matrix of real values,

$b$ is a $n \times 1$ vector of real values, $C$ is a $1 \times n$ vector of real values, and $N$ is a $n \times n$ matrix of real constants with the non-linear coefficients.

The formula of the compensator that is introduced in the bilinear controller is:

$$\frac{u_{flex}(k)}{v_{flex}(k)} = \frac{1 + k_b y_{ref\_flex}(k)}{1 + k_b y_{flex}(k-1)}, \tag{4.9}$$

where $y_{ref}(k)$ is the reference output at which the PID controller was tuned. This term compensates the non-linearities of the plant. More information about how this formula is deduced can be found in [93, 94].

The PID controller is used to send a PWM current ($I$) to the actuator according to the following equation:

$$I = k_p e(k) + k_i \int_0^k e(\tau) d\tau + k_d \frac{e(k) - e(k-1)}{T_s} \tag{4.10}$$

where $I$ is a PWM current , $k_p$ is the proportional gain, $k_d$ is the derivative gain and $k_i$ is the integral gain. $e(k)$ is the error between the reference and the output.

Table 4.3: BPID Controller gains

| Gain | Kp | Kd | Ki | Kb |
|---|---|---|---|---|
| Value | 0.24 | 0.018 | 0 | 1 |

The response of the controlled system provided by the position sensors was compared to the desired reference. Fig. 4.30 shows the position desired reference and the SMA response. This was mounted and tested in the test bench presented in Section 4.4.1. It can be observed that the output follows the reference (the steady-state error is zero) and the system presents an overdamped response. The time to go from 0 to 10000 sensor units is less than 1 second, and the time required to recuperate the initial position is approximately 25 seconds and before entering in the martensite zone approximately 15 seconds.

The test was done with a SMA wire from Dynalloy Company, without Bowden tube: wire length 0.2m, wire diameter 0.51mm, ambient temperature 20°C, recuperation weight 2 kg.

## 4.7 Actuator configurations

This section presents an analysis of different actuator configurations with the objective to choose the adequate SMA based actuator for the rehabilitation device, not only in this field but also in other fields. The actuators was tested in the SMA test bench

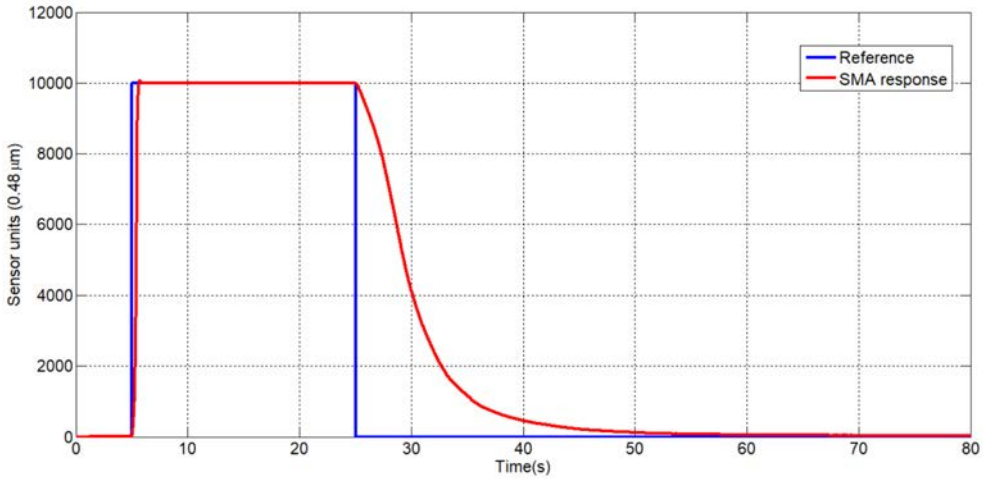


Figure 4.30: SMA position response to a step reference.

presented in Section 4.4.1, and are based on wires with 0.51mm diameter (and in some cases 0.25mm), 0.2m length and test are done at 20°C ambient temperature. The analysis is done in function of the system response over step reference of 10000 sensor units (4.88mm) and in function of the control signal. The PID parameters (4.3) will be maintained throughout the experiments, independently of the SMA diameter. The position response over the SMA controller with the same $k_p$, $k_i$, $k_d$ and $k_b$ gains, will present a different response in function of the plant dynamic (SMA actuator) where we can analyse the time response, and the controller signal giving the possibility to estimate the energy consumption of the each actuator.

### 4.7.1 Simple vs. without Bowden actuator - activation with 90°C

The simple actuator is based on SMA wire for the Dynalloy Inc. Company, which are introduced in the PTFE tube and everything in a Bowden tube. The wire diameter used in this experiment was 0.51mm. In Fig. 4.31 is presented the response of the SMA actuator with the Bowden tube and the response of the actuator without the Bowden tube, when the reference pattern is represented by a step reference with the amplitude of 10000 units of sensor. With the same PID controller parameters, the actuators responses are similar.

The actuator without Bowden cable in the heating stage presents a small amount of overshoot compared with the second case when the SMA wire is introduced in the Bowden cable. This occurs due to the better heat dissipation effect when the SMA wire is in contact with the Bowden and PTFE tube. As a consequence of this effect,

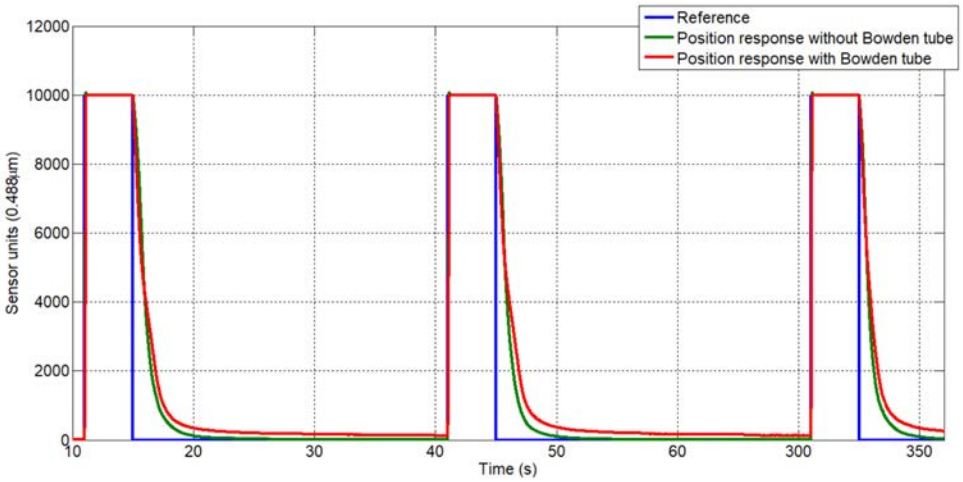


Figure 4.31: SMA of 0.51mm diameter position response with Bowden tube vs. without Bowden tube.

the actuator in the second case presents a slow response. The same effect is identified in the cooling stage, when the actuator recuperates to the initial shape. In this case, the Bowden tube helps in the cooling stage of the SMA wire (Fig.4.32).

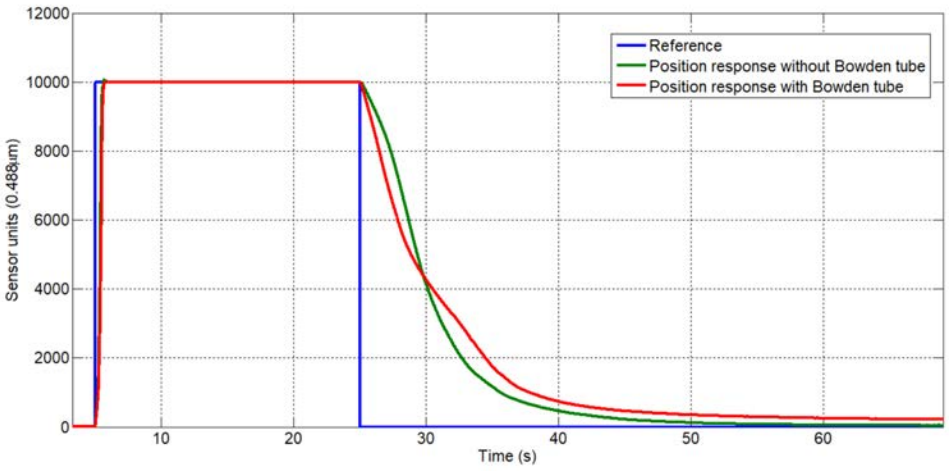


Figure 4.32: SMA actuator with Bowden tube vs. without Bowden tube (Fig. 4.31 enlarged).

Fig.4.32 presents a zoomed part from Fig. 4.31 to highlight the behaviour of the two actuators in the heating respectively cooling stage. As can be seen, the Bowden tube affects in the cooling stage accelerating the actuator initial shape recovering, the heat is transmitted from the SMA wire to the Bowden tube which aids the dissipation

of heat. This is observed in the first recuperation stage when the difference between the ambient environment and Bowden tube temperature is more elevated and the heat exchange is more accelerated. In the second stage when the temperature of the Bowden tube is closer to the ambient temperature, the SMA actuator without Bowden tube presents a better initial shape recovering, the heat exchanges directly with the environment. The Bowden tube in this stage aids to maintain the temperature and slows down the last stage of the cooling of the SMA wire.

In terms of energy consumption, the actuators can be compared in function of their control signals. In practice, the control signal has a great importance that directly affects the dynamics of the system and influences the lifespan. A control signal that easily exceeds the system input or shows oscillating pulses between high values can cause severe damage to the system. The control signal's response of the two actuators with the same PID controller parameters in front to the same reference signal (from Fig. 4.31) can be seen in the Fig. 4.33.

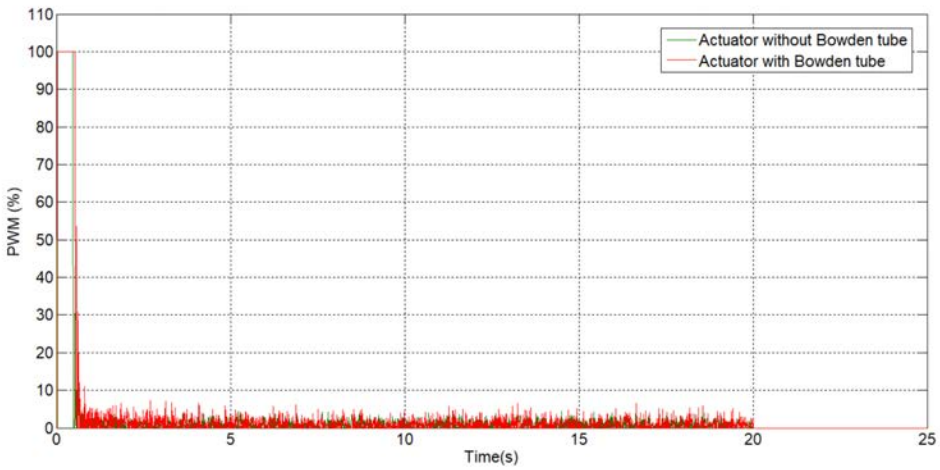


Figure 4.33: Actuators PWM signals with Bowden and without Bowden tube.

Fig. 4.33 presents the control signals of the two actuators following a step reference from 0 to 10000 sensor units and maintaining this position during 20 seconds. The control signal is approximately the same with little differences. Depending on the area of the signals which doing with the axes system observe that the actuator with Bowden tube is little great compared to without Bowden tube. The control signal is directly proportional to the energy consumption, that mean the actuator with the Bowden tube has little more energy consummation compared with the actuator without Bowden tube.

### 4.7.2 Actuator with 90°C activation vs. actuator with 70°C activation

In this section a comparison between two types of SMA wire based actuator is presented. In function of the ambient environment temperature, the candidate wires need to activate at more than 50°C, but the temperature difference between the ambient environment and the wire activation needs to be elevated to accelerate the heat exchange. On the other hand, a high temperature can cause incompatibilities with the rehabilitation devices. Between the candidate wires for the actuator are analysed the wires with the activation temperature at 90°C (high temperature), alloys NiTi from Dynalloy Inc. Company and wires with activation at 70-75°C (low temperature), alloys NiTiCu from SAES Getters [95]. The Cu element added to the NiTi alloy, introduces in the actuator a narrow hysteresis effect.

The experiment set-up is done in the SMA test bench with the wires of high and low temperature of 0.51 mm diameter. The force necessary to recuperate the initial shape in the both cases is represented by the one weight of 2 kg. The response of the two actuators, with the same controller presented in Section 4.6, is showed in Fig. 4.34.

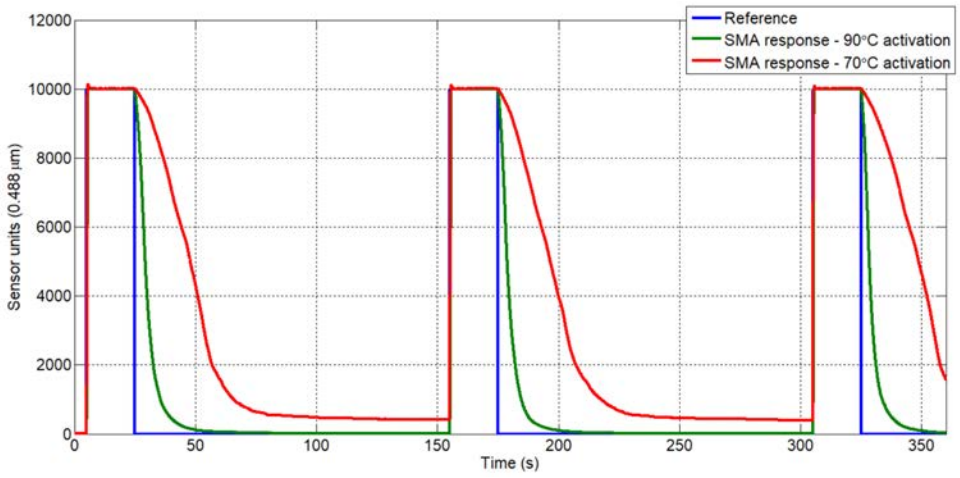


Figure 4.34: SMA actuators response: high temperature vs. low temperature.

As can be seen, in the initial shape recuperation stage the low temperature wire is much slower than the high temperature wire. The thermal transfer between the wires and the ambient environment, from 90°C to ambient temperature respectively from 70°C to ambient temperature, affects the behaviour of the actuators. In the first case, the temperature exchange is more accelerated due to the elevated temperature difference. This leads to a fast actuator initial shape recuperation and thus achieved

set-point. The low temperature wires, slows the actuator movement with approximately 20 seconds of delay compared with the actuator based on high temperature wire. Moreover, the low temperature wire is not capable to recuperate the entire initial shape, resulting in a error presented in permanent regime.

In terms of energy consumption, the PWM signals of the two actuators are compared in Fig. 4.35. The PWM signal area of the low temperature wire is less than the area of the high temperature wire, which implicates a lower energy consumption. This is largely due to the necessary temperature activation (lower) obtained with the Joule effect.

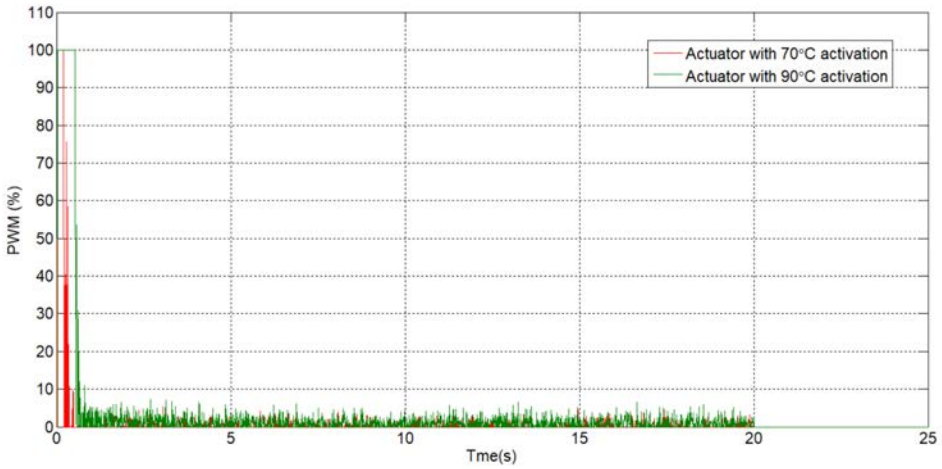


Figure 4.35: Actuators PWM signals with activation in 90°C respectively 70°C .

### 4.7.3 Simple vs. double actuator - activation with 70°C

The double actuator is composed by two or more SMA wires (always an even number), each one on a individual PTFE tube and everything in one Bowden tube (Fig. 4.36). One of the SMAs wires is connected with one end to a fixed part and another end with a terminal which is fixed to the Bowden tube (SMA terminal). Another SMA is connected with one end to the mobile weight, over which is actuated, and the other end is fixed to the other Bowden tube end. The both SMAs wires are connected to the power supply such in Fig. 4.36. Over the Joule effect, the SMAs wires contract and in the same time move the entry structure with the Bowden tube to the fixed part.

A SMA wire, in function of the Dynalloy datasheet contracts 4% of the total length. This means, for the simple actuator, after the SMA wire is heated, the total

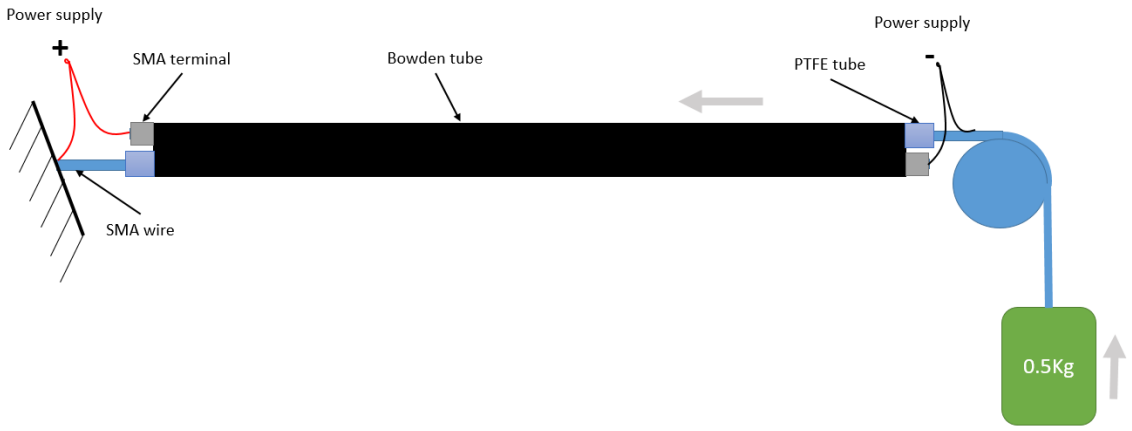


Figure 4.36: Double actuator configuration.

displacement is:

$$d_{simple} = 0.04 * l_{total} \tag{4.11}$$

and for double actuator in the same length:

$$\begin{aligned} l_{total} &= l_{SMAdouble} + 0.04 * l_{SMAdouble} \\ l_{SMAdouble} &= 0.9615 * l_{total} \\ d_{double} &= 0.9615 * l_{total} * 0.04 * 2 = 0.0769 * l_{total} \end{aligned} \tag{4.12}$$

where the $l_{total}$ is the total actuator length, $l_{SMAdouble}$ is the length of each SMA wire from the double actuator, $d_{simple}$ is the total displacement for the simple actuator and $d_{double}$ is the total displacement resulted in the double actuator.

Corresponding with equations 4.11 and 4.12, with the same actuator length the double actuator presents a displacement of 1.9225 times greater. On the other hand, the disadvantage to use this type of actuator compared with the simple actuator is to fix the extremity to a fixed structure (in the simple actuator the extremity of the SMA wire is fixed to the Bowden tube).

If the resistance of the simple actuator is $R_{simple}$, then the resistance of the double actuator can be calculate using the fowling expression:

$$R_{double} = 0.9615/2 * R_{simple} = 0.4808 * R_{simple} \tag{4.13}$$

where $R_{double}$ is the resistance of the double actuator.

The power absorbed by $R_{simple}$ is:

$$P_{simple} = U^2/R_{simple} \tag{4.14}$$

and for double actuator:

$$P_{double} = U^2/R_{double} = U^2/0.4808 * R_{simple} \tag{4.15}$$

where the $P_{double}$ is the power absorbed by the double actuator and the $U$ is the power supply voltage. From equations 4.14 and 4.15, it can be seen that the power absorbed by the double actuator is 2.0799 times greater than the simple actuator, but it obtains 1.9225 times more displacement.

The displacement results and PWM control signal for the simple and double actuator are compared in the test bench. Due to the power electronic restrictions of the test bench presented in Section 4.4.1 the tests are done with the 0.25 mm SMA wire diameter. The control parameters are the same presented in Section 4.6 and the length of the wires for the simple actuator is 0.2m. For the double actuator, the wire dimensions are calculated in function of the equation 4.12. The recuperation force, in function of the wire diameter is generated with 0.5 kg weight. The actuator's position response to a step signal reference is presented in Fig.4.37.

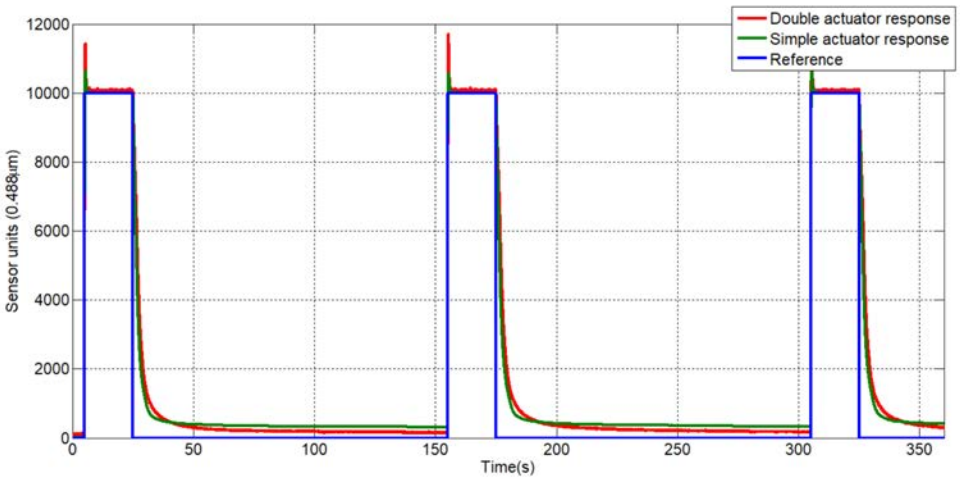


Figure 4.37: SMA double vs. simple actuators response.

In the contraction stage, the actuator's response is relatively similar, the actuators presenting an overshoot. Compared with the response of the actuators based on 0.51mm SMA wire presented in the previous sections, the overshoot presents a small electrical power consumption and the necessity to recalibrate the PID controller parameters. In the initial shape recuperation stage, the double actuator presents a small delay in the last part, due to entry in the martensite zone before the simple actuator.

The PWM control signals of both actuators is presented in Fig. 4.38. As can bee seen, the PWM controller signal generated by the double actuator presents a

relatively high peak compared with the PWM signals of the simple actuator. These high peaks can be cancelled recalibrating the PID controller.

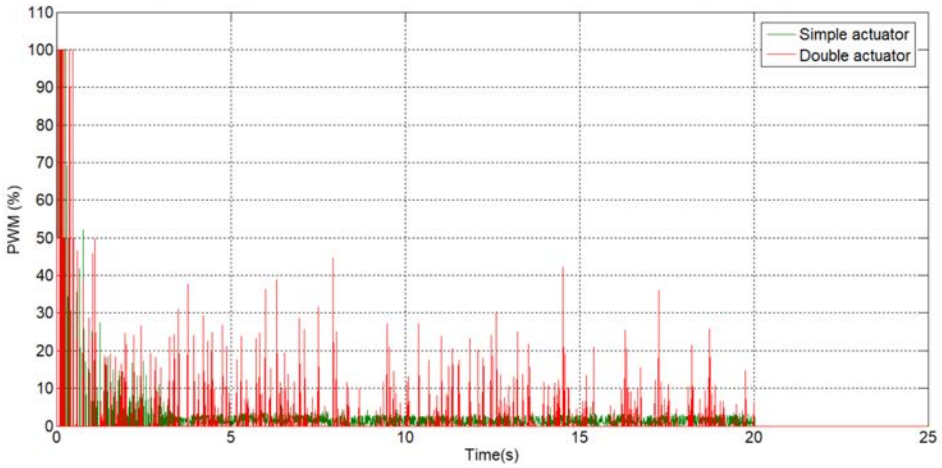


Figure 4.38: PWM control signal for double vs. simple actuator

From Fig. 4.38 is difficult to say if the simple actuator is electrically more efficient, than the double actuator, due to the big differences between the generated signals by the controller. The simple actuator PWM signal present an amplitude which oscillations in a small range during the actuation, compared with the double actuator. In this sense was calculated the average of the PWM control signals which is: 2.0696% for the simple actuator and 2.2283% for the double actuator; a relative similar power consumption. However, this result depend on the PID parameters, the desired reference and the actuation force and it is probable that double actuators have less power consumption than simple actuator in certain cases, considering that need to heat less that the simple actuator, to reach the desired reference.

### 4.7.4 Multiple SMA wires actuator

If the actuator contains multiple SMA wires, it is necessary to decide between two different configurations: all SMA wires inside on single Bowden tube with PTFE tube or a Bowden tube with PTFE tube for each SMA wire. The configuration with parallel SMA wires and a single Bowden tube has some advantages: the size of actuator is more compact; the thermal convention between the SMAs is better; the total energy that is consumed is reduced; and the actuator movement is accelerated. The disadvantage of this set-up can be observed if the cooling stage is analysed. The dissipation of thermal energy is slower, which results in a slower actuator recovery. This property can be deduced from the example presented in Fig. 4.39. This figure shows

a simulation to study the thermal convection of the actuator. This simulation has been performed using the Energy2D software, based on properties of each component: geometry, thermal, optical, mechanical and source. Here were configured parameters like dimensions, temperature coefficient, reference temperature, thermal conductivity specific heat and density. Different situations are drawn: a) Three wires in the tube at 90°C during 20 seconds; b) Three wires after cooling during 10 seconds from 90°C to ambient temperature (20°C); c) and d) represents the same processes but with a single SMA wire inserted in a smaller Bowden cable with PTFE tube. Comparing b) and d), the actuator with three SMA wires has an approximate temperature of 50°C after 10 seconds, and the actuator with one SMA wire has an approximate temperature of 30°C. With these temperatures, according to the Dynalloy characteristics [1], the actuator with three SMA wires has a 0.3% approximate strain after 10 seconds, and the actuator with one SMA wire has a 0.1% approximate strain.

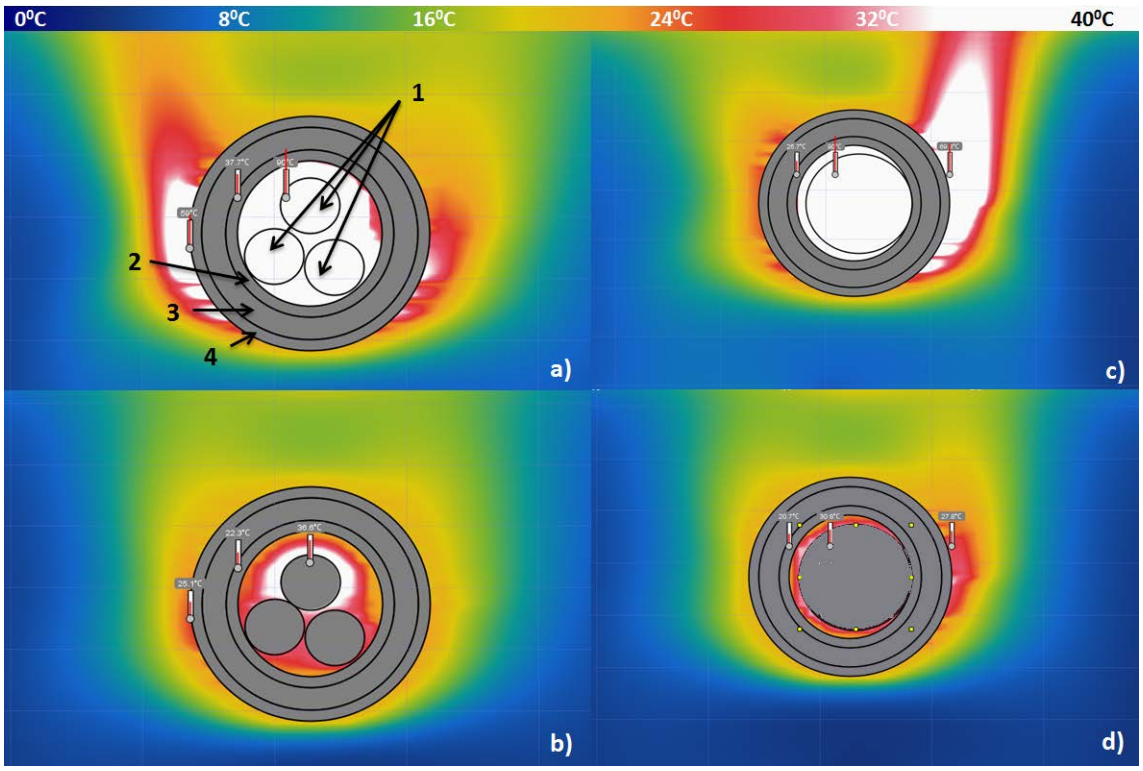


Figure 4.39: Simulation of thermal convection for different setups of the actuator.

In Fig.4.39 is presented the thermal convection for different actuator setups where: 1-SMA wires, 2-PTFE tube, 3-Metal part of the Bowden tube, 4 - Nylon part of the Bowden tube. a) 20 seconds with maximum actuation and three SMA wires. b) 10 seconds of cooling after 20 seconds with maximum actuation and three SMA wires.

c) 20 seconds with maximum actuation and one SMA wire, d) 10 seconds of cooling after 20 seconds with maximum actuation and one SMA wire.

Focusing on the rehabilitations tasks, for patient safety, the actuators are not in direct contact with the human body. They are covered by a protection tube and mounted on the back side of the human body. According to the simulation, if the actuators are contracted at maximum force and displacement during 20 seconds, the external part of the Bowden tube has an approximate temperature of 60°C (Fig. 4.39.a), which in direct contact (90°C) could be dangerous for the user. This type of actuation, maximum contraction during 20 seconds, is not common in this type of rehabilitation tasks.

Fig. 4.40(a) presents the results of real tests with the two configurations (three SMA wires in three different Bowden cables or three SMA wires in a single Bowden tube). Both options were tested with the same control algorithm in a test bench presented in Section 4.1.1 that can simulate the elbow joint of the human body for a person of 70 kilograms. The initial position of the elbow joint is 20 degrees, and the reference follows a sinusoidal pattern with a 30 degrees amplitude and a 30 degrees bias.

In Fig. 4.40(b) is presented the control signal (PWM) corresponding to the actuators response presented in Fig. 4.40(a).

As can be seen in Fig. 4.40(a), the configuration with three Bowden tubes has a slower response in the heating stage. This is caused by its better heat dissipation. This effect can also be observed in the cooling stage, where this configuration has a lower recovery time. After some cycles the difference between both configurations in the cooling stage is more evident due to the heat accumulated in the Bowden tube.

The corresponding control signals using PWM currents are given in Fig. 4.40(b). Although the peaks at the beginning are similar for both configurations (and the energy consumption, which is proportional to the PWM signal), the option with a single Bowden tube has a lower energy consumption during the displacement stage.

### 4.7.5 Gearbox 1:4

The SMA wires is considered a good candidate for rehabilitation devices but in order to mobilize the articulations large displacements are necessary if are does not want to increase the necessary forces moments. For example, for elbow rehabilitation device, with a pulley of diameter $D = 0.03m$ to pass from linear to rotational movement, for 120 degrees angular movement are necessary three SMA wires (0.51mm diameter) with approximately 1.55m of length. If the pulley diameter is reduced, the necessary torque increases and at the same time also the number of the required SMA wires. On the other hand, to maintain the necessary tension force in the SMA wires (if the wires have different tension force this cause the actuator to broke) complicates the

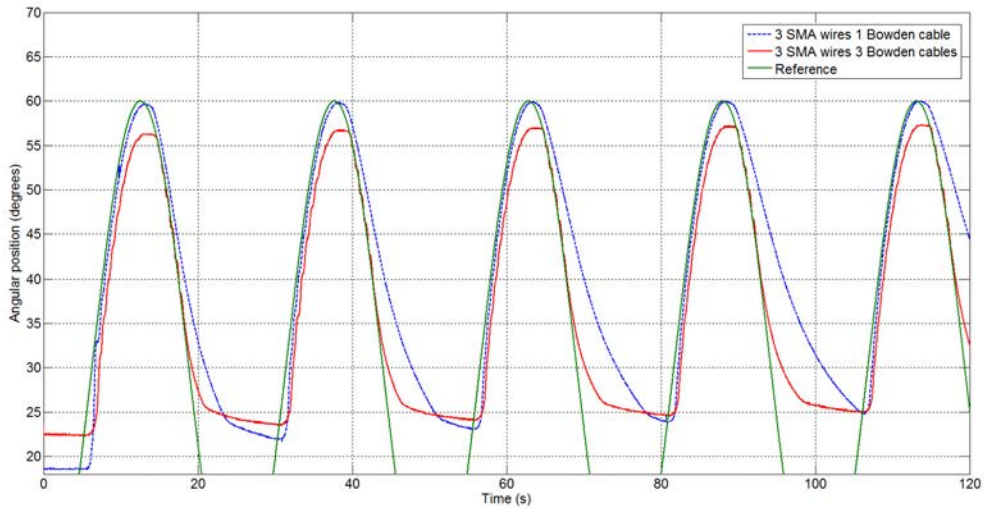


(a)

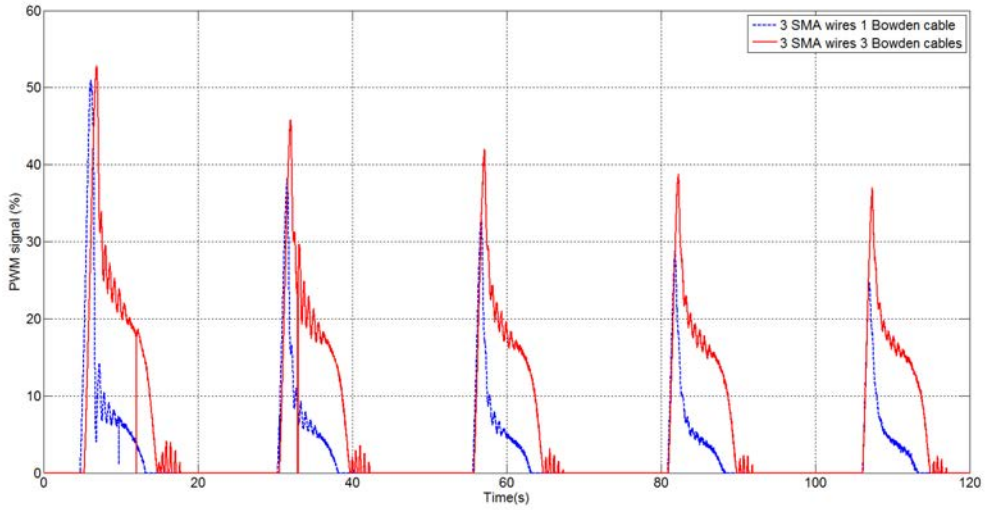


(b)

Figure 4.40: Multiple SMA wires actuator response.

system design in terms of wires installation and calibration tension force.

In this section a gearbox with 1:4 relation is proposed for multiplication of the total wire displacement. The gear is designed in function of the elbow necessary torque mobilization (approximately 3.5 Nm) and the necessary displacement for 120 degrees. The proposed gearbox is composed by: the gear unit, the housing unit and the cover unit Fig. 4.41.

The gear unit is composed by three pulleys: two pulleys for the input movement

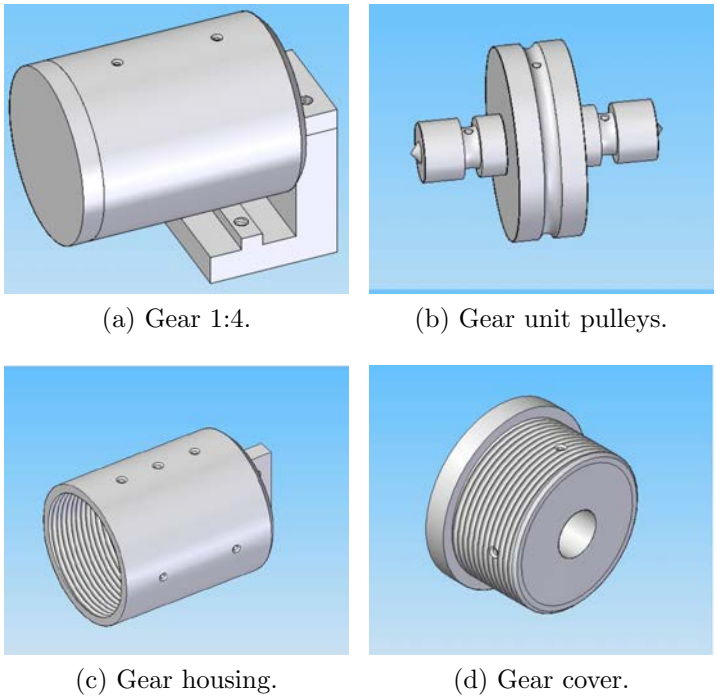

(a) Gear 1:4. (b) Gear unit pulleys.

(c) Gear housing. (d) Gear cover.

Figure 4.41: Gearbox 1:4 structure components.

where the SMA wires can be mounted (from one to five in each one) and the output movement pulley, where one cable is mounted for the output displacement. The input pulleys present a rounded channel where the SMA wires roll. It is important that the distance between the housing wall and the pulleys be less than the diameter wire, otherwise the wire goes out from the channel and can create jams. The wires are connected with the pulleys with the aid of set screws. The diameter of the input pulleys is $d_{input} = 8mm$. The output pulley is similar with the input pulleys and presents a channel with a wire (can be Nylon) which rolled in opposite sense and is fixed with a set screw. The diameter of this pulley is $D_{output} = 32mm$.

For elbow mobilization approximately 3.5Nm is needed, depending of the person weight (in this case 70 kg). If the elbow pulley has a diameter $D_{exo} = 0.06m$, without gearbox three wires of SMA (each wire with 35.6N force) are needed, which produce a total force of 106.8N and 3.204Nm torque. On the other hand, the proposed gearbox has the input pulleys with the $r_{input} = 4mm$ and the output pulley $R_{output} = 16mm$. The multiplication displacement obtained, can be calculated in function of the pulleys radius $R_{output}/r_{input} = 16/4$. In function of this relation for mobilising the elbow with this device, are necessary 12 SMA wires with length of 0.3875m.

For testing the gearbox, three SMA wires with the diameter of 0.51mm where mounted in each input pulley, and a Nylon wire to the output pulley (in actual

configuration, for the channel dimension restriction only maximum five wires in each pulley can be mounted). The response of the actuator to a sine reference and the PWM control signal can be seen in the Fig. 4.42.

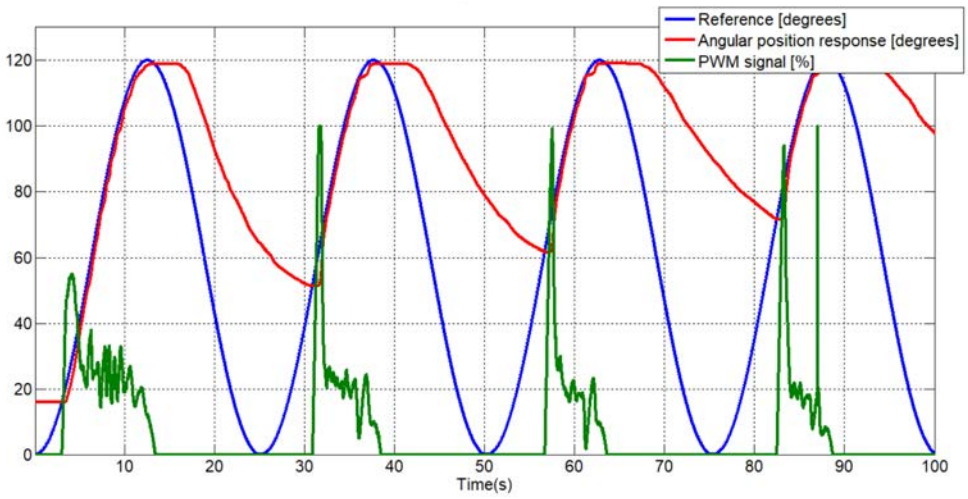


Figure 4.42: Gear 1:4 actuator response.

The actuator response with a gearbox 1:4 in the cooling stage presents a delayed response compared with others configurations. This delayed response is due to the recuperation force, in this case doing with a torsion spring, and the range of movement of the SMA wires (near to the martensite and in the martensite zone). To avoid these inconvenience the initial position can be recuperated with more weight ad for the last inconvenient a possible solution is to mount large length wires, avoiding to work in the marteniste zone and recuperating with more force.

### 4.7.6 Brake gear 1:6

The second gearbox proposed offers the possibility to multiply the displacement six times but can be configured for different relations (less - with the actual components, higher - some components need to be fabricated). In particular, this gear presents one brake which can be activated to maintain a fixed position or to control the initial shape recovering stage (after the SMA wires are cooled) with low power supply consumption. Fig. 4.43 presents the proposed actuator with the brake.

In Fig. 4.43 is presented the break actuator with the output displacement multiplied 1:6 times. In the left part a front view of the actuator where: 1- the terminal part where the SMAs wires are fixed, 2- the terminal part for the Bowden tube (this part is mobile), 3- the brake, 4- a mobile axis which presents in the middle a hole from where the output cable passes, 5- is one SMA wire which actuates the brake,

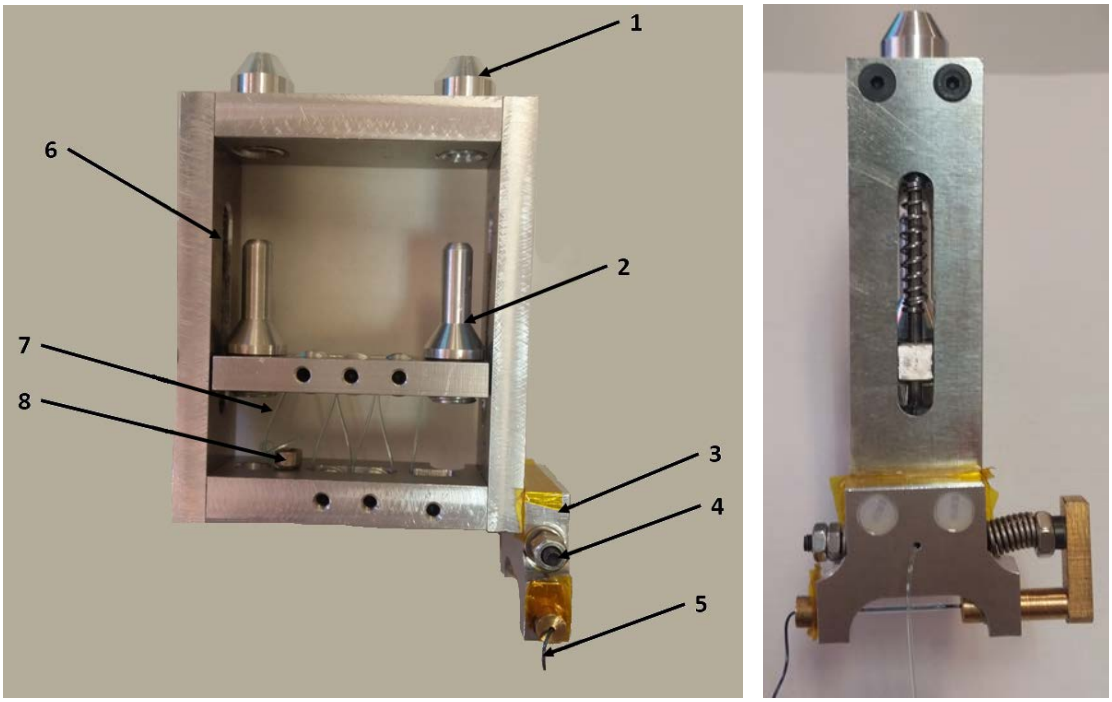


(a) Front view. (b) Lateral view.

Figure 4.43: Brake gear 1:6 actuator.

6- the axis displacement for the mobile part, 7- the output cable, and 8- the point where the output cable is fixed. The output cable gives the multiplied movement.

The SMAs wires are fixed in the actuator terminal and to the other extremity to the Bowden tube. In each Bowden tube can be mounted up to five SMA wires but always the same number of SMAs in each Bowden tube, for the force equilibrium. In the contraction stage the SMA wires actuate over the mobile part of the actuator, producing the displacement of the output wire (nylon wire) over the pulleys. The actuator presents six pulleys each one with a middle channel from the output wire pass. The distance between the pulleys walls is less than the output wire diameter, avoiding to go out from the channel and produce jams. The output pulleys of the mobile part coincide perpendicularly with the output pulleys of the fixed part. According with this, each pulley multiplied the displacement two times. Changing the number of pulleys, the multiplication rate easy can be modified. The current configuration permits to mount 10 SMA wires which give a total force around 356N. The output force with this configuration is 59.3N.

One of the actual limitations of the SMA based actuators is the electrical power consumption when this is actuated by the Joule effect. The proposed actuator

presents a brake which permits to maintain a certain position, blocking the output wire. The brake can be seen in the Fig. 4.43b. This is composed of a fixed part, attached to the actuator and electrically isolated, and a mobile part which is actuated with a SMA wire with a length of 0.025m. The fixed part has a two holes which when the mobile part is actuated are aligned with the hole of the mobile part and permit to pass the output wire. Without actuation the mobile part recuperates the position (closing the pass of the output wire) with the aid of a compressing spring. In function of this when the mobile part is not actuated the output wire is blocked maintaining the current position and reducing the electrical power consumption to 0. Others advantages are the possibility of cooling the actuators when maintaining a fixed position and to control the output position of the actuator in initial shape recuperation stage with the aid of the brake.

## 4.8 Conclusions

In this Chapter where presented the two types of actuators proposed of use them in the rehabilitation devices, for each one developing a simulation model, a test bench where the controls algorithms have been tested and analysed and the controls algorithms for each one.

The USM was identified and modelled based on Hammerstein-Wiener and NARX models able to characterize entire range of movement. In function of the identification, a control algorithm in cascade loop, capable control the motor in position and velocity, was proposed and analysed. In function of the motor characteristics and for better performance a planetary gear with a ratio of 4.3:1 and a magnetorheological clutch were introduced. In combination with these two components the actuator resulted is able to produce a maximum torque of 4Nm and release the output axes in few milliseconds.

In function of the SMA material characteristics and the main objective of this thesis an actuator based on SMA was proposed and analysed. Here a control algorithm based on BPID controller was implemented and a model of the actuator was identified (in this case together with the control algorithm) which will be used in the simulation in the follow Chapters. The performance of the identified model compared with the real behaviour of the actuator was presented. Moreover, has tested and analysed various actuator configurations based on SMA with different SMA materials, with-/without Bowden tube and different mechanical configurations. Was demonstrated that in the case of the SMA based actuator for the rehabilitation device the adequate solution is based on various SMA wires inside of the PTFE and Bowden tube.

In function of this actuators performance and human body characteristics will be chosen the adequate solution to be implemented in the rehabilitation devices.

# Chapter 5

# Biomechanical simulation for rehabilitation devices

This Chapter presents a simulation tool, which gives the possibility to analyse the interaction between the human body and the rehabilitation device. In the majority of the cases the exoskeleton forces to actuate directly over the human body causing discomfort and pain, and for this reason the human-robot interaction (HRI) is one of the principal fields of research in robotic exoskeletons technology. The physical configuration of the exoskeleton and the patient's reaction times for this rehabilitation device both play significant roles in the design of the exoskeleton.

## 5.1 Biomechanics of the human body

Biomechanics is a scientific discipline that has the objective of structuring and studying the mechanical character that exist in living things, fundamentally the human body. Biomechanics is an area of interdisciplinary knowledge that studies models, phenomena and laws that are relevant in the movement and balance (including the static) of living beings.

Centring on the upper limb (the area where the joints of interest for the proposed actuators are), the next three sections presented a brief biomechanics description of the hand and the three articulation interest articulations of interest , the shoulder, elbow and wrist.

### 5.1.1 Shoulder

The shoulder joint is the most dynamic and mobile joint in the human body. It consists of the glenohumeral, acromioclavicular, sternoclavicular, and scapulothoracic articulations and the muscular structures that act on them. These articulations give the possibility to a complex range of motion, measured in terms of flexion and extension in the sagittal plane, abduction in the coronal plane, and internal-external rotation about the long axes of the humerus. The motion of these articulations is better understood when it is analysed for separate components. A schematic depiction of the bony structures of the shoulder and their four articulations is presented in Fig. 5.1.

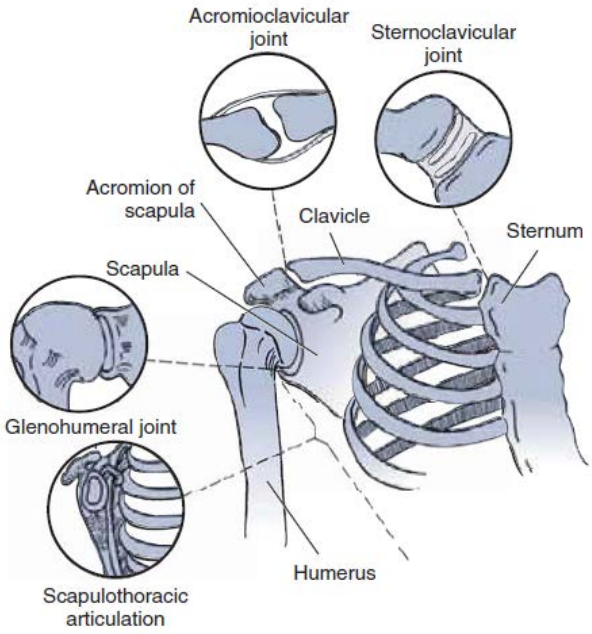


Figure 5.1: Shoulder complex (taken from [25]).

The shoulder articulation moves in three planes: sagittal (which divides the body or organs verticaly into right and left sides), frontal (divides the body or an organ into an anterior (front) portion and a posterior (rear) portion) and transvere divides the body in horizontally in the upper and lower portions. The transverse axis is horizontaly from side to side and perpendicular to the sagittal plane. This axis directs the movements of flexion and extension. The sagittal axis or anteroposterior axis is located horizontally from the front to the back and perpendicular to the frontal plane. This axis directs the movements of abduction and adduction. From the last, the vertical axis has a direction perpendicular to the ground and to the transverse plane. This directs two types of movements, the movements of abduction and adduction horizontal, and internal and external rotation.

In the shoulder movements, when the arm elevation occurs, this is composed by the two movements: glenohumeral (GH) and scapulothoracic (ST) movement. These two movements are interrelated to each other with a specific rhythm of movement called Scapulohumeral rhythm. In the literature Scapulohumeral rhythm is described like a ratio: humeral elevation: scapulothoracal rotation. The overall ratio of 2:1 during arm elevation is commonly used. According to the 2:1 ratio framework, flexion or abduction of 90 degrees in relation to the thorax would be accomplished through approximately 60 degrees of GH and 30 degrees of ST motion. In another study of Scapulohumeral rhythm between children and adults, the mean ratio for the scapular

plane was 2.4:1 for adults and 1.3:1 for children [96].

In the flexion-extension movement, the shoulder presents theoretically 180 degrees of forward elevation (flexion), but practically the average value is 167 degrees for men and 171 degrees in women. The extension or posterior elevation averages is approximately 60 degrees. To complete successfully the Activities of Daily Living (ADL) 120 degrees of flexion and 45 degrees of extension are necessary.

In the frontal plane, the abduction movement can realize 180 degrees and 45 degrees of adduction movement . In ADL 130 degrees of abduction and 15 degrees of adduction are necessary.

For the last part, in the transverse plane we find the movement of adduction and horizontal abduction, where abduction to 120 degrees and adduction to 50 degrees, and the movements of internal and external rotation, where internal rotation to 110 degrees and external rotation to 90 degrees.

### 5.1.2 Elbow

The elbow is a complex articulation, placed between the arm (humeral bone) and forearm (ulna and radius bones). It is composed by the humeroulnar and humeroradial joints (for the flexion-extension movement) and the proximal radioulnar articulation (for the pronation-supination movement). The flexion-extension movement, in the majority of the cases, has an angular range of movement between 0 and 150 degrees, but in the ADL the functional range is estimated between 30 and 120 degrees. In the pronation-supination movement, the averages are 71 degrees of pronation and 81 degrees of supination. In ADL, the total range of pronation is approximately 50 degrees and for supination 50 degrees [25],[97]. During the flexion-extension movement of the elbow joint, the center of rotation changes and this articulation cannot be truly represented as a simple hinge joint.

### 5.1.3 Wrist

The wrist or carpi is the collection of bones and tissue structures that connects the hand to the forearm. This complex set of bones, ligaments, tendons and soft tissues is able to offer a wide arc of movement that increases the function of the hand and fingers, giving it a considerable degree of stability. This joint plays a fundamental role in daily life because its kinetic functions allow the orientation of the hand with respect to the forearm, and the kinetics allow to transmit loads from the forearm to the hand and vice versa. All upper limb joints aim to position the hand so that it can perform the desired tasks, especially the wrist seems to be the key to the function of the hand. The stability of the wrist affects the ability of the fingers to flex and extend [25]. It is a complex joint made up of several joints that make the connections

between the radius bone with the metacarpal bones (radio-carpal), the ulnar-carpal (distal radio-ulnar) space and the connections between the first and second row of the carpals bones (mid-carpal). The carpal bone mass is composed of eight bones arranged in two rows of four: scaphoid, lunate, triquetrum, pisiform, trapezium, trapezoid, capitate and hamate bone.

The wrist joint presents two movements in two planes: the sagittal plane which present the movement flexion-extension (90 degrees of flexion and 85 degrees of extension) and the frontal plane which presents the ulnar and radial deviation (ulnar deviation 45 degrees and radial deviation 20 degrees). In ADL the flexion-extension movement is 15 degrees of flexion and 35 degrees of extension.

### 5.1.4 Hand

The human hand is one of more complex biomechanical parts of the human body. Its structure involves a lot of small bones, articulations, muscles, tendons, ligaments, nerves and blood vessels. The bone structure of the human hand includes eight carpal bones, five metacarpal bones, five proximal phalanges, four intermediate phalanges and five distal phalanges. The position of each bone in the structure of the human hand can be seen in Fig. 5.2.

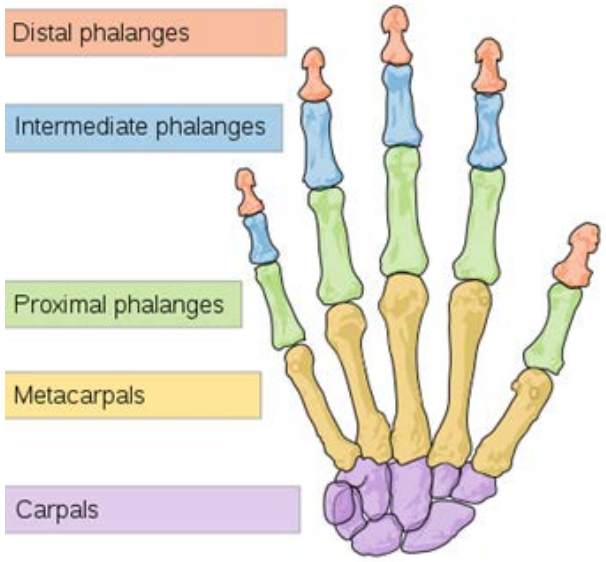


Figure 5.2: Human hand bones

The metacarpal bones connect the carpal bones with the proximal phalanges. Except the for thumb metacarpals joint (the metacarpals joints are the articulation

made between the carpals with the metacarpals bones) have a very limited range of movement compared with the rest of articulations. In this work the four metacarpal articulations for the index finger (II), middle finger (III), ring finger (IV) and little finger (V) were represented as a fixed articulation. The thumb metacarpal articulation has a large range of rotational movement. In this case this articulation was represented as one articulation with 2 degree of freedom.

The proximal phalanges are found in the continuation of the metacarpal bones for the five fingers. Together with the metacarpal bones form the metacarpo-phalangeal joints. These articulations except the thumb metacarpo-phalangeal (MCP) joint present two degree of freedom.

In the continuation of the proximal phalange for the four fingers (II, III, IV and V) we find the intermediate phalanges. The articulation formed between the proximal phalanges and the intermediate phalanges are the proximal interphalangeal joints (PIP). The final bones of the hand are the distal phalanges and with the intermediate phalanges in case of the four fingers (II, III, IV, and V) and the proximal phalanges in case of the thumb finger formed the distal interphalangeal joints (DIP).

Both models for the proximal interphalangeal joints as for the distal interphalangeal joints permit a single rotation movement, having only one degree of freedom.

Although the movement constraints depend of each person, one approach was founded in [98]. The first constraints type refers to the range movement of the four fingers. In this case this type of constraints can be represented using the following inequalities:

$$-30^\circ \leq \theta_{MCP-F} \leq 90^\circ, \tag{5.1}$$
$$0^\circ \leq \theta_{PIP} \leq 110^\circ, \tag{5.2}$$
$$-5^\circ \leq \theta_{DIP} \leq 90^\circ, \tag{5.3}$$
$$-15^\circ \leq \theta_{MCP-AA} \leq 15^\circ \tag{5.4}$$

For the thumb finger the range of movement can be represented with the below inequality:

$$-15^\circ \leq \theta_{TMC-F} \leq 90^\circ, \tag{5.5}$$
$$0^\circ \leq \theta_{MCP} \leq 75^\circ, \tag{5.6}$$
$$0^\circ \leq \theta_{IP} \leq 75^\circ, \tag{5.7}$$
$$-15^\circ \leq \theta_{TMC-AA} \leq 15^\circ \tag{5.8}$$

Other type of constraints refers to the limits imposed on the joints during the finger motion. The motion of the PIP joints and the DIP joints was related through

of the muscle group that actuates in the two articulations. This relation can be approximated with the following relation:

$$\theta_{DIP} = 2/3\theta_{PIP} \tag{5.9}$$

## 5.2 Biomechanical software simulation

Current biomechanical analyses and models do not gather sufficiently complex features for compatibility between human and robotic structures. The robotic design requires simulation tools to test mechanical structures, actuators and control algorithms with real users and without risk. This justifies the need for a complex simulation environment that allows simulation of robotic exoskeleton interaction over the human body, as well as combining the simulation of human body movements with the robotics' actuation.

There are several types of software that are capable of developing and analysing biomechanical models of the human body in inverse dynamics or forward dynamics (e.g., AnyBody® [99], MSMS® [100] [101], BoB® [102], OpenSim® and SIMM® [103], [104]). A brief comparison between some of these models was presented and analysed in Consistency Among Musculoskeletal Models: Caveat Utilitor [105].

On the other hand, Matlab-Simulink® software is widely used in engineering algorithm simulation. It provides a graphical programming language, ideal for developing control systems. Matlab-Simulink® is a system that combines a block diagram interface and temporal simulation capabilities with core numeric, graphics together with the language functionality of Matlab®. The models of the actuators proposed for this research (presented in Chapter 4) were developed in Simulink®. As the actuator models were developed in Simulink and due to the advantages and disadvantages of this type of software for musculoskeletal simulation, BoB® software was selected. All the simulation was developed and tested in the same environment, Simulink®. This environment enabled the analysis of the biomechanical behaviour of the human body, the behaviour of the exoskeleton and its actuator, taking into consideration the viscoelastic part of the human body (such as skin and human tissue) and the exoskeleton lining. The developed simulation environment was able to offer the necessary requirements for complex simulation, and to enable the development of new control algorithms for the actuators, when the exoskeleton is in direct contact with the human body.

## 5.3 Simulation components

The proposed simulation environment allows development of complex systems of control for rehabilitation of the elbow. This simulation includes: actuators, sensors, an exoskeleton, connection between the exoskeleton and the human body, and components of the human body. The simulation environment enables configuring the models of each of these components and simulating their interaction. The scheme of the proposed simulation environment can be seen in Fig.5.3. The actuator model gives the necessary torque for the exoskeleton, which will be transmitted to the human elbow through forces generated within a spring damper linkage which connects the systems. The model of the exoskeleton can be configured with the desired weight and dimension for each of the segments. The components of the human body permit simulation the human musculo-skeletal system and calculation of the motion determined by muscle activation and external forces. Each component will be presented and analysed as shown in the figure below.

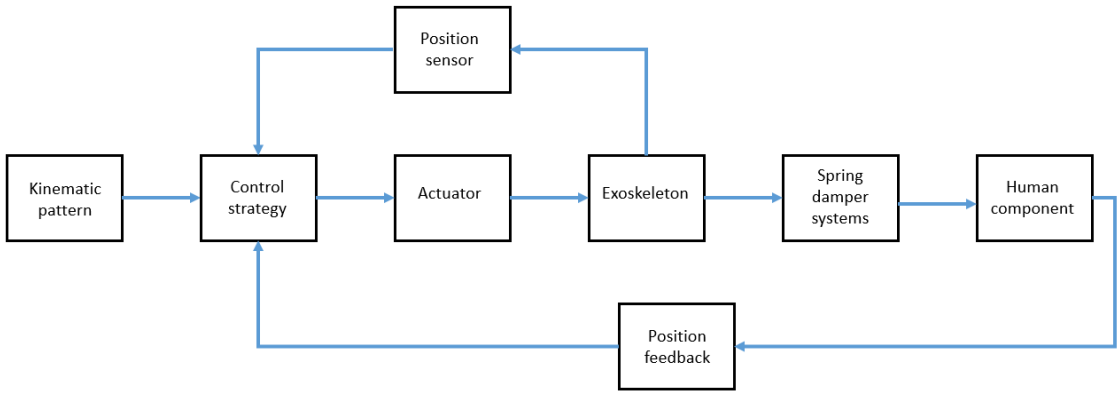


Figure 5.3: Proposed simulation environment

### 5.3.1 Biomechanics of Bodies

Biomechanics of Bodies (BoB®) is the human musculo-skeletal simulation system within Matlab/Simulink®. BoB® consists of 36 skeletal segments and 666 locomotor muscle units [106]. This was developed at Coventry University, United Kingdom, and has two versions: a version for inverse dynamic biomechanics of the human body and another version for forward dynamics of the human body. In inverse dynamics model, BoB® can calculate joint torques, muscle loading distribution and joint contact forces. In forward dynamics, model BoB® can calculate motion due to muscle activation and external forces. BoB® also has extensive post-processing and graphics capabilities.

As BoB® resides totally within the Matlab environment there is a minimal learning curve required for existing Matlab® users, making BoB® particularly suitable for teaching. Additionally, BoB® can be integrated into existing Simulink® models which requires a human component. This application was used in research projects, such as: "Calculation of Muscle Loading and Joint Contact Forces in Irish Dance" [102] [107], "Biomechanical analysis of entry, egress and loading of a passenger vehicle with rear hinged rear doors" [108] and "FES rowing biomechanics: fixed and floating stretcher ergometers" [109].

In this section the forward dynamic version was used. This model has various input ports such as the weight of the person, muscles signals, the application force in the segments (i.e. humerus force, radius force), the inertia in the segments and a signal that represents the rigid body motion (RBM) defined by the translational and rotational movement of the pelvis segment. All of these input ports enable manipulation of the model of the human body. The graphics interface of BoB is shown in Fig. 5.4.

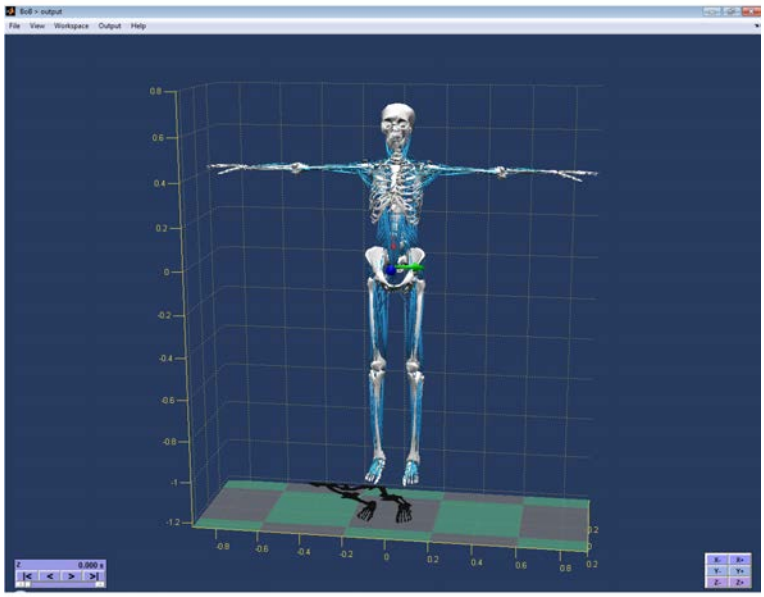

Figure 5.4: BoB interface.

### 5.3.2 Exoskeleton system

Another component of the proposed simulation consists of the exoskeleton model. The kinematic structure of the exoskeleton should consider the variability of the users' anthropometry, the range of motion of the limbs, and also the intra-subject variability of the joint center of rotations during the movements. Other parameters

which must be taken into account are the weight of the exoskeleton, albeit with a overall low inertia, interaction surface between the user and the robot (comfort), the design of the exoskeleton and the system of actuators [110]. In this section one robotic exoskeleton was designed, in order to simulate the assist behaviour of the human elbow in flexion-extension motion (Fig. 5.5). The aim of this is to assist patients in the rehabilitation process and to compensate motor disorders by compensating with the necessary torques. In medical and biomechanical terms, the elbow joint in flexion and extension has a range of movement between 0 to approximately 150 degrees (Section 5.1.2).

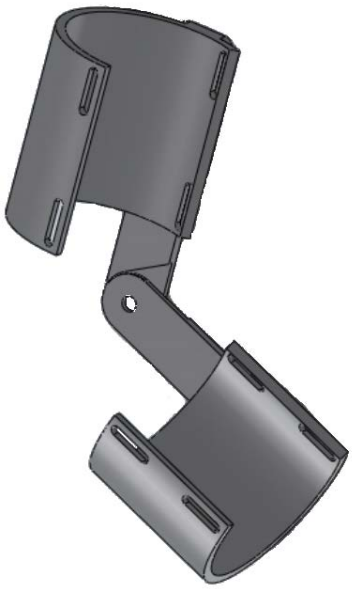

Figure 5.5: 1 DOF proposed elbow exoskeleton for simulation.

The material used to manufacture the exoskeleton is aluminium and the total weight of the exoskeleton does not exceed 0.450 kg (approximately 0.213 kg for the arm exoskeleton and 0.193 kg for the forearm exoskeleton). There is a protective elastic material lining the exoskeleton between the user and the robot that reduces the risk of an uncomfortable patient-robot interaction. In the simulation, the type of protective elastic material is similar to a spring damper system [111]. This parameters are important for better approximation of the simulation to the reality.

In this project, the proposed device will be used only in the simulation environment, the exoskeleton model was developed for this reason. The exoskeleton's characteristics, for example its weight and the spring damper parameters, can be set to represent a wide variety of design configurations.

The actuator used in this simulation is based on USM, and each model was presented in the Section 4.1.

### 5.3.3 BoB Configuration

The human body model (BoB_forward) is able to calculate motion due to muscle activation and the application of external forces. This model consists of a compiled S-function block in Simulink® with various ports for inputs and outputs. Between the inputs ports, one should take into account: one port for the muscle force, 15 inputs ports for the external force applied to the segments, 15 inputs ports for the inertia of the segments, one input port for the body mass of the person and one port for the RBM. The output port produces a signal containing data for the graphics and data storage for post processing[106].

The initial position of the musculo-skeletal model (the position at $t = 0$), coincides with the standard anatomical position and can be seen in Fig. 5.4. In the absence of the muscle forces and the external forces, due to the strength of the force of gravity, the model falls over.

To develop this simulation environment, various steps were necessary to model interaction between BoB and the rest of the components. In order to work only with the upper limb, the first step will be to keep the musculo-skeletal model fixed in space ie the external load acts on the segments with a force capable of keeping the musculo-skeletal model in a stationary position. The second step consists of connecting the exoskeleton model to the human component. In this case the actuator torque from the exoskeleton is applied to the human forearm segment. In both cases, the necessary force was transmitted through a spring damper system between the exoskeleton and the human model. Using this method, we can simulate the soft tissue and avoid any problems associated with the connectivity.

Knowing the initial coordinates of the joint articulations, the objective was to connect this initial point coordinate to static coordinates by spring-damper systems. The input of this type of system would be the coordinate of the fixed point and the coordinate of the real position of the segment and therefore the extension of the spring can be calculated. Because the fixed point of the joint articulation was developed in SimMechanics the initial extension of the spring damper - system is compatible with SimMechanics. The scheme developed in Simulink can be seen in Fig. 5.6.

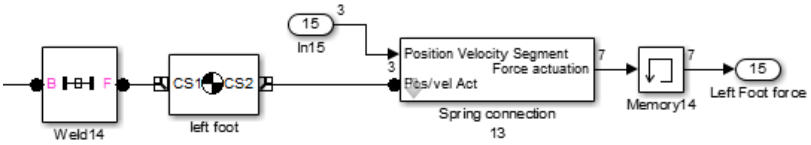


Figure 5.6: Spring-damper connection between the fixed point and the left foot

The configuration of the spring-damper system's is based on the configuration of the spring coefficients and the damper coefficient. For each segment, the spring coefficient was set in relation to its weight. The mass of the segment was set in relation to the total body mass:

$$m_i = P_i * m_{totalbody} \tag{5.10}$$

$$\sum_{i=1}^{n} P_i = 1.000 \tag{5.11}$$

$$m_{totalbody} = \sum_{i=1}^{n} m_i \tag{5.12}$$

where $m_i$ is the mass of the segment $i$, $P_i$ is the mass proportion of the segment $i$ [112], $n$ is the number of body segments, and $m_{totalbody}$ is the total body mass.

The damper coefficient was set in function of the damping ratio parameter $\zeta$ (equation 5.13) in the condition of over-damping, $\zeta > 1$ .

$$\zeta = \frac{c_i}{\sqrt{m_s * k_i}} \tag{5.13}$$

where $c_i$ is the viscous damping coefficient of the segment $i$ , in units of Newton seconds per meter (N* s/m), $m_s$ is the mass of the segment and $k_i$ is the spring constant of the segment $i$.

The spring damper models actuating over BoB can be seen in the Fig. 5.7

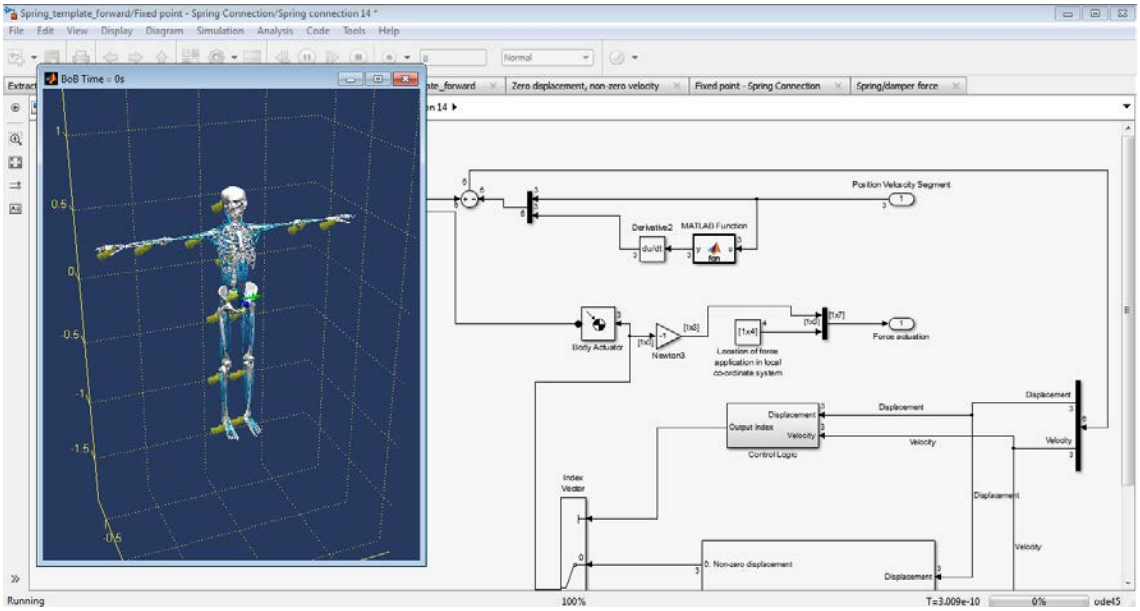


Figure 5.7: Spring-damper forces act over BoB model.

The proposed simulation is used in the rehabilitation of the elbow joint. For this reason, all the joints of the musculo-skeletal model were fixed in space with spring damper systems, and only the hand was released (joint articulation of the wrist).

The model of the exoskeleton was built in Solidworks®. With the option from SimMechanics Link® the model was imported in a SimMechanics environment. The exoskeleton has been positioned as follows: the shoulder points of the exoskeleton coincides with the fixed point of the shoulder joint articulation and the elbow exoskeleton point coincide with the fixed point of the elbow joint articulation. Between real points of the musculo-skeletal model and the fixed point there is a distance of 1cm (representing the soft tissues thickness). The force of the exoskeleton over the upper limb was transmitted from hand force entrance at a variable distance from the hand. In this case it was at a distance of 10cm from the wrist joint articulation.

The position of the upper arm and the exoskeleton with the spring damper system can be seen in Fig. 5.8.

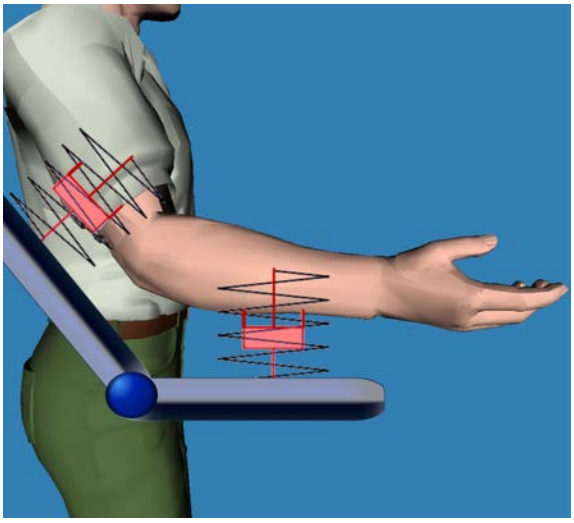

Figure 5.8: Spring-damper connection between the upper limb and the exoskeleton.

The SimMechanics model for the upper limb with the exoskeleton can be seen in Fig. 5.9.

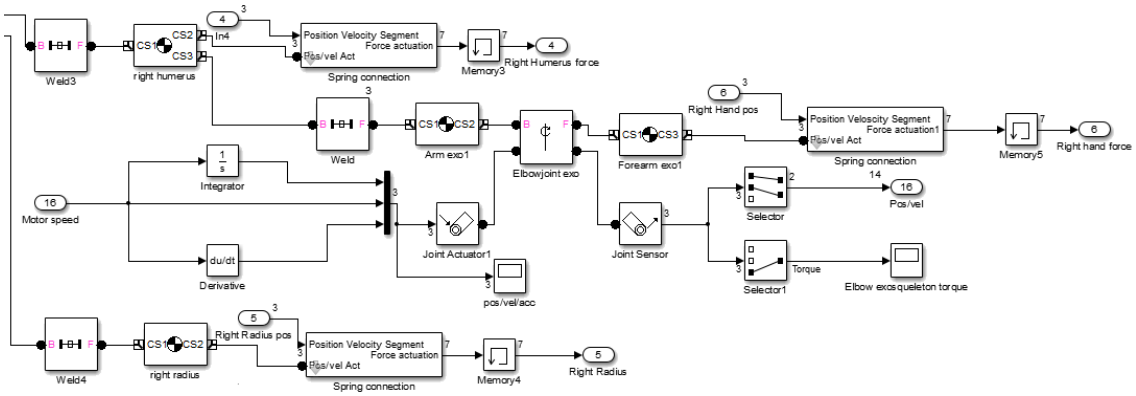


Figure 5.9: SimMechanics model of exoskeleton rehabilitation for the elbow joint

### 5.3.4 Activation of the muscles

The elbow joint is crossed by a large number of muscles that provide extension and flexion movement of the forearm. For extension the muscle includes the triceps, the brachii and the anconeus. For flexion these are the biceps brachii, brachialis and brachioradialis [113]. The BoB_forward model has an input port for the muscle force (the musculo-skeletal model has 666 muscles). A new Simulink® function was developed to control the different activity of the muscles. This function gives the

possibility to simulate partial or integral activity for each muscle, similar to a real case, where a patient has a partial function of the upper limb, after SCI, ACV or other musculo-skeletal disorder. The newly developed function receives as inputs the reference of the exoskeleton, the actual position of the exoskeleton and the force of the muscles. The muscle force can be chosen in relation to the patient capabilities, and as a percentage of the activity of each muscle. The force of the muscles is a function of the movement of the upper limb in flexion and extension.

## 5.4 Preliminary results

This section shows the test results obtained after various simulations on the different muscles' activity, and in different situations. This complex simulation environment is capable of analysing the behaviour of the actuator during a wide range of various rehabilitation activities.

The first configuration of the simulation environment consisted of a musculo-skeletal model with the upper limb in vertical position (perpendicular to the ground), as well as the setting of the exoskeleton position.

Whilst the initial position of the musculo-skeletal model consists of the upper arm being in a horizontal position with the ground, the first two seconds of the simulation consist in positioning the upper limb in vertical position. For this reason the first two seconds were ignored. The first test entails tracking the reference presented in Fig. 5.10 and analysing the behaviour of the actuator in the different situations of muscle activity. In this case the upper limb is perpendicular with the ground.

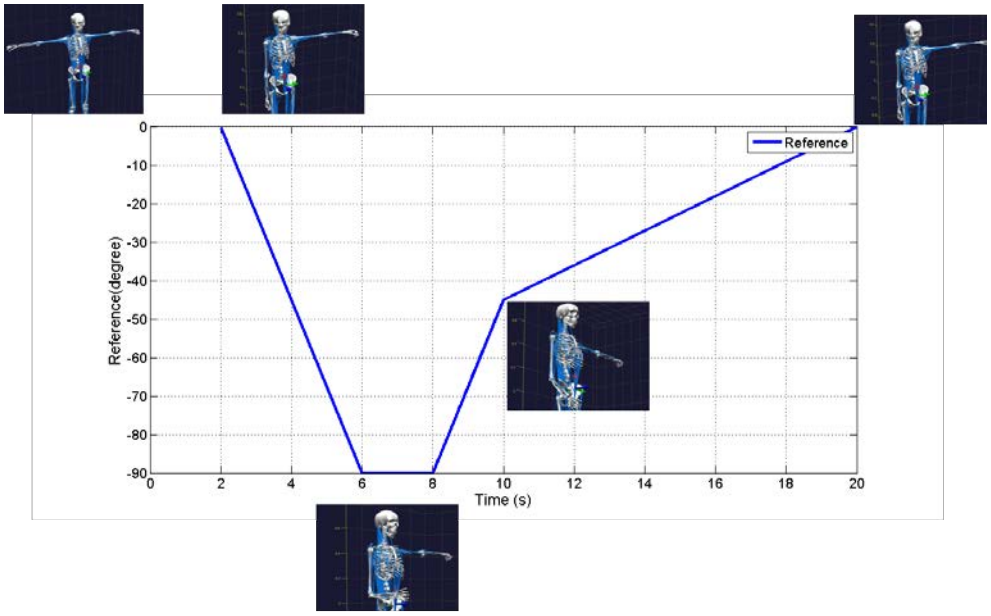


Figure 5.10: Reference position of the elbow.

Fig. 5.11 shows the reference and the response of the exoskeleton and upper limb reference tracking when the USM based actuator is used. The proposed control algorithm for the actuator enabled the exoskeleton to track the reference with minimal error. In the case of the upper limb, the angular error for the elbow joint increased to approximately 3 degrees because of the spring-damper force transmitted from the exoskeleton to the forearm

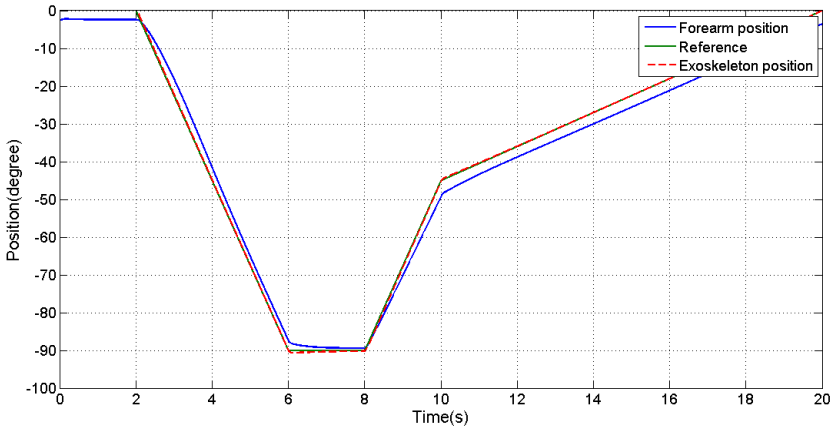


Figure 5.11: Response results of the elbow joint simulation.

The actuator offered the necessary torque for the tracking movement of the exoskeleton. For analysis of the behaviour of this actuator three simulations were released, where the reference trajectory is the same as in Fig. 5.10. In this simulation, as before, the exoskeleton and the upper arm need to follow the reference, but in this case the activity of the muscles was variable. Hence the force of the muscles during flexion and extension of the forearm corresponded to forces of 0N, 5N and finally 10N. The result can be seen in Fig. 5.12.

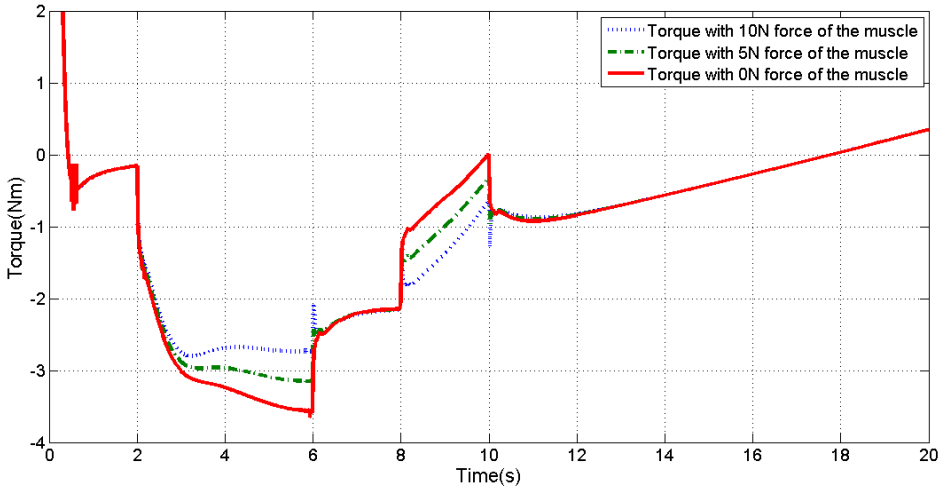


Figure 5.12: The necessary torque for elbow movement with different muscles forces.

As can be seen, if the muscles are active, the necessary torque of the actuator for the exoskeleton is variable. If in the first case when the force of the muscle is 0N, the maximum necessary torque of the actuator is 3.8Nm. In the last case, when the muscles are generating forces of 10N in flexion and 10N in extension, the maximum necessary torque decreases to 2.8Nm.

In the second test the upper limb is in a horizontal position, parallel with the ground. In this case it is not necessary to set the musculo-skeletal model because the initial position coincides with the horizontal position of the upper limb.

Fig. 5.13, presents the reference, the response of the exoskeleton and the response of the upper limb.

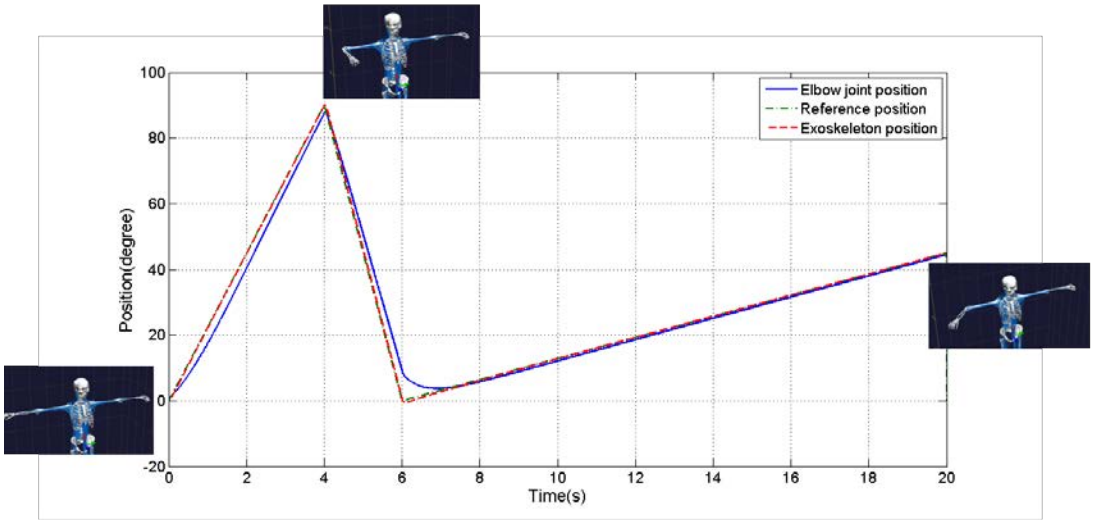


Figure 5.13: Reference position of the elbow joint, exoskeleton position and real position of the elbow joint when the upper arm is horizontal with the ground

In this case, the response in the angular position of the elbow joint is considerably more accurate due to the position of the arm and gravity force direction. This may be observed in the compression and respective extension of the soft tissues (spring - damper systems). Moreover, due to absence of the gravity force, in the flexion and extension of the forearm the necessary movement of the torque is minor. Depending on the reference position (Fig. 5.13) the maximum necessary torque, Fig.5.14 does not exceed 2.3 Nm. As in the first test, the muscle force activity was variable with 0N, 5N and 10N. In the last case, when the force of muscle was 10N, the torque of the actuator in movement between $t = 6$ and $t = 20$ was opposite to muscle force, in accordance with the reference. This means that the force of the muscle produced in the elbow joint has more torque than usual and the actuator was able to compensate this force.

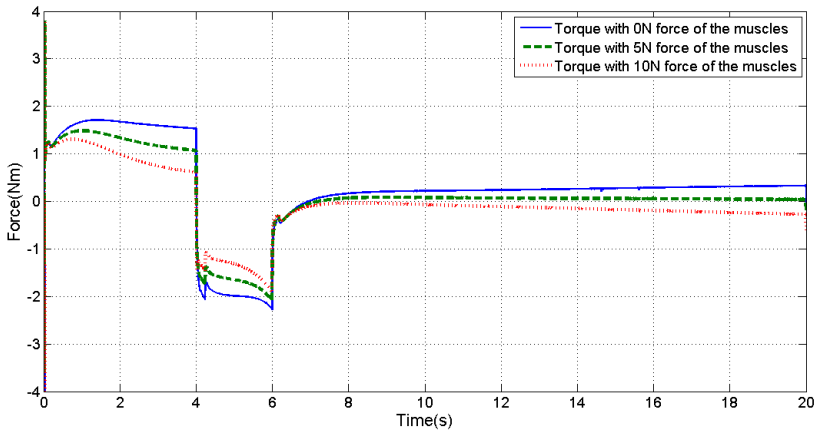


Figure 5.14: The necessary torque with the upper limb in horizontal position.

The simulation environment can simulate different states of muscle activity. This simulation helps in the development of the robotic rehabilitation devices, offering the possibility to simulate exoskeletons with the human body component before the devices are built. Also, the environment offers the possibility to modify percentage of muscle activity for example for a patient who has only partial function of the upper limb after musculo-skeletal disorders.

Similar with the case when the exoskeleton is tested with the USM based actuator in biomechanical simulation software, the actuator based on SMA was tested. The model of USM based actuator and his control algorithm was replaced with the SMA based actuator and simulated in the biomechanical software. The results of this simulation following the the reference presented in Fig. 5.10 can be seen in Fig. 5.15.

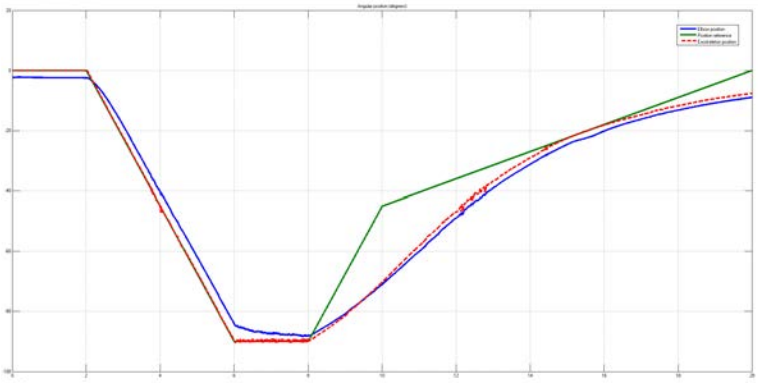

Figure 5.15: Response results of the elbow simulation together with the exoskeleton actuated with the SMA based actuator

It can be seen, the exoskeleton and the elbow joint following successfully the reference from 0 to 100 degrees (in elbow flexion movement) but from 100 to 0 degrees (in elbow extension movement) the error between reference and exoskeleton position is increasing. This results occur due to the actuator behavior which need to recover the initial shape by cooling, exchanging heat between the wires and the environment.

In function of this results we can conclude that the SMA based actuator can be used in the rehabilitation devices where slows movements are required.

## 5.5 Conclusions

This Chapter presents a new simulation environment based on BoB® forward software, which permits analyse the behaviour of the exoskeleton and the actuator, whilst on the presence of the human body components.

The interface of the environment is also responsive, and offers the possibility to change the configuration of the exoskeleton and the actuator type, as well as the possibility of developing further controls algorithm.

Furthermore the preliminary results of the simulation validate the USM actuator to be used in the exoskeleton system on the articulation with less than 4Nm necessary torque.

Due to the torque limitation, for the elbow and shoulder rehabilitation devices, the adequate actuation solution is based on the SMA. In the wrist, the USM based actuator can be used but in terms of actuator weight the SMA actuator is more suitable.

# Chapter 6

# Segmented exoskeleton design for upper limb rehabilitation

This Chapter presents the preliminary design of the upper limb exoskeleton divided in segments, which permits the patient's evaluation and realizes the rehabilitation therapy of each articulation (shoulder, elbow wrist). Initially, these are designed separately with the objective to do the therapy individually for each joint but in the future exist the possibility to combine and use two or more devices at the same time. Throughout the development of these rehabilitation devices, and for a good acceptance of the patients and the therapeutic staff, we have collaborated with the therapists of the LAMBECOM research group of Rey Juan Carlos University of Madrid, Spain. The proposed devices compared with the current solutions as presented in Chapter 2, have a light weight, noiseless operation, and low fabrication costs, mostly due to the actuator type, based on SMA presented in section 4.4.

## 6.1 Shoulder exoskeleton

This section presents the preliminary design of a rehabilitation and patient evaluation exoskeleton for the shoulder joint with three DOF, actuated with SMA based actuators. Due to the actuation system, the proposed exoskeleton presents a light weight, noiseless operation and everything in a simple design structure which implicates a low fabrication cost. The number of actuators and the preliminary designed was calculated after a biomechanical simulation of the human body with a specific category of patients. The mechanical design of the exoskeleton should allow the typical movements of the most common therapies in rehabilitation. This preliminary design has been presented in [114].

### 6.1.1 Shoulder biomechanical simulation

Nowadays, in the development of any robotic device, the simulation tools play an important role due to their capacity to analyse the expected performance of the system designed prior to manufacture. To estimate the necessary torques in the articulations for a specific patient, BoB simulation software in inverse dynamic was used (Section 5.3.1). In this case the simulation was configured with the next parameters: weight 75 kg, height 1.75m, a trajectory in the right shoulder joint from -45 to 120 degrees in flexion-extension and abduction from 0 to 120 degrees with a angular frequency of movement 0.25rad/sec.

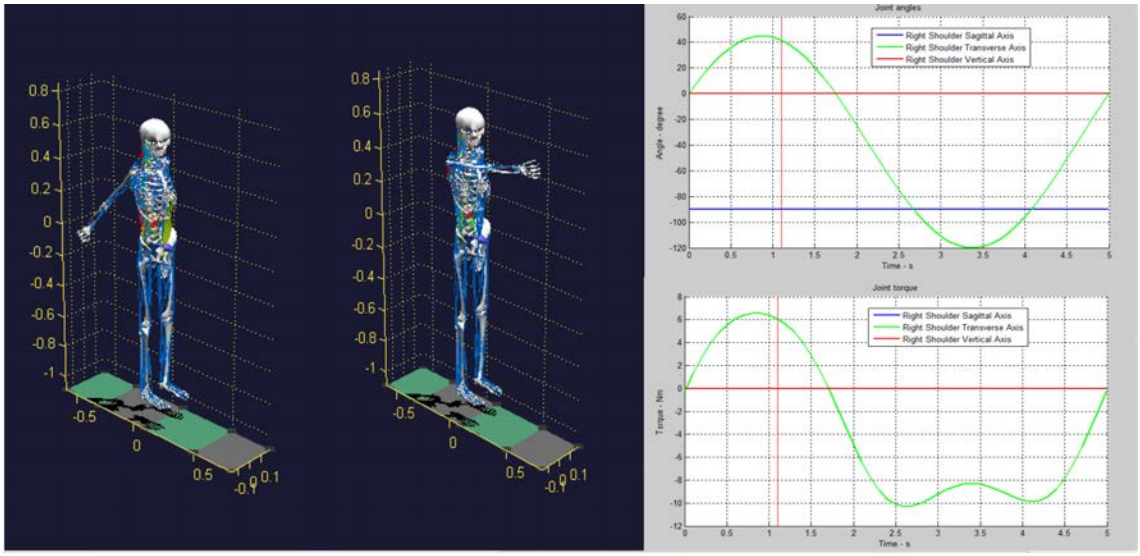


Figure 6.1: Shoulder simulation in inverse dynamic.

In the left part of Fig. 6.1 the BoB simulator is presented configured in the flexion-extension movement of the shoulder joint and in the right part, the input trajectory and the results of the simulation, necessary torque in the shoulder joint. As results from the simulation, to complete the rehabilitation task in the shoulder articulation successfully, a torque no more than 12Nm is required. This case assumes that the patient has definitively lost all the motor function and all the force is given by the exoskeleton.

### 6.1.2 SMA based actuators for the shoulder exoskeleton

The total torque is calculated taking into account the additional weight of the exoskeleton and a possible additional weight in the hand (no more than 10N), the total torque generated by the exoskeleton no surpassing the 12Nm. A simulation script capable of calculating the number of SMA wires and the length was done based on the following assumptions: 12Nm the necessary torque for mobilization of the shoulder and the exoskeleton joint, and ranging the parameters such as: radius of possible pulley to pass from a translation motion to rotary motion, the diameter of the SMA wire, the total force of each SMA in function of the composition (NiTi or NiTi in composition with other alloys). In function of these results an optimal configuration for 165 degrees of angular motion (45 degrees of extension and 120 degrees of flexion) was chosen: 8 SMA wires with a length of 2.2 m and a radius of pulley of 30 mm (Fig. 6.2). Similar, for the abduction-adduction motion 145 degrees was required (120 degrees abduction and 15 degrees adduction) resulting: 8 SMA wires with a length of

2 m and a radius of pulley of 20 mm. The better alloy in this case is NiTi with a diameter of 0.51 mm. Moreover, the SMA wires were introduced in the Bowden tube that in addition to the fixed structure (one of the extremities of the SMA is fixed on the extremity of the Bowden tube) have effect on heat dissipation, presented in Section 4.7.1. The chosen configuration takes into a account aspects such as: aesthetics, the length of wires can't be very large (the wires are mounted on the back side of the exoskeleton user) and the total number of wires which needs to maintain the same force tension.

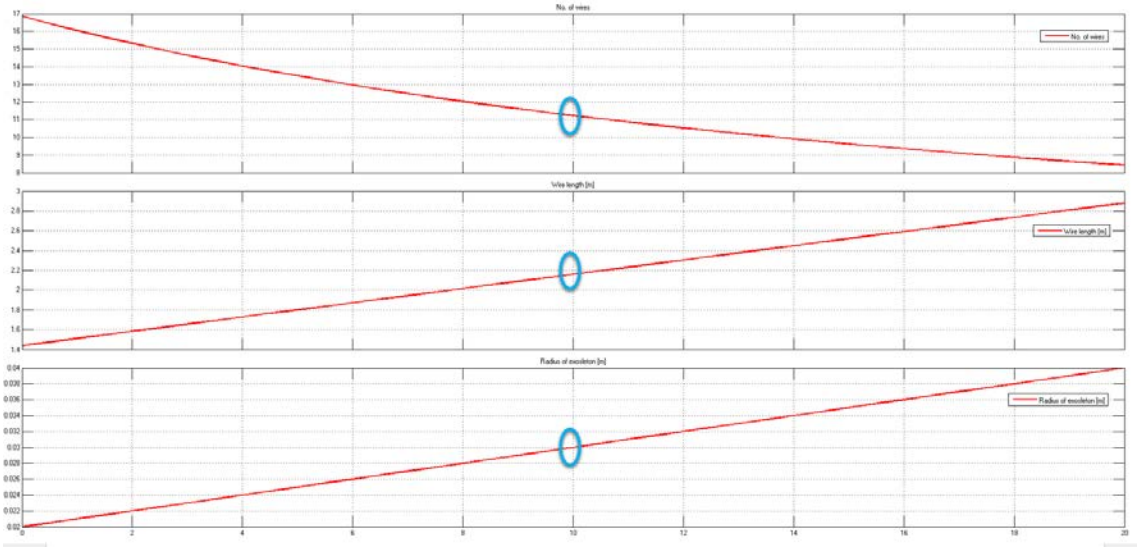

Figure 6.2: Number of wires for the shoulder exoskeleton.

### 6.1.3 Shoulder SMA exoskeleton design

In function of the biomechanical analysis and the chosen actuators an exoskeleton design is proposed in 6.3. This is made of simple parts that give the possibility to facilitate assembly and adjust them in function of the patient's comfort. In addition was designed such a low cost system that can be manufacturing using a 3D printer.

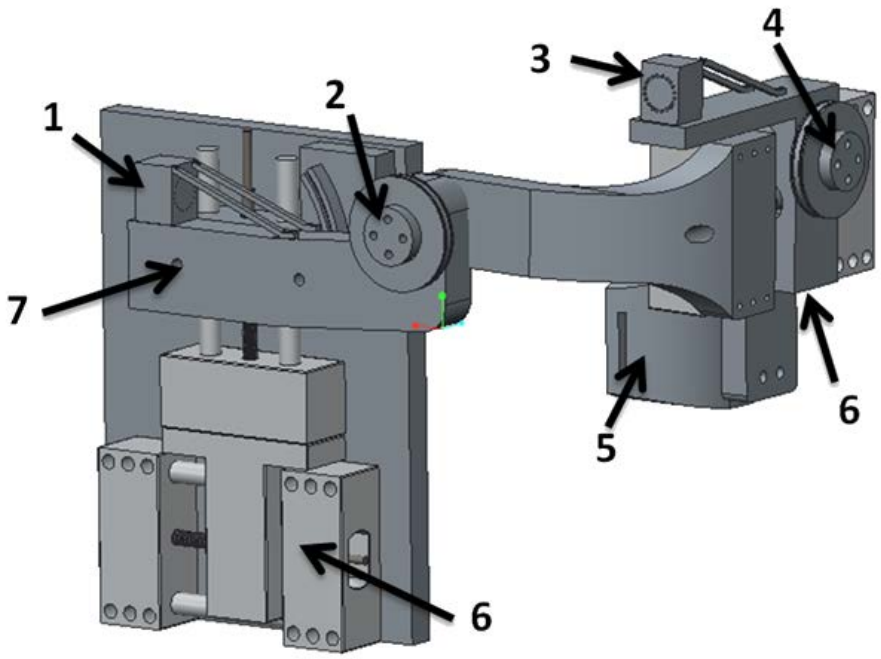


Figure 6.3: SMA shoulder exoskeleton.

The design of the exoskeleton shows three DOFs. The first DOF (2 of Fig. 6.3) gives the possibility for abduction-adduction movement, 4 gives the possibility of flexion-extension movement, 1 and 3 are fixed points for Bowden tube termination, 5 is the attachment point with the arm, 6 is a configurable system in function of the patient and 7 permits a passive scapulohumeral movement necessary in abduction movement.

Based on parameters such as: mobility, comfort, safety and easiness to put the exoskeleton on the patient, the proposed design of the exoskeleton compared with the current solution presents a significant evolution. The main advantages are given by the SMA based actuators that drastically reduce the weight of the structure, less than 2.5 kg, and at the same time with a very low noise - due to the lack of gears and motors in the mechanism. For the comfort, all intern parts in contact with the patient were covered with a very soft hypoallergenic material.

## 6.2 Elbow exoskeleton

The elbow is a complex articulation composed by the humeroulnar and humeroradial joints (for the flexion-extension movement) and the proximal radioulnar articulation

(for the pronation-supination movement). During the flexion-extension movement of the elbow joint, the rotation center changes and this articulation cannot be truly represented as a simple hinge joint. In this section the design of two types of exoskeletons for the elbow joint will be presented. The first one present one DOF which is actuated in the flexion movement and another one presents two DOFs actuated in flexion-extension and pronation-supination. The design and characteristics of the two models will be further detailed and highlighting.

### 6.2.1 1 DOF elbow exoskeleton

The exoskeleton design for the elbow with one DOF for flexion-extension, use like rotation center the properly patient elbow joint articulation. Compared with the current solutions, that align the exoskeleton axis with the elbow axis, this exoskeleton offers an ergonomic physical human-robot interface with a comfortable interaction. The exoskeleton is actuated with an SMA based actuator having minimum rigid parts, only for guiding the actuators. Thanks to this unusual actuation system, the proposed exoskeleton presents a light weight, low noise in operation with a simple designed 3D-printed structure. This exoskeleton design focuses on the patient's evaluation and rehabilitation therapy for the flexion with certain limitation in extension movements of the elbow. This exoskeleton design was presented in [115].

#### Elbow biomechanical simulation

A complex simulation of the elbow joint in the forward dynamic environment was presented in the Chapter 5. It demonstrated that for the elbow mobilization (considering the exoskeleton weight of the forearm approximately 0.193 kg) and without muscle force aid, a torque of 3.8 Nm in the elbow joint is required.

To estimate the necessary torques in the joints for a specific patient, the second option is to use the BoB simulation software in inverse dynamic mode. This is capable of simulating the inverse dynamic behaviour of the human body, receiving as inputs the height, the weight, and the motion joints (additional inputs such as the external inertia or the external forces on the human body can be received). After simulation, the results or outputs represent, among other data, the joints torques and the muscle forces.

For the elbow joint, the software is capable of simulating only the movement in flexion-extension. In this case, a pilot study for this articulation was done configuring the simulator for a specific group of persons with the next parameters: weight of 70 kg, height of 1.7 m, a trajectory in the right elbow joint between 0 and 150 degrees (where the 0 degrees is considered the maximum elbow extension), and a maximum frequency of movement equal to 0.25 Hz. In addition, in the right hand, a force of 20 N was applied. This force represents an approximation of the exoskeleton weight included

in the simulation. As can be seen in the simulation results (Fig. 6.4), to complete the rehabilitation task successfully in the elbow articulation for the flexion-extension movement, a torque of approximately 3.5 Nm is necessary. This case assumes that the motor function is completely lost and that all the force is generated by the exoskeleton. This result is similar with the result in forward dynamic simulation.

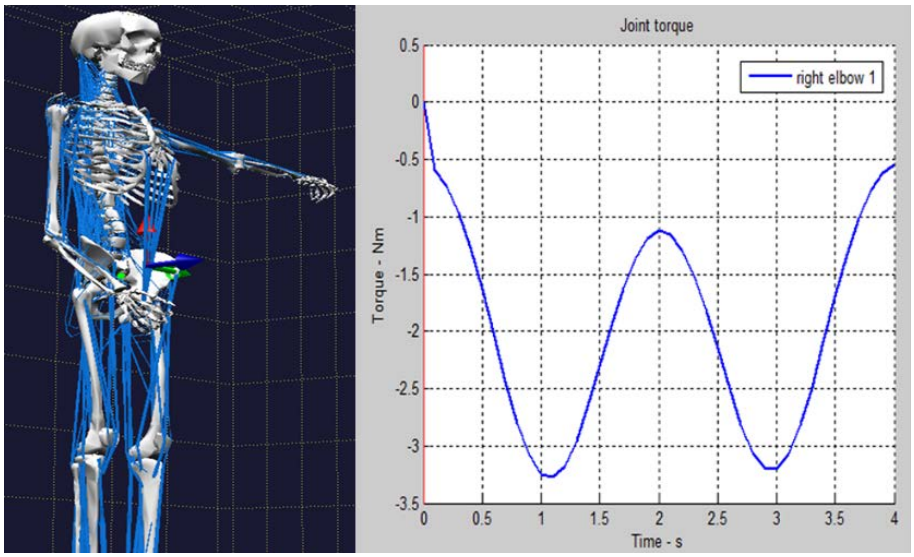


Figure 6.4: Elbow simulation in inverse dynamic.

The simulation software, BoB, is not capable to simulate the second DOF (pronation-supination), and the torque of this joint has been fixed to 1 Nm. This value is above the torque required for this movement [116] and is used in the design of the elbow exoskeleton with two DOF.

### SMA based actuator for the elbow exoskeleton

The simulation presented in Section 6.2.1 estimates the necessary torque in the elbow joint to be approximately 3.5Nm. In function of this number, the actuator structure can be calculated and defined. Similar with the shoulder case, the Matlab script was used to estimate the actuator structure. If the exoskeleton presents a pulley to pass from linear to rotating movement between 0 and 120 degrees (ADL activity) the simulation result is: three wires of SMA (considering that each SMA wire gives a force more than 35.6 N) with a length of 1.6 m and the pulley radius of 0.03 m (Fig. 6.5).

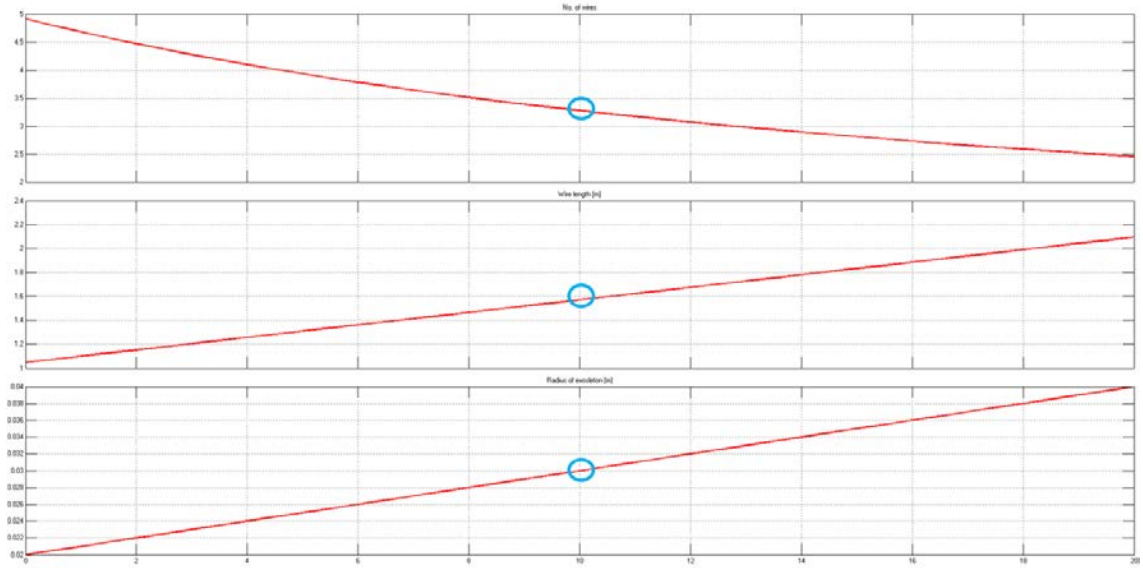

Figure 6.5: Number of wires for the elbow exoskeleton.

In the exoskeleton with one DOF, a pulley is not required because the center of rotation is the patient proper elbow. In this case, in order to calculate the SMA wire length for the actuator, the exoskeleton must be worn by the trial and the structure should be set on the correct position for the biceps and forearm. In case of selected subject, the contraction distance needed for a flexion-extension movement for elbow joint -considering a range of movement from 0 to 150 degrees (maximum flexion)- is around 0.075 m and form 0 to 120 degrees approximately 0.06 m. These values have been found experimentally, measured with a nylon thread and can vary slightly depending on the patient.

Next it is necessary to calculate the SMA wire length. Therefore, it is important to know that a SMA wire can vary until a 4% of its total length. In Fig. 6.6 the actuator with its dimensions is presented.

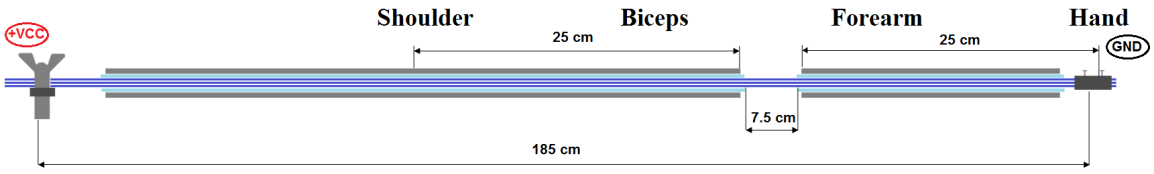


Figure 6.6: Elbow actuator for one DOF exoskeleton.

### 1 DOF SMA elbow exoskeleton design

Fig. 6.7 presents the parts of the first version of the exoskeleton.

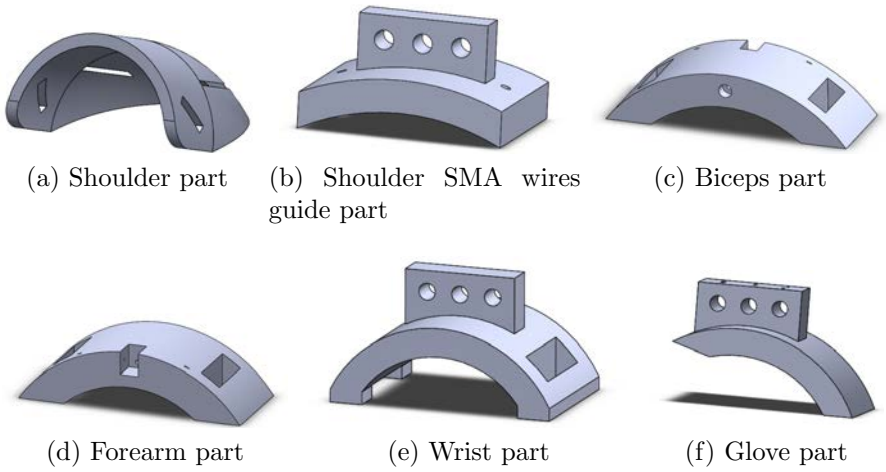

(a) Shoulder part (b) Shoulder SMA wires guide part (c) Biceps part

(d) Forearm part (e) Wrist part (f) Glove part

Figure 6.7: Elbow exoskeleton 3D printed parts.

The main function of the shoulder part defined in Fig. 6.7a is to fix the exoskeleton to the patient's arm, in order to avoid exoskeleton part displacements and to optimize the movement produced by the SMA wires contraction. The part defined in Fig. 6.7b is placed over the shoulder part as shown in Fig. 6.8, and its main utility is to guide the SMA actuators and to minimize mechanical losses. Parts defined in Fig. 6.7c and Fig. 6.7d are used to fix the exoskeleton to the human body and to ease the movement generation of SMA actuators because of the memory effect. Part defined in Fig. 6.7e is essential. As the exoskeleton is built for flexion-extension for elbow medical rehabilitation, the degree of freedom for supination-pronation must be cancelled, so the patient's wrist is blocked. Finally, the part defined in Fig. 6.7f is fixed to a glove over the hand and it is used for crimping process.

Every part must be placed according to Fig. 6.8:

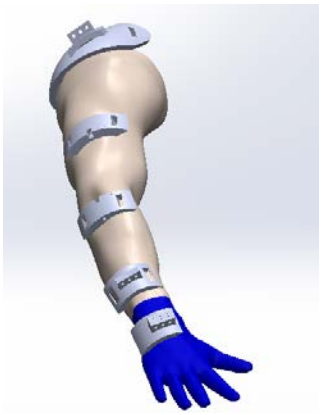

Figure 6.8: Design of a wearable exoskeleton for elbow medical rehabilitation.

The real built exoskeleton is shown in Fig. 6.9. The estimated weight of this exoskeleton is 0.6 kg approximately, without taking into account electronics. This low weight eases the comfort and medical rehabilitation process of the patient.


Figure 6.9: Wearable exoskeleton for elbow medical rehabilitation with Shape Memory Alloy actuators.

The crimp process is the technique that allows to fix the SMA wires so that, when the wires contract, there are no mechanical losses and that contraction is exclusively used to generate the actuator movement.

In this project, the crimp system for SMA wire-based actuators for an elbow medical rehabilitation exoskeleton is built with two parts: on the one hand, for crimping

the SMA wires on the hand glove part, a metallic piece of an electric connector that tightens the wires with two screws is used, which is placed inside the part defined in Fig. 6.7f. On the other hand, for crimping the SMA wires on the shoulder part, a metric four thumbscrew is required, as it is shown in Fig. 6.10.

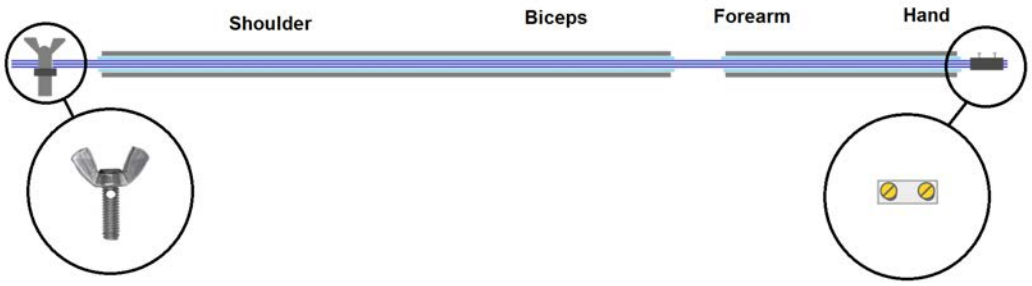


Figure 6.10: SMA wires crimp process for elbow exoskeleton actuators.

The crimp process as follows:

- First of all, the exoskeleton is placed over the patient's damaged arm and the end of the SMA actuator is fixed to the glove over the metallic piece, previously described.
- Next, the patient move his arm up to initial position with extended elbow ($\theta_{(k)}$=0 degrees) and the SMA wires are tightened without tightening the screw.
- Finally, the thumbscrew and the nut are tightened, and now, the SMA wires are totally tensioned when the patient's arm is in initial position.

### Sensors

A Flex Sensor, by Spectra Symbol, is a resistive sensor whose resistance varies depending on the bending angle. The flex sensor's resistance changes when the metal pads are on the external bottom of the curve. It is used in robotics because of its light weight and its simplicity. It is recommended to pin up the base to avoid damage on the connector due to flexion efforts.

In this project, the flex sensor is used to measure the exoskeleton's angular motion which coincides with the patient's elbow joint angle, for flexion-extension movements in real time. The sensor is positioned over the elbow joint with the aid of the arm cover. The sensor signal is used as feedback signal for the control loop and, along with the reference signal, it is possible to calculate the error signal for every instant. The relationship between the elbow flexion angle and the electrical resistance presents a linear behaviour.

In Fig. 6.11, the electrical installation for the flexion sensor with voltage divider configuration with a resistance $R = 10K\Omega$ and 3V power supply voltage, is shown. The power supply voltage is 3V because the analog inputs of the STM32F4 microcontroller can only read signals with amplitude up to 3V.

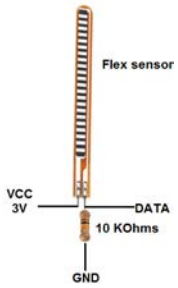


Figure 6.11: Electrical connections for FlexSensor.

The electric signal from the Flex Sensor, is read by a STMicroelectronics board and is transformed into continuous values by a 10-bit Digital-Analog Converter. Next, a conversion from voltage to degrees is necessary, taking into account minimum and maximum resistance of the Flex Sensor input voltage and elbow movement range. As it is a resistive sensor, the voltage variation of the sensor depending on the elbow position is linear. Finally, an average filter of 11 samples is applied to avoid peaks and to smooth the elbow signal position there is a 0.11 seconds delay and the sample time is $T_s$=0.01s.

Finally, the experimental response of the flex sensor measures the elbow angle in flexion-extension movements as shown in Fig. 6.12.

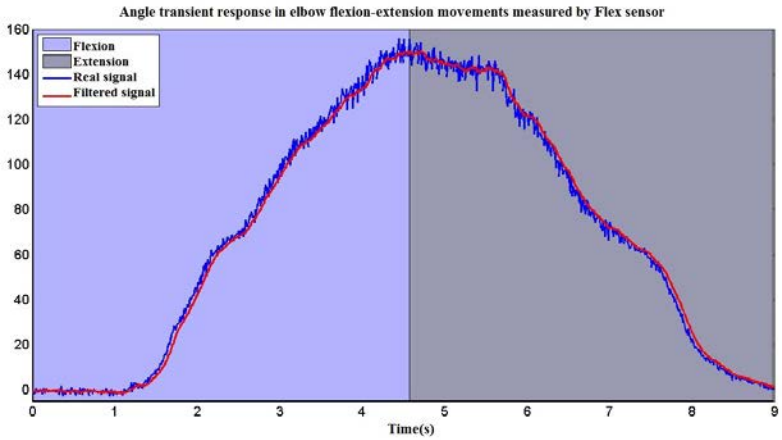


Figure 6.12: Elbow joint time response for flexion-extension movements.

### Results

The proposed design is characterized by low weight, nearly 0.6 kg for the whole structure with actuators. Th structure demonstrates noiseless operation in order to get comfortability, portability and adaptability with low cost and innovative materials.

In this way, experimental tests using the control presented in Section 4.6 are defined to check those characteristics of comfort and efficiency for a medical rehabilitation device.

The preliminary results of an experimental test carried out with a person from the laboratory staff, are shown below in Fig. 6.13. The person's characteristics are: 1.8m height, male, with a weight of 80 kg and 23 years old. A step reference signal is the input for the system and the response is analysed.

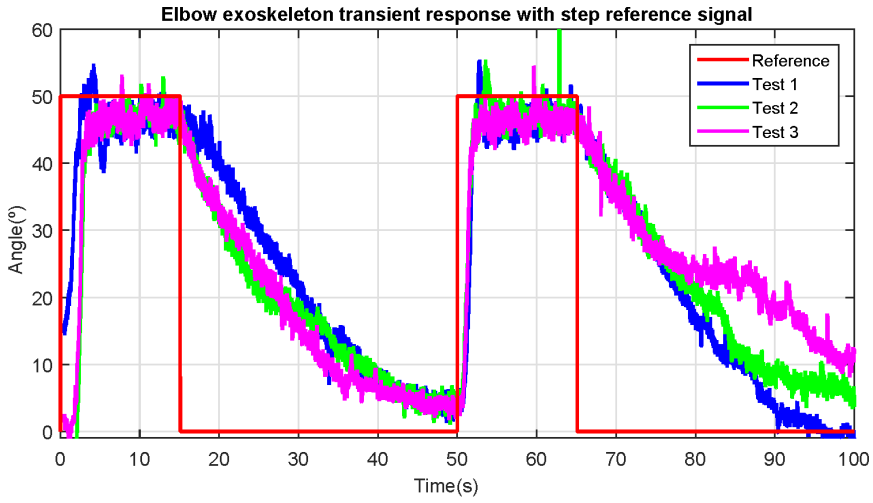


Figure 6.13: Elbow exoskeleton time response in experimental tests with step reference.

The reference signal is defined as a step signal because the performance of the control system can be easily analysed. If the SMA actuators respond fast and accurate to a step signal, the transient behaviour is expected to be controlled for heating/cooling processes for slower changes in the reference signal.

The elbow range of motion is approximately 150 degrees and the SMA actuators are sized for this range. In this case, the reference signal set-point is 50 degrees. This difference between reference signal set-point and elbow range of motion was because it was thought that a 50 degree reference set-point would represent a better and precise behaviour than if the limit of the elbow motion range was reached, because for example the CVA patients usually have a decreased range of motion and the rehabilitation starts step by step and increases the motion gradually.

A comparative study of the elbow exoskeleton time response for step reference signal is carried out for three experimental tests in Fig. 6.13. Results repeatability for SMA wires heating/cooling processes is observed. On the one hand, the heating process is defined as a 4.5 seconds time response due to the control system and power electronics actions on SMA actuators. On the other hand, the cooling process is slower, almost 25 seconds. In this case, the cooling method is air convection at room temperature. Depending on the final application, there are several solutions to improve and accelerate the cooling process the use of an antagonist actuator [117], that is, a double actuator formed by an actuator responsible for flexion movement and an actuator responsible for extension movement, taking into account the heating/cooling processes for each one to avoid wire rupture due to a stress increasing when the wires is heated, or, use springs to accelerate the recovering process of the original shape of SMA wires. The average error in stationary state is 3.42 degrees in case of positive steps.

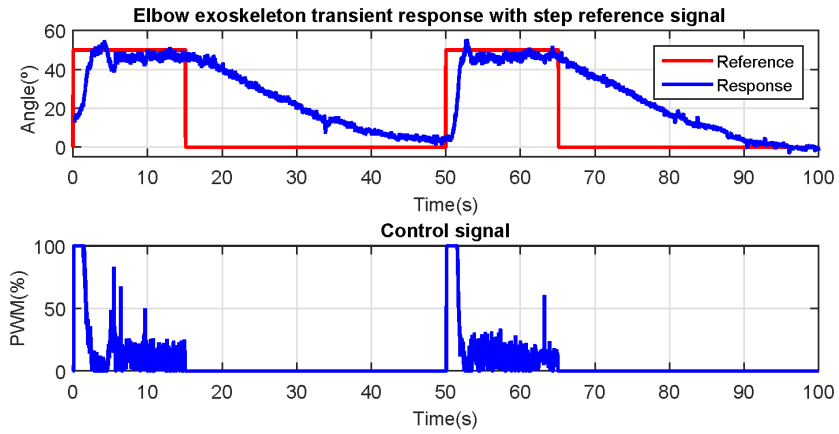


Figure 6.14: a) Elbow exoskeleton transient response with step reference signal b) PWM control signal.

Lastly, the control signal is analysed for a step signal reference test (Fig. 6.14), and it is observed that the PWM control signal is maximum when a step in the reference signal occurs. In this instant, the power consumption of a SMA actuator is maximum (160 W approximately, depending on the SMA actuators voltage power supply). The power consumption is minimum when the exoskeleton keeps the current position in stationary state and during the cooling process.

### Proposed design for the second version of one DOF exoskeleton

With the goal to increase the patient comfort in the rehabilitation therapy, a second design for the elbow exoskeleton with one DOF was proposed. This second design is based on the first one, but with the difference to reduce the rigid parts and in the same time the total weight of the device. The rigid parts from the Fig. 6.7 was eliminated and the whole structure of the exoskeleton was done over a commercial zippered cycling jacket. The Bowden tube, which in the first design has extremities in the exoskeleton parts, in the second design the Bowden tube stop in the small metallic pieces which serve connectors for the SMA actuators (and such a crimp pieces). These pieces are sewn on tapes that allow the exoskeleton to be set in function of the patient. This structure reduces the total weight to 0.3 kg. The resulting design can be seen in Fig. 6.15.

Figure 6.15: Second version of the 1 DOF elbow exoskeleton.

Both versions of the wearable exoskeletons are considerate as low weight devices compared with the current solutions, they have a noiseless operation and implicate low cost in fabrication. This structures have been tested in flexion actuation with a healthy person (the results are presented in Fig. 6.14. The extension movement is done with the gravity force [115].

### 6.2.2 2 DOF elbow exoskeleton

The mechanical design of the exoskeleton follows the concepts and requirements given in Sections 5.1.2, 6.2.1 and 6.2.1. The CAD structure of the exoskeleton is displayed in Fig. 6.16, where 1- attachment points, 2- fixed structure for supination-pronation, 3- actuator termination, 4- pulley for linear to rotational transformation. The preliminary design and results was presented in [118], [119] and [117].

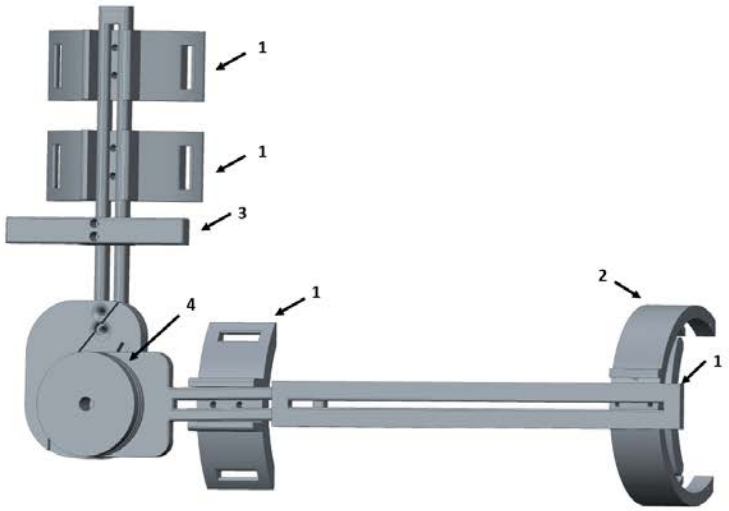


Figure 6.16: Elbow SMA exoskeleton design.

For the flexion-extension movement, taking into account that the actuator presents a linear movement and that in the elbow joint a rotation movement is needed, a 0.06 m diameter pulley is introduced. Considering this diameter, the necessary torque is approximately 3.5 Nm, the desired range of movement between 0 and 120 degrees (ADL), and the force of the SMA wire, an actuator with three SMA wires of 1.5 m length is required. This means that, since each wire produces 35.6 N, the torque of the elbow joint is approximately 3.5 Nm. This torque can be obtained during tens of millions of cycles when each SMA wire works with the optimal characteristics (35,6 N force). Considering the decrease of lifetime when the actuator force is raised, if the maximum force of each cable is increased to 118 N, the torque in the elbow

joint is 10.62 Nm, but the lifetime of the actuator is reduced to a few thousands of cycles. Moreover, the actuator structure allows to easily insert another SMA wire to increase the total torque. In addition, it is possible to install a torsion spring which is helpful for the flexion-extension movement. The torsion spring helps to recuperate the initial position of the actuators (extension movement) when the patient executes the rehabilitation task with the arm horizontal to the ground. The gravity does not have effect on the elbow joint in flexion-extension. In the extension movement, the necessary torque depends of the position of the arm (the gravity force) and the torsion spring force. In function of this, the necessary torque for the forearm extension is less than 3.5 Nm and an actuator based on two SMA wires is proposed.

For the pronation-supination movement, the CAD can be observed in Fig. 6.17(a) and the real device is shown in Fig. 6.17(b). This design consists of a fixed part connected to the forearm, and a sliding part connected to the hand. The actuation of the sliding part, with two antagonist actuators, generates the pronation-supination movement of the forearm. According to the proposed mechanism for the fixed part, with an internal diameter of 0.1 m, two SMA-based actuators are required, each one with one SMA wire of 2 m length. With this configuration, the forearm can be moved 50 degrees in pronation and 50 degrees in supination, representing the necessary movement of the ADL. The length of the actuators is not a concern, considering the flexibility characteristic of these actuators. The shape of the cable can be adapted to the shape of the human body. A summary of the system configuration depending on the movement can be seen in Table 6.1.

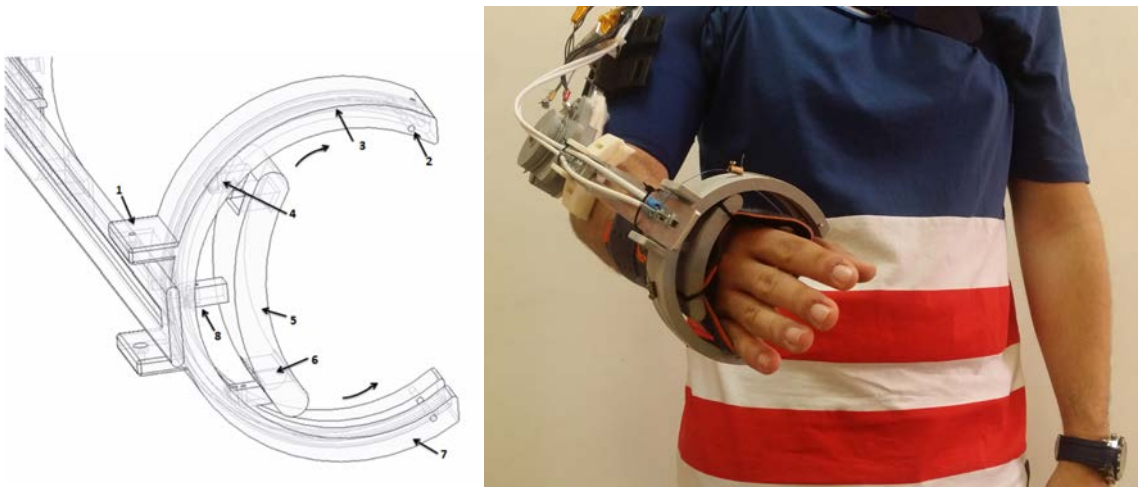


(a) (b)

Figure 6.17: Elbow SMA exoskeleton pronation-supination parts.

In Fig. 6.17(a) is presented a CAD structure for the pronation-supination parts

where 1 - actuator termination for Bowden cable, 2 - shaft for pulley, 3 - canal slip, 4 - terminals for traction cable hold, 5 - sliding part, 6 - attachment point (to the hand through a belt), 7 - fixed part, 8 - sliding point. In Fig. 6.17(b) is presented a prono-supination partreal of elbow SMA exoskeleton.

Table 6.1: Exoskeleton actuators.

| Movement | SMA wires | Maximum force [N] | Length [m] | Weight [kg] |
|---|---|---|---|---|
| Flexion | 3 | 354 | 1.5 | 0.16 |
| Extension | 2 | 236 | 1.5 | 0.15 |
| Pronation | 1 | 118 | 2 | 0.1 |
| Supination | 1 | 118 | 2 | 0.1 |

The exoskeleton is made from simple parts which give the possibility of easy assembly. Different configurations can be defined depending on the patient. Each component can be easily made with a 3D printer. The exoskeleton has four attachment points with the human body, connected to the arm (two of them), the forearm, and the hand (Fig. 6.16). The attachment points are adjustable in function of the patient. The hand connector presents one DOF, which gives the possibility of pronation-supination of the forearm. For the safety of the patient, the exoskeleton movement is mechanically limited between 0 and 150 degrees. In order to increase the comfort, all internal parts in contact with the patient are covered with a soft hypoallergenic material. Comparing with the current solutions, due to the lack of gears and motors in the mechanism, the proposed rehabilitation device presents a light weight. The whole structure with the actuators weighs less than 1 kg. A 960W DIN Rail Power Supply (24Vdc/ 40A) is used to provide the necessary energy to the actuators. The weight of the Power Supply unit is 1.9kg. In addition, it presents a noiseless operation characteristic, which increases the comfort of the patient in the rehabilitation process. The final version of the exoskeleton installed on the human body can be seen in Fig. 6.18.

The control algorithm of the actuation system and test results with this structure is detailed in the Chapter 7.

## 6.3 Wrist exoskeleton

This section presents the exoskeleton design for wrist rehabilitation and evaluation with two DOFs actuated with SMA wires. This is designed in function of a patient: male, 1.75 m height and 75 kg weight. The preliminary design of this exoskeleton was presented in [120].

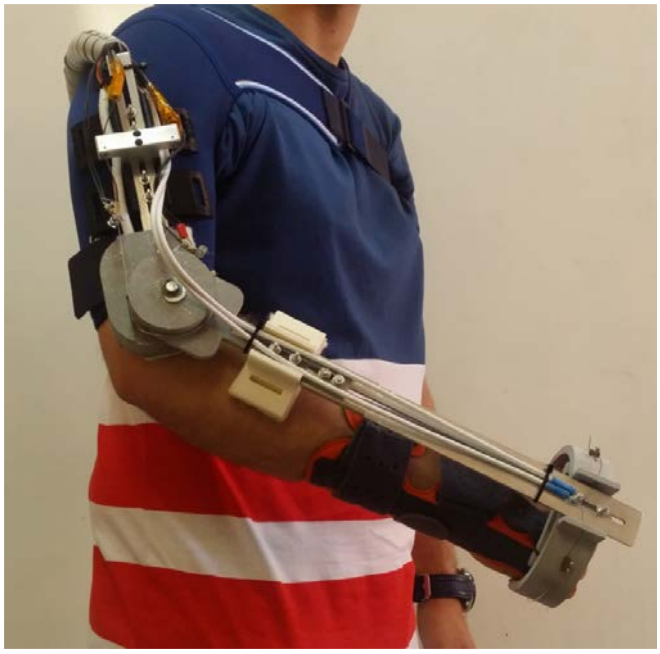

Figure 6.18: Elbow SMA exoskeleton design.

### 6.3.1 Wrist biomechanical simulation

Similar to the case of the shoulder and the elbow to estimate the necessary torque in the wrist, BoB software in inverse dynamic has been used. This case was configured with the parameters of the male patient, and the wrist movement trajectory with 90 degrees of flexion and 85 degrees of extension at a frequency of 0.25 Hz. This frequency is considerate the maximum frequency in which the rehabilitation therapy was done. The actuator shows a slow response compared with this frequency. The simulation results for successfully completing the rehabilitation therapy, needed in the wrist articulation is 0.3 Nm (Fig. 6.19).

In the case of radial deviation and ulnar deviation (abduction and adduction), although the orientation of the hand may change, the pairs of the wrist joint may not exceed 0.3 Nm. In this simulation we have assumed the worst case in which the patient has complete loss of motor function of the joint and all the force must be performed by the exoskeleton.

### 6.3.2 SMA based actuators for the wrist exoskeleton

To estimate the number of wires, the length and the necessary contraction distance, the script of Matlab/Simulink was used. The total torque in the wrist was set in function of the biomechanical simulation at 0.5 Nm. The simulation results (presented

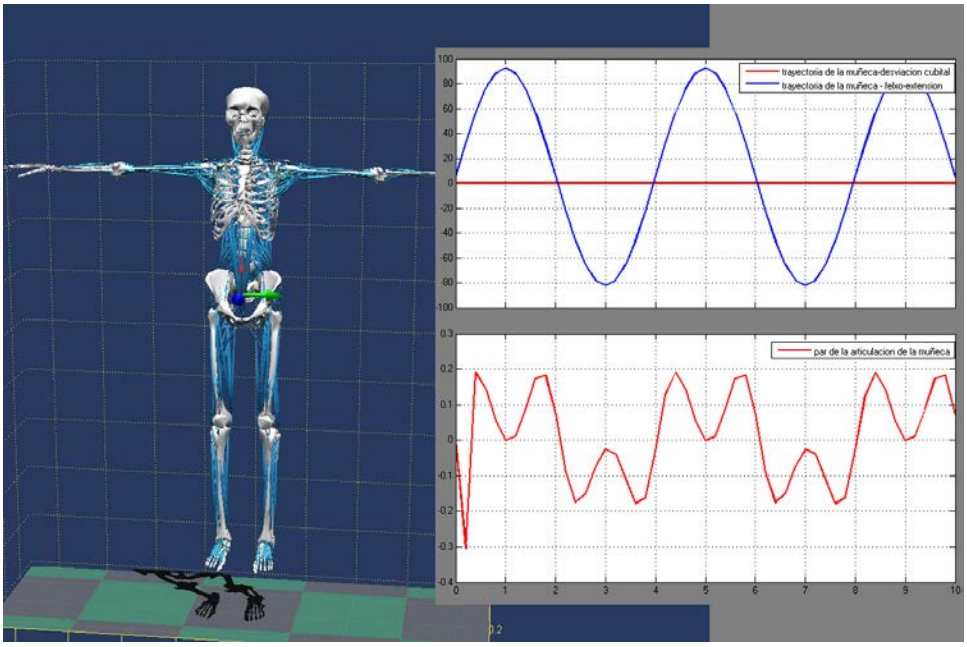


Figure 6.19: Wrist simulation in inverse dynamic.

in Fig. 6.20) demonstrate that for the wrist mobilization one SMA wire for each movement is needed, and in function of the radius (to pass from linear movement to rotative movement) the total length wire it may vary from 0.5 to 1.8 m.

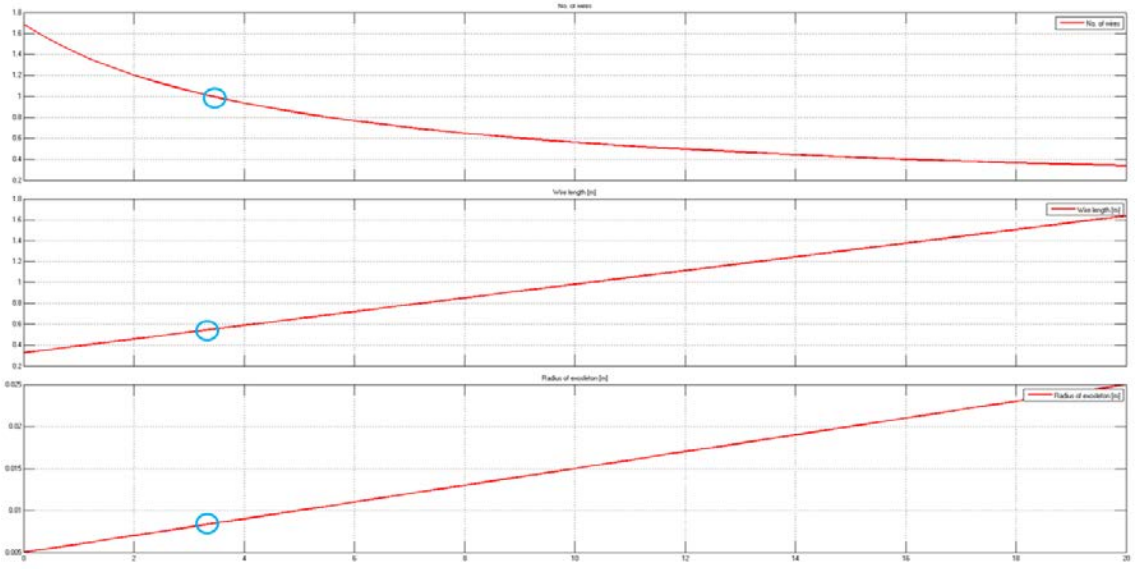

Figure 6.20: Number of wires for the wrist exoskeleton.

The total number of actuators used in the wrist SMA exoskeleton with two DOFs are: one actuator for the flexion movement, the extension movement doing with he elastic component, and two actuators, one for the radial deviation and another one for ulnar deviation. The last two actuators will be controlled in antagonist movement which algorithm will be presented in the Chapter 7.

### 6.3.3 Wrist SMA exoskeleton design

In function of the biomechanical analysis and the actuators simulation, the wrist SMA exoskeleton design is shows in Fig. 6.21. The entire exoskeleton design is placed over a glove which permits a better fixation with the human body. On the other hand, using a glove decreases the setup time, by simply placing it over the human hand being more easy. The points of subjection with the human body allow to transmit the forces generated by the exoskeleton directly to the hand and the forearm . Through the intermediary of the glove material and the exoskeleton's protective material, the pressures on the skin are cushioned by maintaining a comfortable interaction between the robot and the human body.

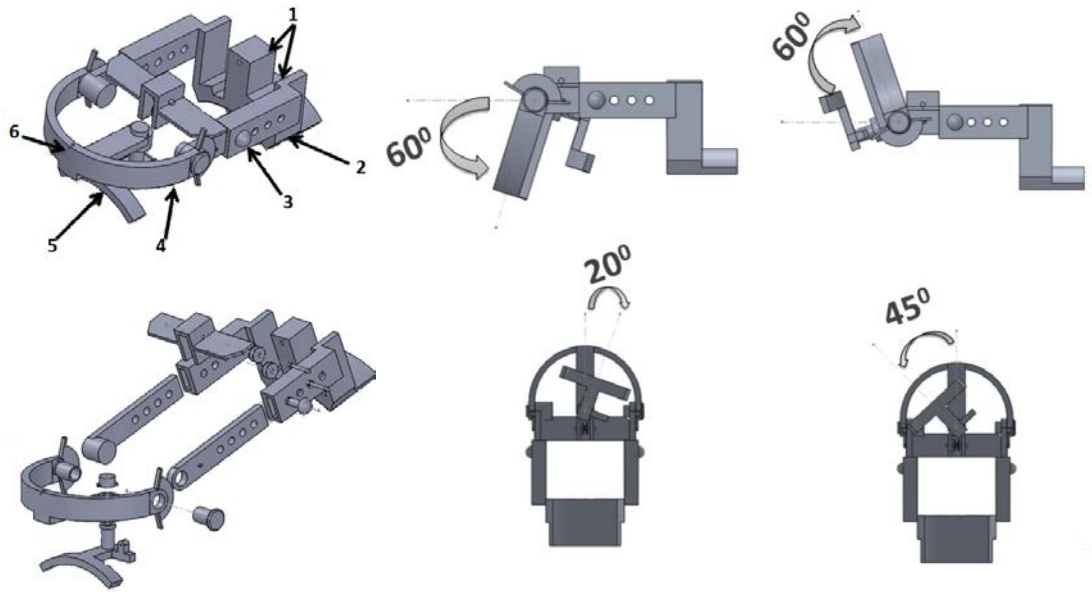


(a) (b)

Figure 6.21: Wrist SMA exoskeleton design.

The exoskeleton has been designed with simple parts that facilitate assembly and can be adjusted in function of the anthropometric characteristics of the patient

(Fig. 6.21a) where: 1 - termination part of the Bowden tube, 2 - fixed point of attachment with the forearm, 3 - adjustment system in function of the patient, 4 - DOF for flexo-extension, 5 - DOF for ulnar deviation and radial deviation, 6 - point of actuator restraint). It has also been designed as a low-cost device whose parts can be manufactured with a 3D printer. The design of the exoskeleton presents two DOFs: one for flexion-extension and one for ulnar and radial deviation. In flexion-extension axes the rehabilitation device have a torsion spring that helps to recover the initial shape of the actuator. In addition, the device is mechanically restricted to a certain range of motion by 60 degrees in flexion, 60 degrees in extension, 45 degrees in ulnar deviation, and 20 degrees radial deviation for the patient's safety (Fig. 6.21b) ).

In each axis of rotation the exoskeleton has a rotary position sensor (Bourns 3382G-1-103G) which will be used to close the control loop and save the required data for the analysis of the evolution of the patients' recovery.

This design has significant improvements compared with the current solutions such as portability, comfort, safety and ease of installation. The main advantage is given by the use of actuators based on SMA wires, this reduces the total weight of the device to approximately 0.15 kg. At the same time it present noiseless operation due to the absence of reducers and motors in the mechanism. The structure of the exoskeleton will be fixed to the hand and forearm by the intermediary of a glove that also aims to protect the contact between the human body and the rehabilitation device.

## 6.4 Conclusions

In this Chapter was presented the preliminary design for a segmented wearable upper limb exoskeleton actuated with SMA based actuators (without motors) which permit to reduce drastically the weight of the exoskeleton (less than 2.5 kg for the shoulder, less than 1 kg for the elbow and less than 0.15 kg for the wrist) and presents a noiseless operation that increase the comfort of the system. On the other hand the devices present low cost fabrication, with low cost electronics and actuators, which can be adjustable depending on the patients.

The exoskeleton design is presented separately in four rehabilitations devices: one for the shoulder, two for the elbow and one for the wrist, which permit the rehabilitation therapy separately for each joint. The possibility to use two or more rehabilitation devices at the same time to do the rehabilitation therapy for various joints is limited on function of the incompatibility between the devices. Currently the design of the shoulder exoskeleton permits to be used with one DOF elbow exoskeleton or wrist exoskeleton, but the wrist exoskeleton can't be used with the 2 DOF elbow exoskeleton (incompatibility of prono-supiantion system with the wrist movements).

The shoulder SMA exoskeleton design was proposed but was not build physically

because it implicates more fabrication costs and that were considered prior to manufacture. The actuator control algorithms, and preliminary results can be tested and analysed on the elbow rehabilitation device, the actuation system presents similitude.

The one DOF exoskeleton was built and tested over the human body. The current configuration presents a maximum actuation angle for the flexion movement between 0 and 100 degrees. The two DOF exoskeleton design, was build and the system actuation and results are presented separately in the next Chapter.

The wrist SMA exoskeleton was built with the 3D printer. Due the fragility of some parts, it is necessary to redesign or manufacture them in aluminium prior to test.

# Chapter 7

# SMA based elbow exoskeleton with 2 DOF: set-up and tests

In Chapter 6 was presented the design of the segmented upper limb exoskeleton design which is a proposed to use in the rehabilitation therapy and evaluation of the patient. This Chpater presents the control strategy based on a simple four-term bilinear PID controller presented in Chapter 4, the operation mode of the exoskeleton and the results. All the tests are presented over a two DOF elbow SMA exoskeleton. Depending on the desired therapy, the position reference and the control performance can be chosen to meet different requirements:

- reading sensors data (without actuation), necessary for evaluation and diagnosis of the patient.
- passive therapy in flexion movement and recuperation of the initial position (extension movement of the elbow joint) with the aid of the gravity force and the torsion spring;
- passive therapy in extension movement and recuperation (flexion) of the initial position is done by the patient;
- passive therapy in antagonistic movements, two actuators for flexion and extension, respectively;
- active therapy, the reference is generated in function of the electromyography signals;

All experimental tests were performed in the same conditions as the simulation set-up (presented in the Chapters 5 and 6) but with different frequency of movement. Each control strategy (for each movement) is explained in the following sections.

The pronation-supination movement is governed by two SMA wires that produce the antagonistic movements. This offers the possibility to work in a passive modeby reading reading only sensors data (when the device is not actuated and it only makes the data acquisition).

## 7.1 Operating mode

Concerning the type of assistance, the exoskeleton is designed to offer three operating modes: reading sensor data, passive mode which separately includes movement of flexion, extension and flexion-extension, and the active mode. This types of assistance as separately analysed in the follow sections.

### 7.1.1 Reading sensors data

In the reading mode, the exoskeleton is not actuated and it only reads the sensors data. In this mode, the actuators control is not activated and the exoskeleton only needs the connection with the PC for microcontroller and sensors power supply and data acquisition. Without control, the exoskeleton joints move freely. Some tests in the passive mode have been performed with a healthy person. The data acquisition from the sensors can be seen in Fig. 7.1.

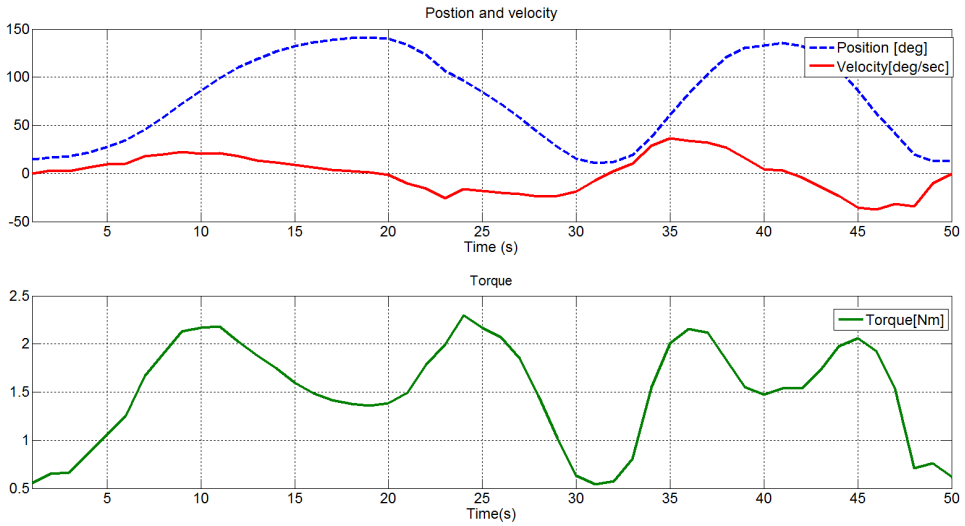


Figure 7.1: Data acquisition and processing: position, velocity and torque.

After data processing, the software returns the position of the elbow joint in degrees, the velocity in degrees/second, and the estimated torque in the elbow joint in Nm. The estimated torque has been calculated using the biomechanical equations for the human body for the elbow motion (position, velocity and acceleration) and the subject weight and height. These formulas are based on [121] and [122]. The estimated torque considers that the human body is in anatomical position and that it only moves the elbow in flexion - extension.

### 7.1.2 Passive mode

The control strategy used in this mode is based in the BPID controller presented in Chapter 4. In this mode three types of rehabilitation therapy are possible: actuating only in flexion movement, actuating only in extension movement or actuating in flexion-extension movement.

### Flexion movement

To demonstrate the performance of the control algorithm with the exoskeleton, the response of the controlled system provided by the position sensors was compared to the desired reference. This was tested and analysed with two references types: tracking a step and tracking a sinusoidal reference.

#### Step response

Fig. 7.2 shows the angular position reference and the output when the device is mounted in the test bench (see section 4.1.1). It can be observed that the output follows the reference (the steady-state error is zero) and that the system presents an overdamped response. The time to go from 0 to approximately 120 degrees is less than 10 seconds, and the time required to recuperate the initial position is approximately 30 seconds (considering that it is not necessary to get to 0 degrees and is enough to move between 30 and 120 degrees in ADL). In this case, only the flexion actuator was activated and the initial position was recuperated with the aid of the gravity force and the torsion spring placed in the shaft of the exoskeleton. Flexion time can be minimized to approximately 1 second by changing the controller gains. However, the time of the extension movement depends on the recuperation force and the ambient conditions (temperature). It has to be said that this example is an extreme case because the actuator varies from the initial position in martensite phase (at low temperature) to the maximum position in austenite phase (at high temperature). If the position reference does not cover the maximum range of the actuator and the austenite phase is not reached, the time of recuperation remarkably decreases.

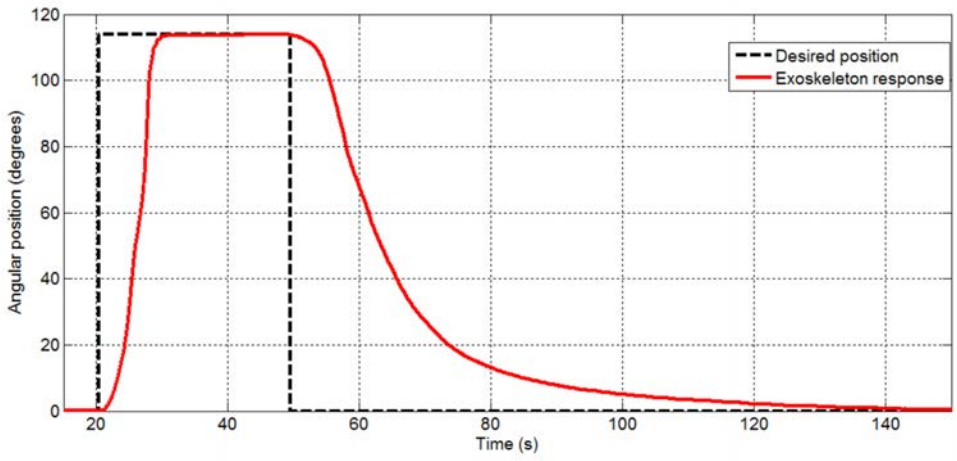


Figure 7.2: Exoskeleton position response to a step reference.

The movement of the exoskeleton is relatively slow in the extension movement and it could only be used in slow rehabilitation tasks, especially during the first phase of the rehabilitation process. A solution could be to increase the total length of the actuator. In this case, the same displacement could be obtained without the maximum range and the recuperation would be faster. This would have an effect on the mechanical structure of the exoskeleton and some parts would need to be adapted.

**Sinusoidal response**

The second test highlights the behaviour of the exoskeleton with a sinusoidal reference signal (Fig. 7.3). In this case, the angular position reference is a sinusoidal signal with an amplitude of 80 degrees and a frequency of 0.2 rad/sec. With the same controller gains, the exoskeleton response is capable of tracking with accuracy the reference signal during the flexion movement. In the extension movement, due to the lack of control (no signal is sent) and the capacity (of the actuator) to recuperate the initial position in the cooling phase, the response presents an elevated error. Besides, this error increases with working time. Due to the frequency of the input signal, the actuator does not have time to dissipate the accumulated heat. According to the actuator response detailed in Section 7.1.2, the system needs approximately 30 seconds to dissipate the accumulated heat. This means that the sinusoidal cycle needs a frequency of 0.046 rad/sec to have an optimal performance. The increase of error shows a linear behaviour, and it is represented in Fig. 7.3 with an orange dashed line.

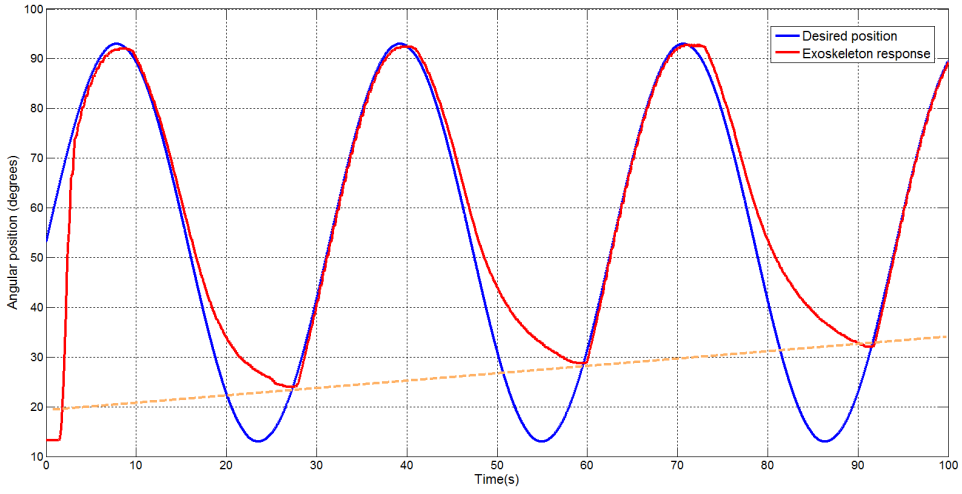


Figure 7.3: Exoskeleton position response to a sinusoidal reference. The orange line represents the error increment through the heat accumulation.

### 7.1.3 Extension movement

In the extension movement, the rehabilitation device is only actuated in the extension movement and the flexion movement it is performed by the patient. This configuration is used with the patients with disorders in extension movements. In this configuration the exoskeleton was tested with a sinusoidal pattern of reference presented in the Fig. 7.4.

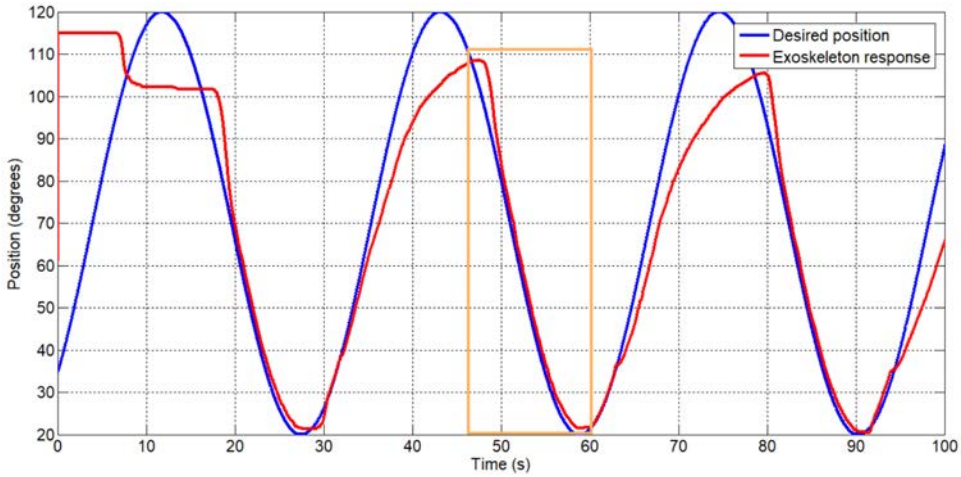


Figure 7.4: Exoskeleton position response to a sinusoidal reference in the extension movement.

In Fig. 7.4 is presented the behaviour of the exoskeleton in the extension movement over a health person. In the orange rectangle, the exoskeleton tracking the extension movement with the aid of the extensor actuator. As can be appreciated the flexion movement is free and in extension movement the actuator forcing the exoskeleton to track with the minimum error the reference.

### 7.1.4 Antagonistic movements

In the antagonistic movements layout, two actuators are configured in the elbow joint: one of them with three SMA wires for the elbow flexion, and the other one with two SMA wires for the elbow extension. Through this design, it is possible to abandon the use of the torsion spring in the elbow joint because the extension movement is made by the actuator. The initial setup includes the torsion spring in the elbow exoskeleton articulation. The next tests have been made with the extension and flexion actuators with sames parameters used in simulation.

Considering the principle of work of this type of actuators presented in Chapter 4, it is necessary to introduce temperature sensors because the information provided

by these sensors is used in the control algorithm. These sensors are placed in the terminals of the actuators to measure the temperature of the wires in real time. The control signal takes into account the temperature of each actuator to avoid the breakage of the wires. Switching control signals from one actuator to another can lead to breakage if the temperature of the wires is not considered. The constraint that is introduced in the model is that, to activate an actuator, the temperature of the antagonist actuator needs to be lower than a value that is fixed empirically (60°C). For example, if the flexion wires are activated with a temperature of approximately 90°C and (suddenly) the control algorithm switches to activate the extension wires with an elevated control signal, the temperature constraint interrupts the signal to avoid breakage.

The control scheme in this case is based on two BPID controllers in parallel (Fig. 7.5). The exoskeleton movement is still controlled in angular position.

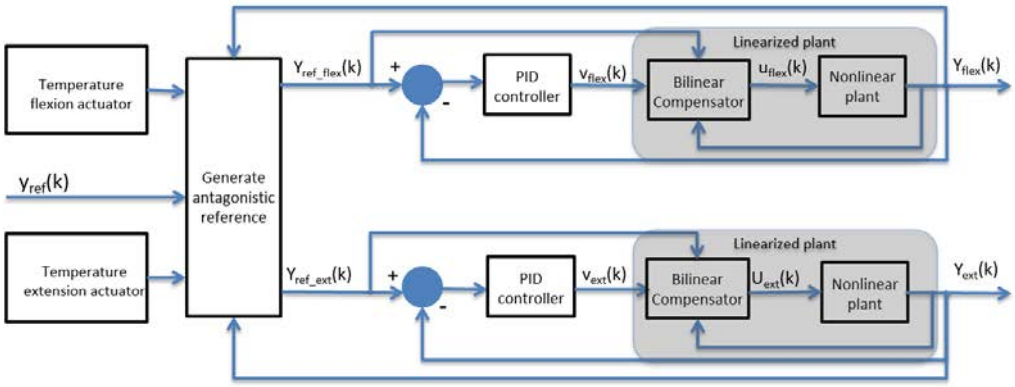


Figure 7.5: Antagonist control scheme with two parallel four-term BPID controllers.

The control algorithm receives only the pattern of reference, which is the desired angular position for the elbow joint. This reference, depending on the actual position (the feedback signal from the position sensor), generates two reference signals for the flexion and the extension movements, respectively. The control signal of one of these two references is fixed to zero, and the other one represents the positive difference between the desired reference and the actual position. The temperature condition intervenes in the control algorithm when the temperature of the antagonist actuator is higher than 60°C (interrupting the control signal). Because of the cooling time and, in order to obtain a continuous movement in the antagonist control approach, it is recommended to use sinusoidal references. For the step reference, a delay equal to the time required to cool the wires may occur. This can be annoying in the rehabilitation

therapy.

Fig. 7.6 displays the response of the exoskeleton in antagonist mode when the pattern of reference is represented by a position sinusoidal signal with an amplitude of 100 degrees and a frequency of 0.2 rad/sec. The antagonist controller achieves a high accuracy when tracking the position reference. Compared to the flexion movement controller presented in Section *Sinusoidal response*, the error in the extension movement is drastically reduced. Moreover, using this type of controller, the rehabilitation therapy does not depend on the position of the forearm, it does not need the gravity force, and the spring torsion force for the extension movement is not required.

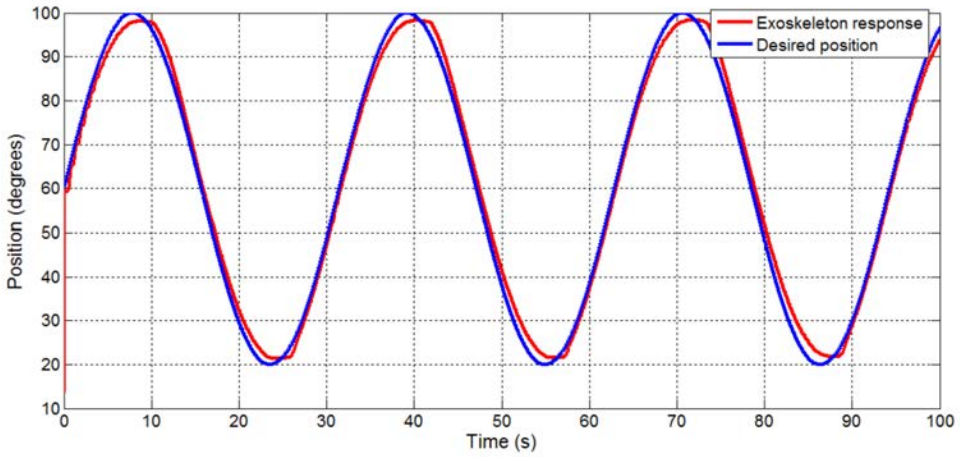


Figure 7.6: The pattern of reference angular position of the exoskeleton and the response of this actuated in antagonist movement.

The control signals corresponding to the two BPID controllers when the pattern of reference is the signal of Fig. 7.6 can be seen in Fig. 7.7. From the general reference (the desired angular position of the exoskeleton), two distinct references are generated for the flexion and the extension movements, respectively. The control signals (PWM) of these references are activated alternatively, the blue signal corresponding to the flexion movement and the red signal corresponding to the extension movement.

In Fig. 7.6, it can be observed that the starting point of the reference is different from the actual position of the exoskeleton. Nevertheless, the system presents a quick response and it reaches the desired position in less than one second. This can be identified in the control signal of Fig. 7.7, showing a greater amplitude in the first part.

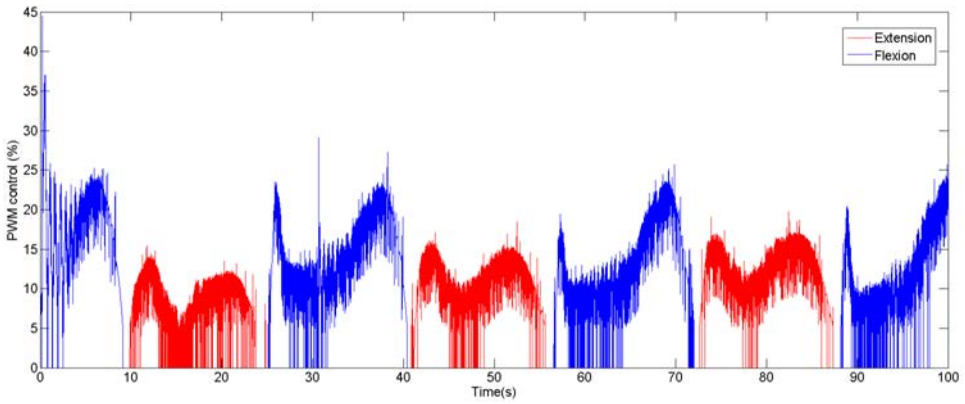


Figure 7.7: Control signal of the antagonist controller corresponding to the reference signal.

### 7.1.5 Active mode

Myoelectric signals (MES) contain information from where data about user movement intention in terms of muscular contraction can be extracted. This information can be detected using surface electrodes (sEMG) [123]. These signals were used in control of prosthetics and rehabilitation devices such a ''on-off" control [124], proportional control in position or assistive torque [125], [126], and distinguish between different kind of motion [127], [128].

This section presents the algorithm used to generate the desired reference in position and torque based on sEMG signals and pressure sensors. The sEMG signals were captured at 1000 Hz frequency with a circuit made in Carlos III University of Madrid. These signals were preprocessed, firstly the raw EMG was filtered with the high-pass filter using a zero-lag fourth-order recursive Butterworth filter to remove movement artifacts, then a full wave rectified was used, and after that in the absolute value was filtered using a Butterworth low-pass filter to cut-off frequency. After this process the algorithm for online calibration overrides the first two seconds (where the used circuit perturbation happens) and uses the next 18 seconds to detect the maximum signal for normalization process. In this time the patient is required to flex the forearm to the maximum. The normalized signal, $E_{norm}$, was calculated with the equation 7.1:

$$E_{norm} = \frac{E_{act} - E_{min}}{E_{max} - E_{min}} \tag{7.1}$$

where $E_{act}$ is the actual sEMG signal, $E_{min}$ is the minimum value of the sEMG signal in the first 20 seconds and $E_{max}$ is the maximum value of the sEMG signal in the first 20 seconds.

In order to generate the position reference pattern with a good precision, two

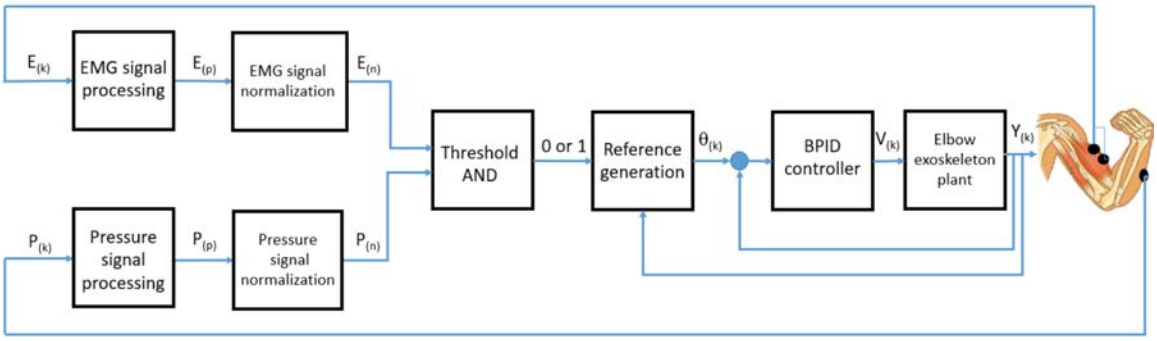


Figure 7.8: High level control of the exoskeleton based on sEMG signals

types of signals have been used, the sEMG normalized signal and the pressure sensor signal. These two signals were logically compared to detect the intention of movement. The binary result in function of the actual position of the joint generates a position reference using two type of increment: one for fast actuation (used when the actual position of the elbow joint is different to the position of the actuator reference) and another increment used to generate the reference pattern following the sEMG normalized signal over the threshold value.

In Fig. 7.8 is presented the high level control algorithm of the exoskeleton based on surface sEMG signals, for active rehabilitation therapies with the reference pattern generated in position.

Here the signals represent:

- $E_k$ represents the sEMG signal of the biceps muscle.
- $P_k$ represents the pressure signal of the sensors which will be placed between the human arm and the exoskeleton.
- $E_p$ represents the processed sEMG signal. Here the signal is filtered and passed to absolute value.
- $P_p$ represents processed pressure signal after calibration.
- $E_n$ represents the normalised sEMG signal after calibration. The calibration time default is 20 seconds.
- $P_n$ represents the normalised pressure signal after calibration.
- $\theta_k$ is the desired angle for the elbow exoskeleton generated by the sEMG and pressure signal.

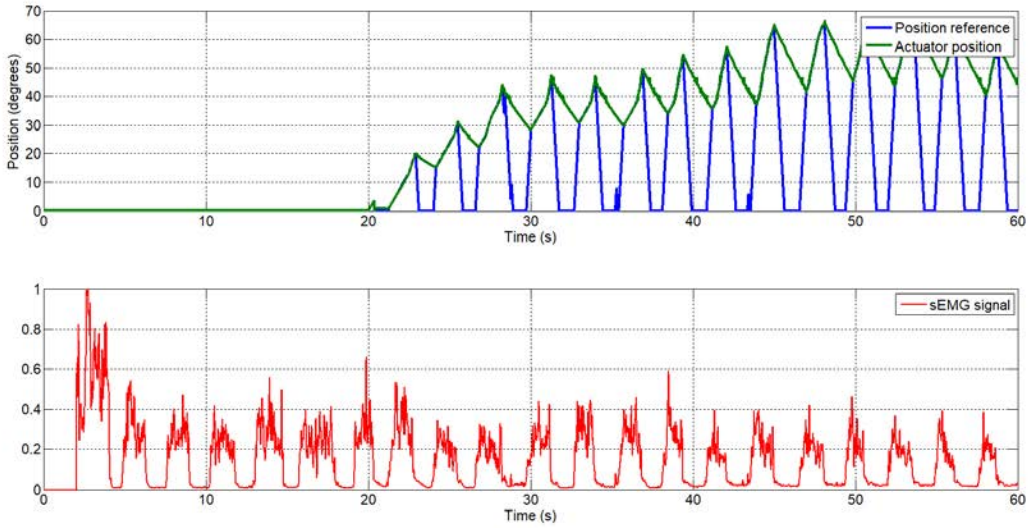


Figure 7.9: The generated position reference by the sEmg signal in simulation.

- $V_k$ is the PWM control signal for the exoskeleton actuators.
- $Y_k$ is the real exoskeleton angular position.

The torque reference pattern consist an assistance torque (a certain percentage of the required torque for mobilization of articulation) from the exoskeleton for the rehabilitation therapy. The reference pattern (torque reference), is calculated in function of the biomechanical model of the human body and the exoskeleton parameters. The biomechanical model of the human body, estimate the necessary torque to mobilization the elbow in function of the patient position, weight and height. In function of this torque and the sEMG signal, a percentage of assistance in torque was generate such input reference. This is directly proportional with the sEMG signal, a decision if the patient want to continue with the movement.

### Results in simulation

The first results of the two algorithms were tested in the simulation with the SMA actuator model presented in 4.4.2. For the sEMG data acquisition, the electrodes were placed along the biceps muscle fibers and on the midline of the belly of the muscle, considering that the sEMG signals have the greatest amplitude.

In Fig. 7.9 the generated reference in function of the sEMG signal in simulation is shown. Here the red signal is the sEMG signal normalized between 0 and 1. The position reference pattern was generated in function of this sEMG signal and the

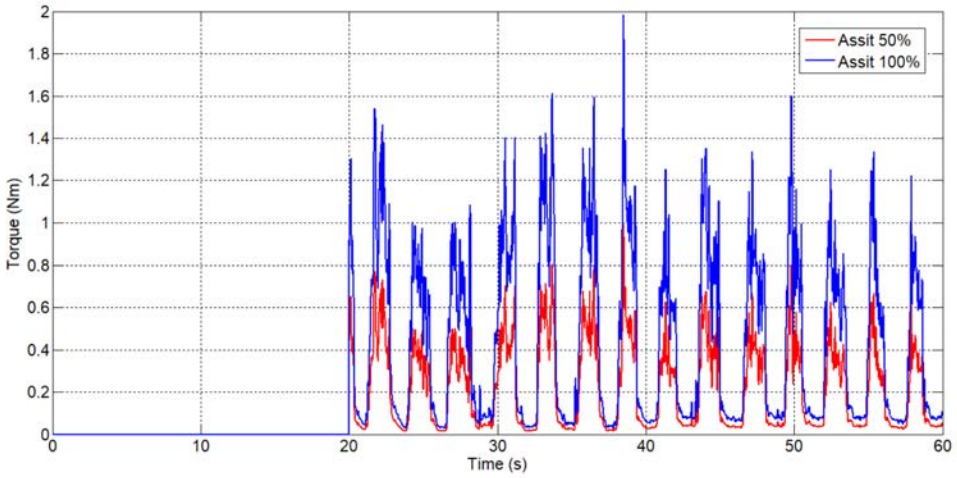


Figure 7.10: The generated torque reference by the sEmg signal in simulation.

actual position of the actuator which coincides with the angular position of the SMA exoskeleton. The first 20 seconds were ignored for online calibration of the algorithm.

In the torque assist movement, the reference was generated in function of the biomechanical model of the human body considering that the rehabilitation is executed standing or sitting, and in function of the sEMG signal placed over biceps muscle. A similar idea is presented in [125] but there, they do not take into account the biomechanical structure of the human body.

In Fig. 7.10 was presented the pattern reference in torque assist for one patient with mass of 70 kg and a height of 1.73 m in two cases: the exoskeleton assists the patient with the total torque, 100% (blue signal) and the exoskeleton assist with 50% of the total torque (red signal).

### 7.1.6 Results with the real SMA exoskeleton

The EMG based control algorithm was tested with the real elbow SMA based exoskeleton with two DOFs presented in Chapter 6 generating the position reference. This was tested with a healthy person of 1.73 height and 70 kg weight. The results of the test can be seen in Fig. 7.11.

In Fig. 7.11 was presented the reference position signal (blue signal) generated by the sEMG signal (green signal) and the real position exoskeleton (red signal). In the first $t_c = 20 seconds$ the exoskeleton user calibrates the algorithm doing movements of flexion-extension of the elbow joint. After calibration, when the algorithm detects the movement intention this starts to generate the reference position for the control algorithm, which follows the reference with the exoskeleton.

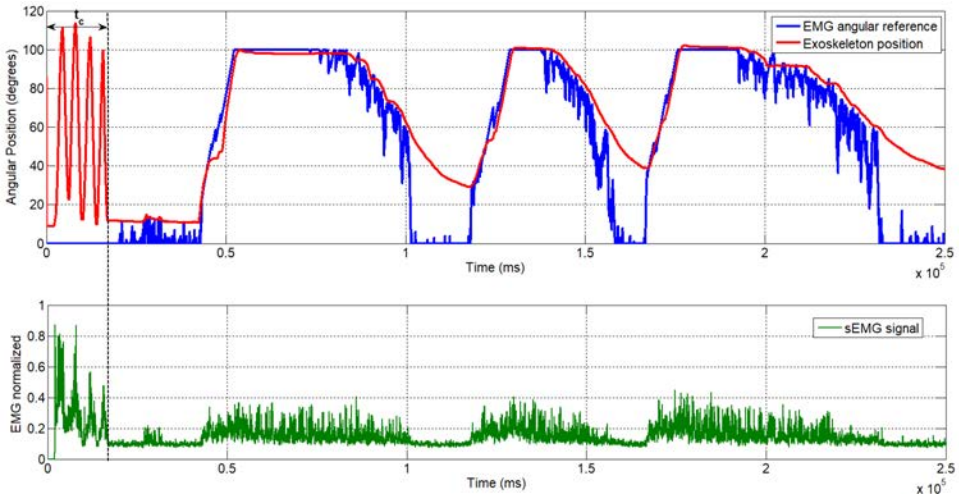


Figure 7.11: Position reference and response generated by the sEMG signal

In all these tests the pressure sensor signal is not present and the variable algorithm of this was set to "active", which mean that the reference is generated only with the EMG signal. Inserting the pressure signal, the precision of the control algorithm in intention of movement increase.

## 7.2 Elbow exoskeleton characteristics

In this section are presented the characteristics of the elbow SMA exoskeleton with two DOFs in terms of usability in the rehabilitation therapy. The exoskeleton permits the rehabilitation therapy for the elbow with two DOFs: flexion-extension and supination-pronation.

- In flexion-extension the exoskeleton can be operated between 0 and 150 degrees (for patient safety, the exoskeleton is mechanically restricted between these values). Usually, it is expected that the exoskeleton works similarly as in ADL, doing one movement between 30 and 120 degrees.

- In prono-supination the human forearm can be moved between 71 degrees of pronation and 81 degrees of supination. The exoskeleton is mechanically restricted and actuated on 50 degrees of pronation and 50 degrees of supination.

Mechanically the elbow SMA exoskeleton consists of a simple and comfortable structure, which permits a fast collocation over human body. The necessary time for collocation is approximately one minute. Default the exoskeleton is set for a person

of approximately 1.70 - 1.75 m height, but can be easily adjusted for persons of 1.40 m to 1.80 m.

The electronic hardware is based on the STM32F407VG microcontroller which manages the controls algorithms for all actuators, and the exoskeleton sensors: for the angular position, actuators temperature and EMG. The microcontroller, EMG hardware and power stage for the actuators is placed in a box with the dimension of 16x15x5cm and 0.1 kg weight.

The entire exoskeleton structure with the actuators and hardware box have a weight of 0.96 kg. The Power Supply necessary to provide the energy to the actuators (A 960 W DIN Rail Power Supply 24Vdc/40A), has a weight of 1.9 kg. The exoskeleton is considerate portable, can be easily transported from one place to another but needs to be connected to the electrically network.

### 7.2.1 Therapy with the exoskeleton

The proposed process therapy with the elbow SMA exoskeleton starts with the collocation of the exoskeleton over the human body. After that, the rotation axis of the elbow and the exoskeleton need to remain aligned, the set points with the human body can be modified in function of the patient to align the axis. After this process of adjustment the therapy can start with the data acquisition (without actuation) to evaluate the patient. In this case information such as angular position and frequency are necessary to define the passive and active rehabilitation therapy trajectories. On the other hand, in data acquisition mode, the necessary data is saved for the medical stuff to evaluate the patient. In this mode the available information is the angular position, velocity and the estimated elbow torque of the patient (it is considered that the therapy is done while standing).

The exoskeleton permits two types of therapy's in passive respectively active mode.

- In passive mode can be chosen between three types of actuations: flexion , extension or flexion-extension. In flexion respectively extension movement the exoskeleton is tested with a sinusoidal trajectory with an amplitude of 60 degrees, bias 60 degrees ( between 0 and 120 degrees) and a frequency of 0.2 rad/sec (0.0318Hz). With this configuration a good result is guaranteed and the session time of therapy don't be exceed 240 seconds. The time between the sessions (necessary to cooling the actuators) need to be between 5 and 10 minutes in function of the ambient temperature. If the session exceeds 8 cycles (240 seconds), the actuator is not capable to recuperate the initial shape because the heat accumulation and introduces in extension (when actuate in flexion) or flexion (when actuate in extension) a increasing error with each cycle, approximately 5 degrees/cycle. This error is directly proportional with the frequency.

In flexion-extension, due to the actuation in the flexion respectively extension movement a heat accumulation in the two actuators occurs, this restricts the system to maximum 5 cycles of movement at a frequency of 0.2rad/sec. After this period, similar as in the case of flexion or extension movement, the actuators need to cool during 5 -10 minutes. If the systems is not stopped after 5 cycles the two actuators don't recuperate the initial shape and can rupture easily. In this case due to the antagonistic actuation the position error is minimal.

- In active mode the exoskeleton tracks a reference generated by the EMG signal. This means that the patient needs to present muscular activity which can be read with the sEMG electrodes. This mode is tested in the flexion movement, placing the sEMG over the biceps muscle. The set-up of this therapy mode, after the exoskeleton collocation and the patient evaluation, implicate the calibration of the algorithm, where the patient during 20 second needs to do flexion and extension movements and after that in function of the normalized EMG amplitude, the threshold can be set to change the sensitivity of reference generation. Similar such as in passive mode, after 8 cycles the system need to stop for the actuators cool down.

## 7.3 Tests with healthy people

A series of tests was carried out with the exoskeleton and some volunteers from the RoboticsLab laboratory from UC3M. The subjects (two males and one female) with age between 20 and 40 years old. The necessary data such as weight, height and other data for each subject is presented in the Table 7.1.

Table 7.1: Subjects.

| Subject number | Gender | Age | Weight | Height |
|---|---|---|---|---|
| 1 | male | 23 | 75 | 1.73 |
| 2 | male | 40 | 75 | 1.75 |
| 3 | female | 20 | 70 | 1.7 |

The tests are similar with patients in rehabilitation therapy, data acquisition was done to evaluate the subjects and afterwards have been achieved a rehabilitation therapy in passive mode was done.

### 7.3.1 Data acquisition mode

After the exoskeleton collocation over human body and adjustment in function of each subject, the subjects were asked to realize two cycles of flexion - extension. It

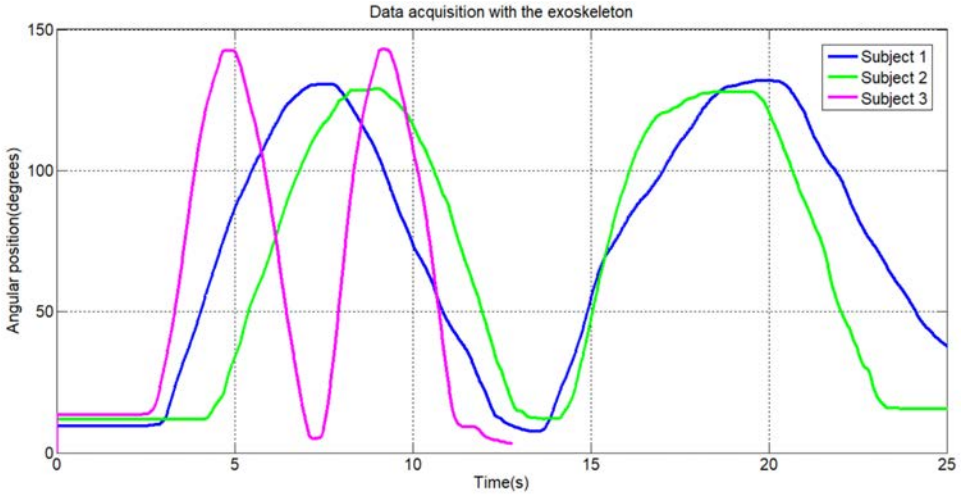


Figure 7.12: Data acquisition - angular position

can be highlighted that for the subjects 2 and 3 at is the first time they tests the exoskeleton and don't have previous experience with this type of devices. After data acquisition with the exoskeleton, the angular position of each subject can be seen in the Fig. 7.12.

In function of the body structure of each subject, it can be observed that the first two subjects realize a flexion - extension movement between 20 to approximately 130 degrees and the third subjects reaches a higher amplitude, approximately 145 degrees. These data are important to set the maximum values of the rehabilitation trajectories and this way the patient's discomforts and pain is avoided. Here, the healthy subjects reach higher amplitude but in the case of patients with flexion - extension movement disorders they present a limited amplitude and in function of the therapist indication, the rehabilitation therapy trajectory grows gradually.

The same environment of data acquisition offers the possibility to analyse the angular velocity of the elbow. For the same movement presented in the Fig. 7.12, the corresponding angular velocity is presented in Fig. 7.13. The first two subjects presents low velocities, making slow movements and the last subject realizes the movement faster. With this option, the evolution of the patient in time can be analysed.

Due to the fact that the therapy tests were done while standing, in function of the characteristics of each subject (weight and height) with the aid of the biomechanical model, the torque in the elbow can be estimated. These results can be seen in the Fig. 7.14.

These results represent an estimated torque in function of the forearm position and the biomechanical upper limb model. For this estimation no pressure or force

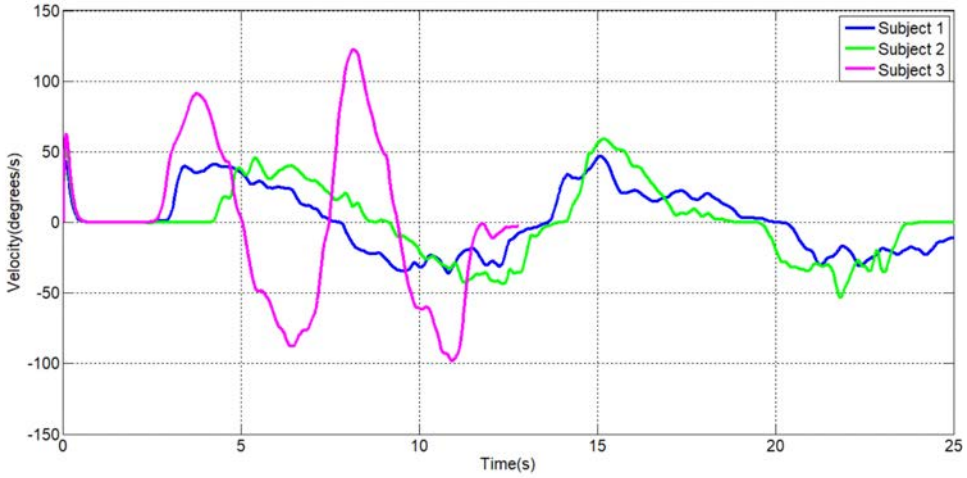


Figure 7.13: Data acquisition - angular velocity

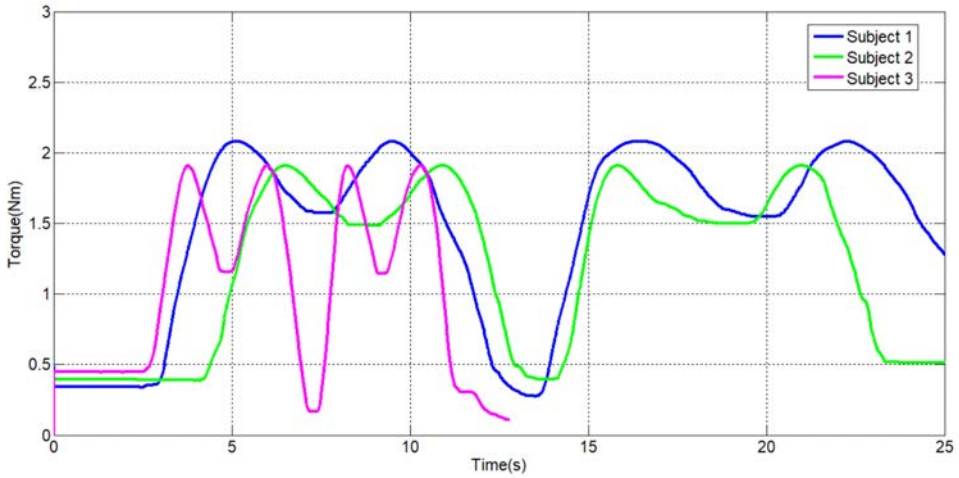


Figure 7.14: Data acquisition - torque estimation

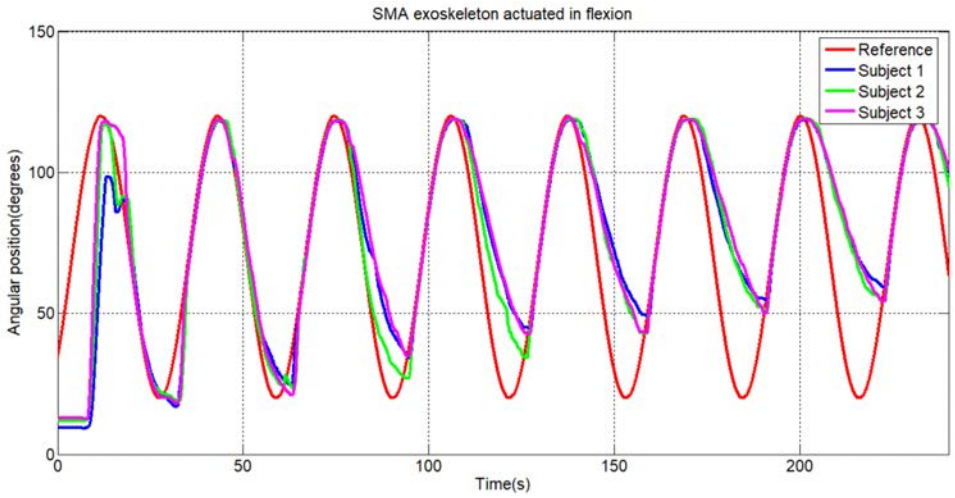


Figure 7.15: Flexion movement - angular position

sensors were used.

### 7.3.2 Passive mode

In the passive mode, the three types of therapies are tested: flexion, extension and felxion - extension.

#### Flexion movement

In flexion movement, the rehabilitation trajectory is represented by the sinusoidal movement between 20 and 120 degrees and with a frequency of 0.2 rad/sec. In this case only the flexion actuator is activated and the extension movement is done by the subject with the aid of the gravity force. The results can be seen in the Fig. 7.15.

In flexion movement the exoskeleton and in the same time the elbow track the desired reference during the 8 cycles, approximately 240 seconds. Due to the heat accumulation and the lack of actuator extension, in the extension movement an error which increase in time can be observed. If in the first cycle this error is minimal, in the last cycles this grows with approximately 30 degrees.

The PWM signals for each subject can be seen in Fig. 7.16. The heat accumulation can be observed in the control signal, if in the first cycles the control signal still 100% in the last cycles this decreases, being necessary to heat less to track the reference. In function of the biomechanical characteristics the necessary torque to the articulation mobilization is variable for each subject. This variation can be observed in the control signal, the pink signal corresponds to the female subject with less weight, which

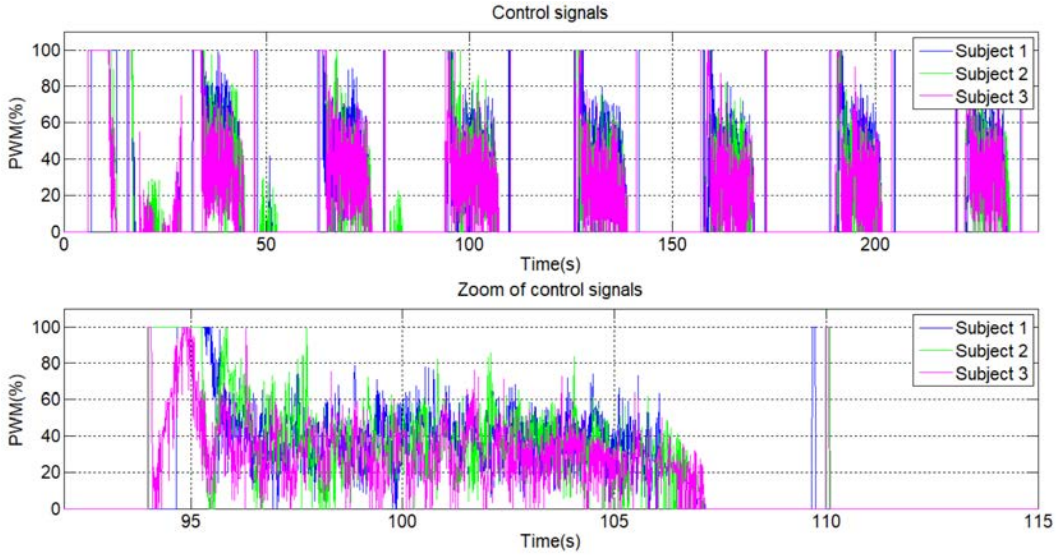


Figure 7.16: Flexion movement - PWM control signals

implicates less torque to mobilize the joint. This is observable presenting a lower amplitude.

### Extension movement

In extension movement the exoskeleton is actuated only in the movement of extension. In this case the actuator of flexion is not actuated and the user of the exoskeleton needs to do the flexion movement. In the extension movement the exoskeleton assists the user to track the position reference. The tests with the subjects, 8 cycles and respectively 5 cycles can be observed in the Fig. 7.17.

In Fig. 7.17 are presented the response signals in angular position of the extension therapy for the healthy subjects where in the flexion movement the subject doesn't have assistance and realize only the movement and in the extension movement the exoskeleton is actuated and obligates the subject to track the reference.

The corresponding control signal of the extension movement is presented in Fig. 7.17 can be observed in Fig. 7.18.

### Flexion-extension movement

The last passive therapy mode is represented by the flexion-extension movement. In this mode both movements are actuated in the antagonistic with two actuators in function of the control algorithm presented in the Section 7.1.4. The results with subjects test of the exoskeleton controlled in position can be seen in Fig. 7.19. Here

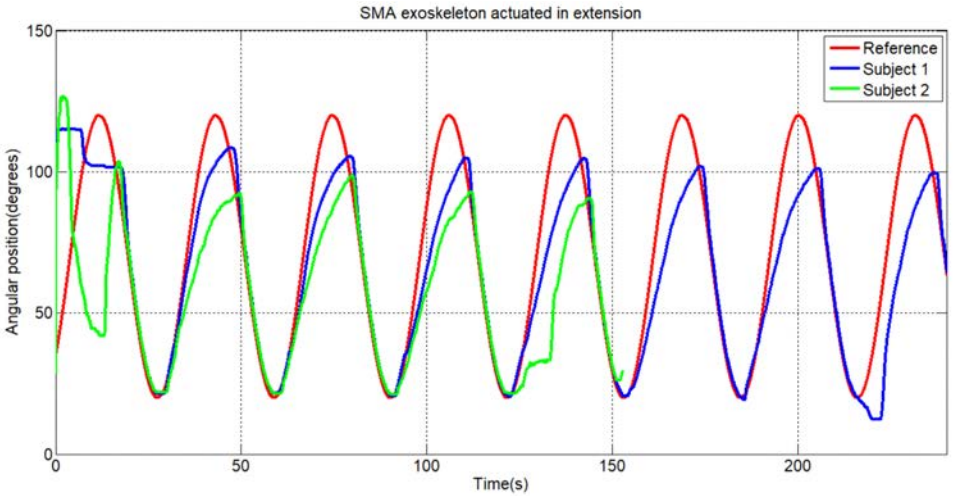


Figure 7.17: Extension movement - angular position

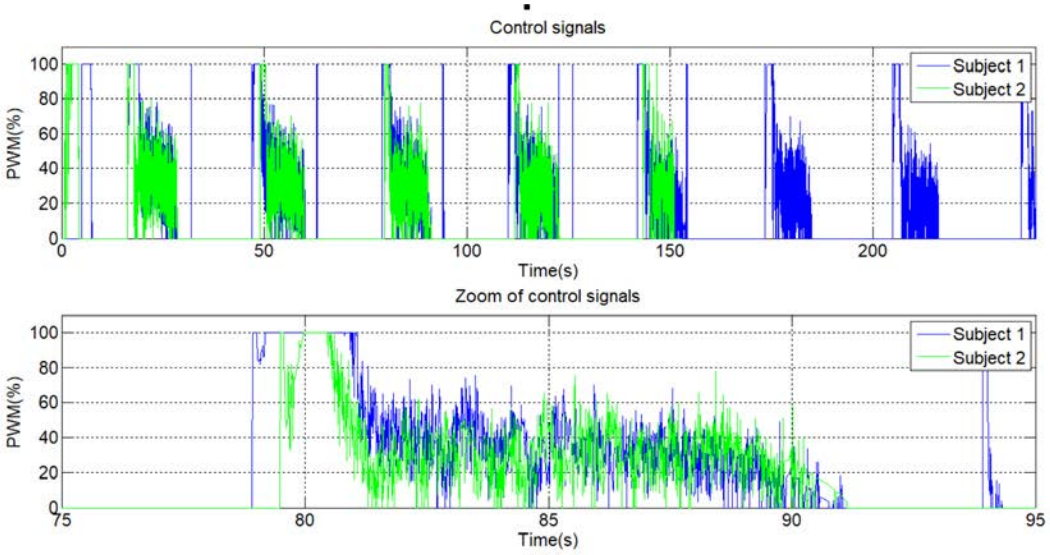


Figure 7.18: Extension movement - PWM control signals

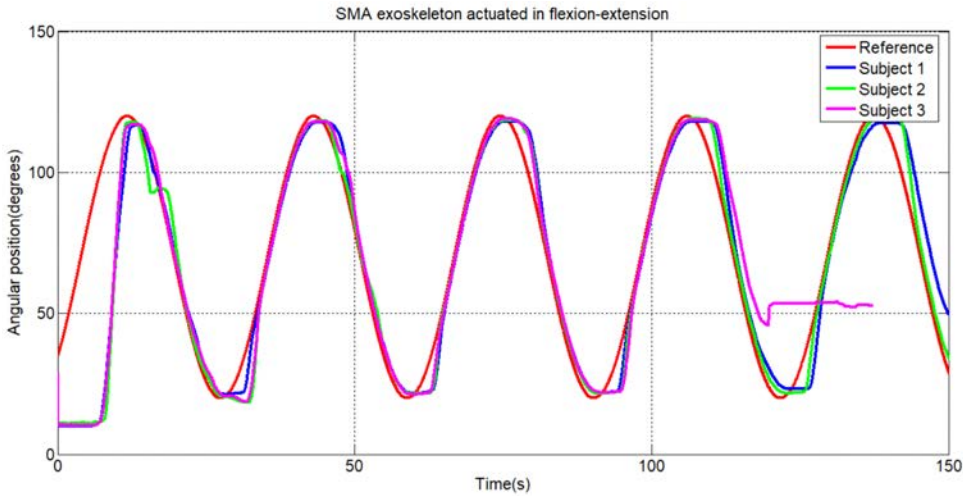


Figure 7.19: Flexion - extension movement - angular position

the actuation time is limited due to the heating of the actuators, and in this case the tests are done during 5 cycles respectively 4 cycles.

The control signals of the flexion and extension actuators can be seen in the Fig. 7.20. Similar with the flexion and extension movement this presents a higher consumption in the first cycle where the actuators are cold and in the last cycle where the both actuators are warm and resist each other during the movement.

## 7.4 Validation tests with patients

The exoskeleton documentation with its characteristics and operation mode have passed the ethics committee of research from Rey Juan Carlos University of Madrid which a favorable response. This certificate gives the possibility to do test for device functionality evaluation with patients. The tests currently are ongoing, searching patients in various centres of rehabilitation such as Lambecom group from Rey Juan Carlos University of Madrid, Hospital Rey Juan Carlos from Mostoles and San Vicente Clinic of Mirasierra. In this section the first results with a patient will be exposed.

A female patient from Lambecom group from Rey Juan Carlos University of Madrid tested the rehabilitation device. Her has suffered an ischemic stroke in the left middle cerebral artery territory which have produced a right hemiparesis in the upper limb.

The test start with the data acquisition for evaluate the patient. For this reason some data was needed from the patient: female, 48 kg weight, 1.55 m height. This data are used for inverse dynamic analysis of the elbow joint.

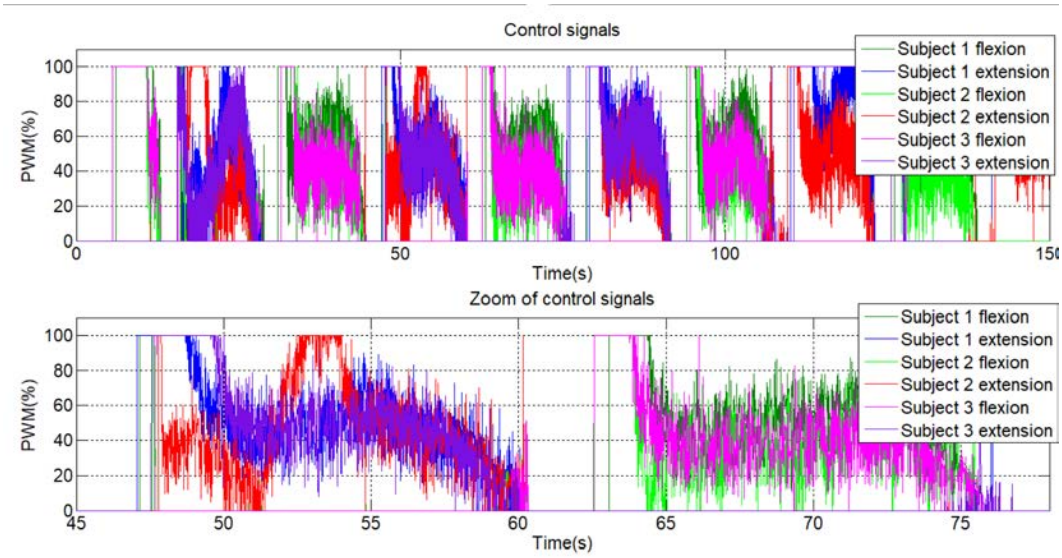


Figure 7.20: Flexion - extension movement - PWM control signals

### 7.4.1 Data acquisition mode

The first step after the exoskeleton was collocated over the human body of the patient, consist in evaluate the patient for set the therapy tasks. In this case, the patient was asked to do some flexion - extension movements (without forcing the elbow joint). In this sense, the maximum and minimum position angle was saved. As can be appreciated in Fig. 7.21, the patient is in an advanced state of rehabilitation, can doing slow movements between 20 and 140 degrees.

The angular velocity of elbow joint during the data acquisition process can be seen in the Fig. 7.22.

In function of the patient characteristics, biomechanical model and the data from the sensors have been estimated the torque of the elbow joint. The result of this estimation can be seen in Fig. 7.23.

### 7.4.2 Passive mode

#### Flexion movement

Similar to the tests with healthy people, the rehabilitation trajectory is represented by the sinusoidal movement between 20 and 120 degrees and with a frequency of 0.2 rad/sec. In the flexion movement only the flexion actuator is activated and the extension movement is done by the patient with the aid of the gravity force. The angular position of the elbow joint following the sinusoidal reference can be seen in

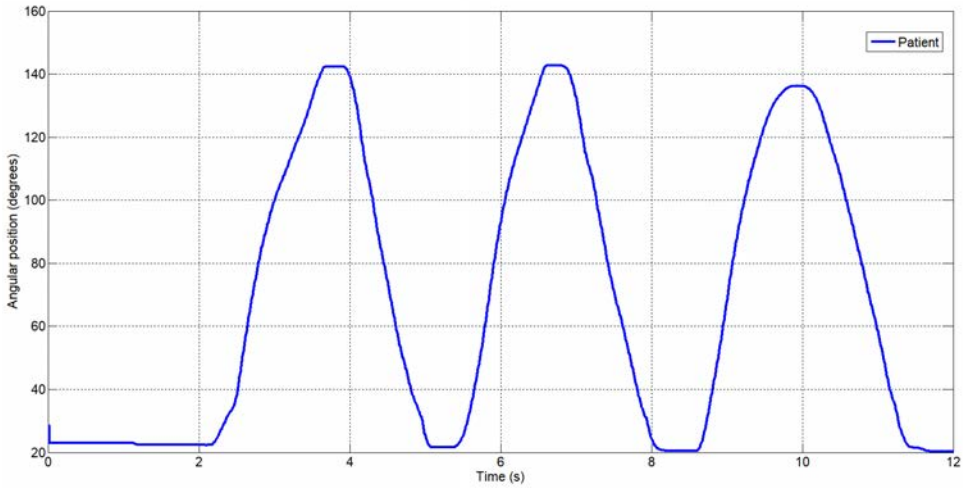


Figure 7.21: Data acquisition - angular position

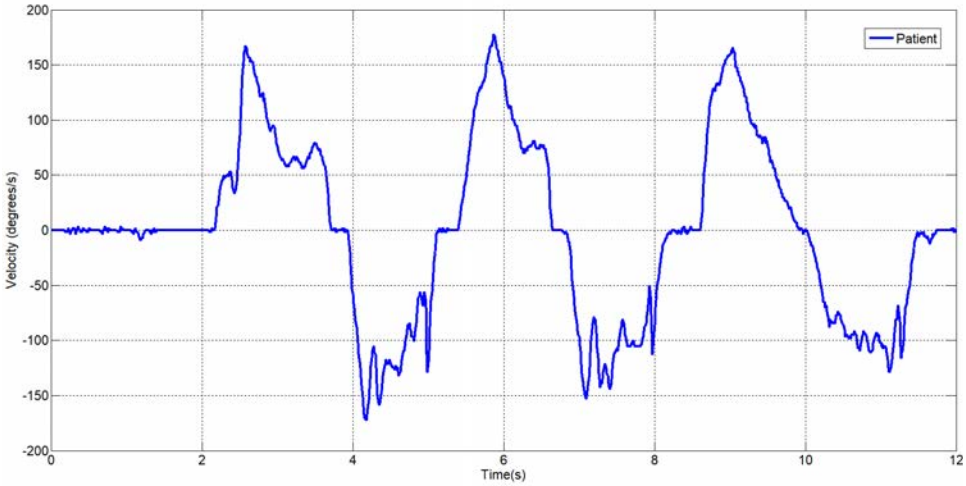


Figure 7.22: Data acquisition - angular velocity

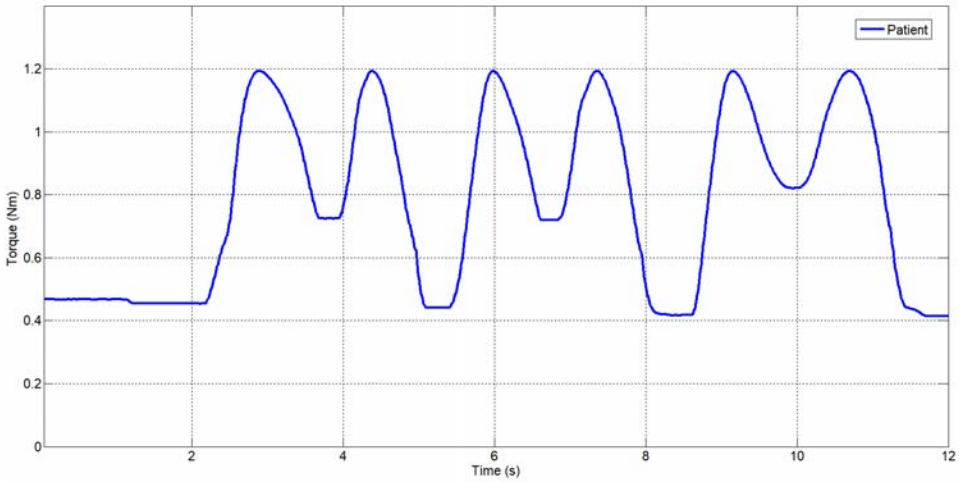


Figure 7.23: Data acquisition - elbow torque

Fig. 7.24.

The control signal corresponding to the flexion movement presented in Fig.7.24 can be seen in Fig. 7.25.

**Flexion - extension movement**

The second test was done in flexion - extension movement. In this case the flexion respectively extension actuators were activated ensuring that the elbow joint done a sinusoidal movement between 20 and 120 degrees. The angular position of the elbow joint following the sinusoidal movement can be seen in Fig. 7.26.

The control signal corresponding to the flexion - extension movement can be seen in Fig. 7.27.

After the tests, the patient was prayed to complete the Quebec questionnaire, only the first 8 questions, regarding with the rehabilitation device. The response corresponded with a number between 1 and 5 where 1 not satisfied at all and 5 very satisfied. The results was:

1. the dimensions (size, height, length, width) of your assistive device?
   **5**

2. the weight of your assistive device?
   **5**

3. the ease in adjusting (fixing, fastening) the parts of your assistive device?
   **5**

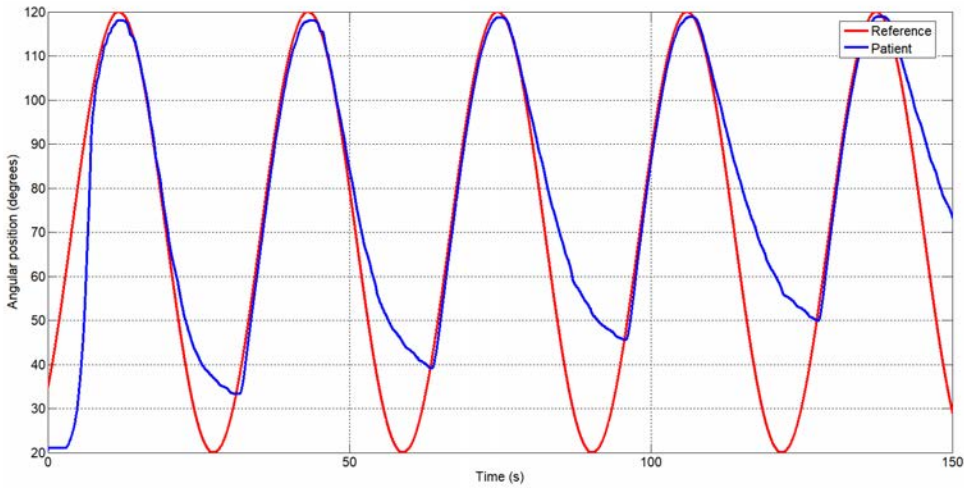


Figure 7.24: Flexion movement

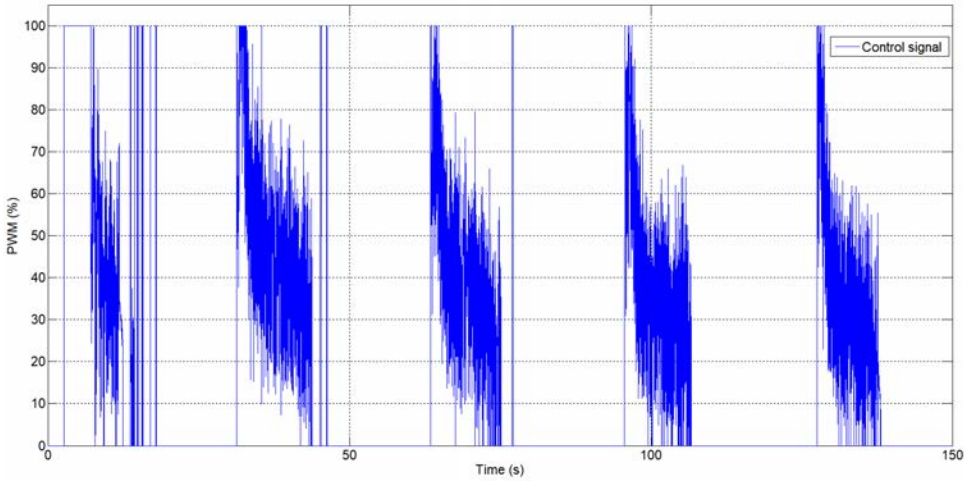


Figure 7.25: Flexion PWM signal

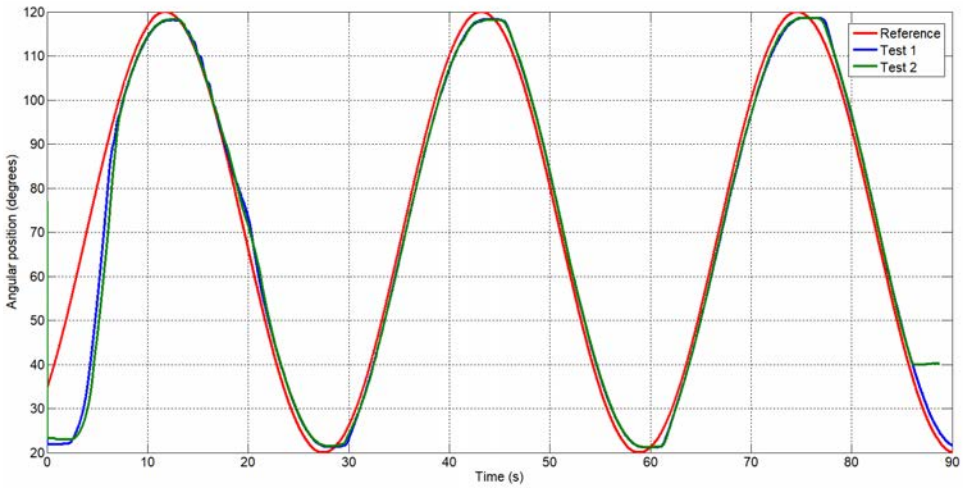


Figure 7.26: Flexion -extension movement

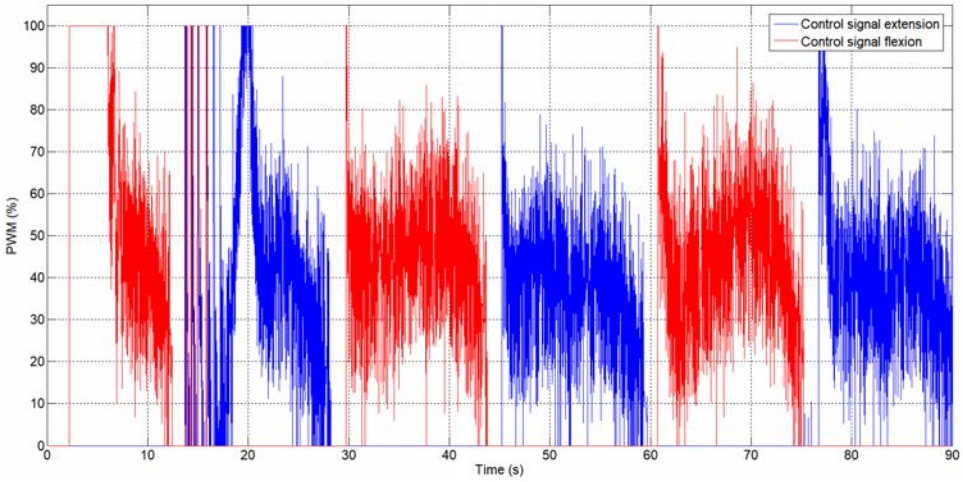


Figure 7.27: Flexion-extension PWM signal

4. how safe and secure your assistive device is?
   **5**

5. the durability (endurance, resistance to wear) of your assistive device?
   **5**

6. how easy it is to use your assistive device?
   **3**

7. how comfortable your assistive device is?
   **5**

8. how effective your assistive device is (the degree to which your device meets your needs)?
   **4**

It is worth mentioning that the patient which used the exoskeleton don't interacted with the settings program for therapy. For this reason on the question number 6 she told us that she cant answer exactly. On the question number 8, due to the patient was in an advanced stage of therapy she don't considerate the exoskeleton very useful but she strongly recommend for patients in the first and middle stage of therapy.

# Chapter 8

# General conclusions and future works

## 8.1 General conclusions

The disorders provoked after ACV, SCI or other neuromuscular injuries, leave behind traumas at the neuromuscular and muscular levels which affect the motor level and hinder the normal ADL of the person who suffered the trauma. This disorder of motor level can be totally or partially recovered thanks to a rehabilitation therapy which consists largely in repetitive movements with a aid of the therapist. Robotic rehabilitation come as an aid to the therapist. The rehabilitation device demonstrated an good acceptance factor by the patients and involve a financial cost reduction over time, more accuracy, effective and fast rehabilitation and a better patient involvement in the rehabilitation therapy. Nevertheless, the rehabilitation device can be improved in terms of fabrication costs, efficiency in the rehabilitation therapy, weight, dimensions (portability) and comfort.

The overall aim was to offer new actuation solutions for the rehabilitation devices from the category of non-linear actuation systems and generate a simulation environment where the actuation system can be tested with together human body and the interaction behaviour can be analysed. A new design based on the proposed actuator for upper limb rehabilitation is proposed and tested in simulation and with real persons.

In this work, were analysed two types of non-linear actuators (USM and SMA materials) which were proposed as an alternative solutions for actuation systems for rehabilitation devices. In function of the relation force-weight, and the joints of interest, the use of the USM was dropped (in the joints such elbow and shoulder) and the SMA based actuator was chosen as main candidate (Chapter 4). For each type of actuator, was developed a simulation model and a control algorithm which was tested in a test bench. For the SMA based actuator different mechanical configurations were analysed in terms of frequency response and energy consumption.

To analyse the behaviour of the proposed actuator together with the human body component, a simulation environment based in BoB forward dynamics was developed. This simulation tool permit to simulate the mechanical structure of the exoskeleton with the actuator, his control algorithm, and human body component. The forward dynamic version of the BoB permits to vary the muscle force and in this way simulates the patients with partial disorders in the motor function. This is done thanks to developed algorithms capable of compensating this missing force with the aid of the exoskeleton (Chapter 5).

A novel design of a segmented exoskeleton for the upper limb rehabilitation and patient evaluation based on SMA actuators was proposed. This consists in a separately exoskeleton for each upper limb joint: for shoulder (3 DOF, where two are actuated and one is passive), for the elbow joint (two proposed designs with 1 DOF

respectively 2 DOF) and for the wrist with 2 DOF (Chapter 6). This designs represent an alternative solution for the current rehabilitation upper limb exoskeletons which compared with these, is characterized by low weight, a low fabrication cost, presents a noiseless operation and is easy to use.

The elbow SMA based exoskeleton with 2 DOF presents three mode of operation: data acquisition mode necessary for the patient evaluation and therapy set-up, passive mode where three type of assisted rehabilitation mode are available: flexion movement, extension movement and in flexion-extension movement, and active mode where the position reference is generated by the muscle activity (Chapter .7). A pilot study with health subjects in the UC3M RoboticsLab was done to highlight the features of the rehabilitation therapy with the exoskeleton. Moreover the exoskeleton was tested successfully in the Lambecom Group of Rey Juan Carlos University of Madrid, with one patient which suffered an ischemic stroke and after this trauma presents a hemiparesis of the right upper limb.

### 8.1.1 Contributions of the dissertation

This dissertation has made the following contribution to the field:

- A review of commercial rehabilitation devices for the upper limb.
- A novel actuator design based on SMA for rehabilitation devices
- A simulation environment which gives the possibility to analyse the behavior between the rehabilitation device and the human body component.
- The first exoskeleton based on SMA actuators which gives the possibility to minimize the total weight of the device, presents a noiseless operation and reduces the fabrication costs.

### 8.1.2 Publications

#### Journal Publications

- **D. Copaci**, E. Caño, L. Moreno, and D. Blanco *New design of a soft-robotics wearable elbow exoskeleton based on Shape Memory Alloy wires actuators*, Applied Bionics and Biomechanics, 2017.
- A. Flores, **D. Copaci**, Á. Villoslada, D. Blanco, L. Moreno *Sistema Avanzado de Protipado Rápido para Control en la Educación en Ingeniería para grupos multidisciplinares*. Revista Iberoamericana de Automatica e Informatica Industrial (RIAI), 2016.

- A. Villoslada, A. Flores, **D. Copaci**, D. Blanco, L. Moreno, *High-displacement flexible Shape Memory Alloy actuator for soft wearable robots.* Robotics and Autonomous Systems, 2015.

- A. Flores, **D. Copaci**, D. Blanco, L. Moreno, J. Herrán, I. Fernández, E. Ochoteco, G. Cabañero, H. Grande *Innovative Pressure Sensor Platform and its Integration with an End-User Application.* Sensors 06/2014; 14(6). DOI:10.3390/s140610273.

**Book Chapters**

- **D. Copaci**, A. Flores, F. Rueda, I. Alguacil, D. Blanco, L. Moreno, *Wearable elbow exoskeleton actuated with Shape Memory Alloy.* Converging Clinical and Engineering Research on Neurorehabilitation II, 10/2016.

- **D. Copaci**, A. Flores, D. Blanco, L. Moreno, *Shoulder exoskeleton for rehabilitation actuated with Shape Memory Alloy.* RoboCity16 Open Conference on Future Trends in Robotics, chapter 5, 05/2016.

**Conference Proceedings**

- **D. Copaci**, D. Blanco, L. Moreno *Wearable elbow exoskeleton actuated with Shape Memory Alloy in antagonist movement.* Joint Workshop on Wearable Robotics and Assistive Devices, International Conference on Intelligent Robots and Systems. IROS 2016, Daejeon, Korea; 10/2016.

- **D. Copaci**, D. Blanco, I. Guerra, S. Collado-Vazquez, M. Pérez De Heredia, *Exoesqueleto actuado por SMA para movilización de la muñeca*, XXXVI Jornadas de Automática, Madrid, 2016.

- I. Alguacil, E. Monge, **D. Copaci**, D. Blanco, M. Pérez De Heredia, S. Collado-Vazquez *Diseño de un Exoesqueleto por Segmentos para Evaluación y Tratamiento del Miembro Superior* 54 Congreso Nacional de la Sociedad Española de Rehabilitación y Medicina Física (SERMEF), 2016 *(Poster).*

- **D. Copaci**, A. Flores, Á. Villoslada y D. Blanco, *Modelado y Simulación de Actuadores SMA con Carga Variable*, XXXVI Jornadas de Automática - 2015, Bilbao, 2015.

- **D. Copaci**, A. Flores, D. Blanco, F. Martin. *Modelado de motores USM para robotica de rehabilitacion.* XXXV Jornadas de Automática; 09/2014.

- **D. Copaci**, A. Flores, D. Blanco, L. Moreno *Herramienta de simulacion para el desarrollo de exoesqueletos basada en Matlab-Simulink.* XXXV Jornadas de Automática, Valencia, 3-5 Septiembre 2014; 09/2014.

- **D. Copaci**, A. Flores, J.C. Garcia-Pozo, D. Blanco *Simulacion de la mano humana mediante Matlab/Simmechanics.* XXXV Jornadas de Automática; 09/2014.
- **D. Copaci**, A. Flores, A. Martin, D. Blanco, L. Moreno *Ultrasonic Motor Based Actuator for Elbow Joint Functional Compensation.* ROBOT2013: First Iberian Robotics Conference, Madrid; 11/2013.
- A. Flores, **D. Copaci**, A. Martin, D. Blanco, L. Moreno *Smooth and Accurate control of multiple Shape Memory Alloys based actuators via low cost embedded hardware*, International Conference on Intelligent Robots and Systems. IROS 2012.
- A. Martin, A. Flores, D. Blanco, **D. Copaci**, L. Moreno *Lightweight Magnetorheological Based Clutch Actuator for quick response times.* ACTUATOR 2012 13th International Conference on New Actuators, Bremen, Germany; 06/2012.
- A. Martin, A. Flores, D. Blanco, **D. Copaci**, L. Moreno *Elbow functional compensation using a lightweight magnetorheological clutch.* Annual International Conference of the IEEE Engineering in Medicine and Biology Society. IEEE Engineering in Medicine and Biology Society. Conference 08/2011; 2011. DOI:10.1109/IEMBS.2011.6091290.

### 8.1.3 Other dissemination activities

- Award for the better work of simulation and modelation of the year 2014, Herramienta de simulación para el desarrollo de exoesqueletos basada en Matlab-Simulink, XXXV Jornadas de Automatica 2014, Valencia, Spain.
- *USM y SMA - dispositivos de actuación para exoesqueletos* , Speaker - I$^{st}$ International Congress of Software Engineering, Telecommunication, Electronics and Graphic Design, ESPOCH, Riobamba, Ecuador.

## 8.2 Future works

The work presented in this dissertation sets out several research areas for further research, which can be divided in three sections:

SMA actuator design

- Currently the SMA actuator presents a low frequency movement response especially in the recuperation of the initial shape where this process depends on the ambient temperature. To improve the actuator design based on SMA in terms of energy efficiency and cooling methods to grow the frequency of the movement

an possible solution can be a double brake where the mechanical energy can be stored in a spring.

- The Bowden tube together with the PTFE is a good solution for force transmission and heat dissipation independently of the actuator shape, but is still limited: after hundreds of operating cycles has been detected a rupture on the PTFE tube due to the frictions and SMA heat; after some repetitive cycles the Bowden tube is very hot and cooling the SMA wires take long time; the separation between the actuator and exoskeleton structure can be improved in terms of electrically isolation. On these issues, a research in alternative materials which don't conduct electricity, can easily band, resist to the heat, and have the necessary rigidity to transmit the force can be a good solution.

Simulation environment

- The simulation environment can be improved in a generalization set-up where the simulation can be easily configured in function of the exoskeleton characteristics (weight, length, and actuator) and muscle activity.

- The currently connection between the exoskeleton and human body is represented by spring-damper systems which represent an approximation of the soft tissues behaviour. This approximation can be improved by readjusting the spring damper parameters in function of each patient segment and adding more contact points.

Upper limb exoskeleton

- If the elbow exoskeleton is on more advanced stage (manufactured and tested with patients), the shoulder and wrist exoskeleton still such as proposed design. The last two need to be analysed and optimized for design improvements and the fabrication is required for real tests with patients.

- At this moment the exoskeleton can be controlled in three modes: reading sensors, passive mode and active mode (with the aid of sEMG signals). For more efficient therapy where the patient is motivated to execute the tasks, improved methods of control and new sensors (such inertial, pressure, torque) can enable a natural interaction between the patient and the robot.

- For patient motivation and evolution analysis, a patient - exoskeleton - therapist software interface is necessary. In the case of patient - exoskeleton a video game can be a good solution, instead the interface exoskeleton - therapist needs to give the possibility to choose the rehabilitation therapy (range of movement angle, frequency of movement), give the possibility to download information

about each patient in terms of recovery evolution (angular positions, velocity, torques, etc.)

- Increase the usability and autonomy of the systems that provide the therapy.

# Bibliography


[1] "Technical characteristics of flexinol® actuator wires f1140rev i.2." http://www.dynalloy.com/pdfs/TCF1140.pdf. Accessed: 2016-12-8.

[2] S. Corporation, "Ultrasonic motor instruction manual," 2004.

[3] "Hyper project - about hyper." `http://www.neuralrehabilitation.org/projects/HYPER/index.htm`. Accessed: 2017-08-10.

[4] "Robohealth project." `http://www.ieef.upm.es/proyectos/RoboHealth/`. Accessed: 2017-08-10.

[5] K. K. Andersen, T. S. Olsen, C. Dehlendorff, and L. P. Kammersgaard, "Hemorrhagic and ischemic strokes compared stroke severity, mortality, and risk factors," *Stroke*, vol. 40, no. 6, pp. 2068–2072, 2009.

[6] A. de Ama Espinosa, *Hybrid walking therapy with fatigue management for spinal cord injured individuals*. PhD thesis, Carlos III de Madrid, 2013.

[7] T. H. Williams, N. Gluhbegovic, and J. Y. Jew, "The human brain: Dissections of the real brain," in *The Human Brain: Dissections of the Real Brain*, Department of Anatomy and Cell Biology, The University of Iowa, College of Medicine, 1997.

[8] "Sci recovery - spinal cord injuries." `http://www.sci-recovery.org/`. Accessed: 2016-08-10.

[9] "Hocoma - armeo." `https://www.hocoma.com/solutions`. Accessed: 2016-09-10.

[10] "Bionik." `http://bionikusa.com/`. Accessed: 2017-08-10.

[11] "Kinetek - wearable robotics." `http://www.wearable-robotics.com/kinetek/`. Accessed: 2017-08-10.

[12] "Tyromotion." `http://tyromotion.com/en/`. Accessed: 2017-08-10.

[13] "Bkintechnologies - kinarm exoskeleton." `http://www.bkintechnologies.com/bkin-products/kinarm-exoskeleton-lab/`. Accessed: 2017-08-10.

[14] "Cyberdyne - single joint." `https://www.cyberdyne.jp/english/products/SingleJoint.html`. Accessed: 2017-08-10.

[15] R. Espinoza, M. Destarac, J. Garcia, R. Acebrón, L. Puglisi, and C. García, "Orte-sistema robotizado para la rehabilitación del miembro superior," in *Jornadas Nacionales de Robótica, Spanish Robotics Conference*, Editorial CEA-IFAC, ISBN: 978-84-697-3742-2, 2017.

[16] T. G. Sugar, J. He, E. J. Koeneman, J. B. Koeneman, R. Herman, H. Huang, R. S. Schultz, D. E. Herring, J. Wanberg, S. Balasubramanian, P. Swenson, and J. A. Ward, "Design and control of rupert: A device for robotic upper extremity repetitive therapy," *IEEE Transactions on Neural Systems and Rehabilitation Engineering*, vol. 15, pp. 336–346, Sept 2007.

[17] N. Vitiello, T. Lenzi, S. Roccella, S. M. M. D. Rossi, E. Cattin, F. Giovacchini, F. Vecchi, and M. C. Carrozza, "Neuroexos: A powered elbow exoskeleton for physical rehabilitation," *IEEE Transactions on Robotics*, vol. 29, pp. 220–235, Feb. 2013.

[18] C. Pylatiuk, A. Kargov, I. Gaiser, T. Werner, S. Schulz, and G. Bretthauer, "Design of a flexible fluidic actuation system for a hybrid elbow orthosis," in *2009 IEEE International Conference on Rehabilitation Robotics*, pp. 167–171, June 2009.

[19] H. Kobayashi and H. Nozaki, "Development of muscle suit for supporting manual worker," in *2007 IEEE/RSJ International Conference on Intelligent Robots and Systems*, pp. 1769–1774, IEEE, 2007.

[20] J. Stein, K. Narendran, J. McBean, K. Krebs, and R. Hughes, "Electromyography-controlled exoskeletal upper-limb–powered orthosis for exercise training after stroke," *American journal of physical medicine & rehabilitation*, vol. 86, no. 4, pp. 255–261, 2007.

[21] T. Sashida and T. Kenjo, *Introduction to ultrasonic motors*. New York, NY (United States); Oxford Univ. Press, 1993.

[22] J. M. Jani, M. Leary, A. Subic, and M. A. Gibson, "A review of shape memory alloy research, applications and opportunities," *Materials & Design*, vol. 56, pp. 1078–1113, 2014.

[23] L. Fumagalli, F. Butera, and A. Coda, "Smartflex® niti wires for shape memory actuators," *Journal of materials engineering and performance*, vol. 18, no. 5-6, pp. 691–695, 2009.

[24] L. Ljung, "System identification: Theory for the user," *Englewood Cliffs*, 1987.

[25] M. Nordin and V. Frankel, *Basic Biomechanics of the Musculoskeletal System*. Wolters Kluwer/Lippincott Williams & Wilkins Health, 2012.

[26] "World health organization." `http://www.who.int/en/`. Accessed: 2016-08-20.

[27] "Post-stroke rehabilitation." `https://stroke.nih.gov/materials/rehabilitation.htm`. Accessed: 2016-08-10.

[28] K. J. Wisneski and M. J. Johnson, "Quantifying kinematics of purposeful movements to real, imagined, or absent functional objects: implications for modelling trajectories for robot-assisted adl tasks," *Journal of NeuroEngineering and Rehabilitation*, vol. 4, no. 1, p. 7, 2007.

[29] N. R. Sims and H. Muyderman, "Mitochondria, oxidative metabolism and cell death in stroke," *Biochimica et Biophysica Acta (BBA) - Molecular Basis of Disease*, vol. 1802, no. 1, pp. 80 – 91, 2010.

[30] G. Kwakkel, B. J. Kollen, J. van der Grond, and A. J. Prevo, "Probability of regaining dexterity in the flaccid upper limb impact of severity of paresis and time since onset in acute stroke," *Stroke*, vol. 34, no. 9, pp. 2181–2186, 2003.

[31] K. Nas, L. Yazmalar, V. Sah, A. Aydin, and K. Ones, "Rehabilitation of spinal cord injuries," *World Journal of Orthopedics*, vol. 6, pp. 8–16, Jan. 2015.

[32] P. Maciejasz, J. Eschweiler, K. Gerlach-Hahn, A. Jansen-Troy, and S. Leonhardt, "A survey on robotic devices for upper limb rehabilitation," *Journal of NeuroEngineering and Rehabilitation*, vol. 11, no. 1, p. 3, 2014.

[33] Q. Wang, P. Markopoulos, B. Yu, W. Chen, and A. Timmermans, "Interactive wearable systems for upper body rehabilitation: a systematic review," *Journal of neuroengineering and rehabilitation*, vol. 14, no. 1, p. 20, 2017.

[34] H. S. Lo and S. Q. Xie, "Exoskeleton robots for upper- limb rehabilitation: State of the art and future prospects," *Medical engineering & physics*, vol. 34, no. 3, pp. 261–268, 2012.

[35] "Instead technologies for helping people." `http://www.instead-technologies.com/`. Accessed: 2017-08-10.

[36] T. Morishita and T. Inoue, "Interactive bio-feedback therapy using hybrid assistive limbs for motor recovery after stroke: Current practice and future perspectives," *Neurologia medico-chirurgica*, vol. 56, pp. 605–612, September 2016.

[37] M. A. Destarac, C. E. G. Cena, R. J. S. Pazmiño, M. J. R. Urbina, J. L. López, and R. E. Gómez, "Modeling and simulation of upper brachial plexus injury," *IEEE Systems Journal*, vol. 10, no. 3, pp. 912–921, 2016.

[38] M. A. Destarac, C. E. G. Cena, and R. S. Pazmiño, "Simulation of the length change in muscles during the arm rotation for the upper brachial plexus injury," in *Converging Clinical and Engineering Research on Neurorehabilitation II*, pp. 1263–1268, Springer, 2017.

[39] J. G. Montaño, C. E. G. Cena, L. J. M. Chamorro, M. A. Destarac, and R. S. Pazmiño, "Mechanical design of a robotic exoskeleton for upper limb rehabilitation," in *Advances in Automation and Robotics Research in Latin America*, pp. 297–308, Springer, 2017.

[40] R. Song, K. y. Tong, X. Hu, and L. Li, "Assistive control system using continuous myoelectric signal in robot-aided arm training for patients after stroke," *IEEE Transactions on Neural Systems and Rehabilitation Engineering*, vol. 16, pp. 371–379, Aug. 2008.

[41] M.-H. Milot, S. J. Spencer, V. Chan, J. P. Allington, J. Klein, C. Chou, J. E. Bobrow, S. C. Cramer, and D. J. Reinkensmeyer, "A crossover pilot study evaluating the functional outcomes of two different types of robotic movement training in chronic stroke survivors using the arm exoskeleton bones," *Journal of neuroengineering and rehabilitation*, vol. 10, no. 1, p. 1, 2013.

[42] Q. Li, D. Wang, Z. Du, Y. Song, and L. Sun, "semg based control for 5 dof upper limb rehabilitation robot system," in *2006 IEEE International Conference on Robotics and Biomimetics*, pp. 1305–1310, Dec. 2006.

[43] M. Chen, S. Ho, H. F. Zhou, P. Pang, X. Hu, D. Ng, and K. Tong, "Interactive rehabilitation robot for hand function training," in *2009 IEEE International Conference on Rehabilitation Robotics*, pp. 777–780, IEEE, 2009.

[44] M. D. Ellis, T. Sukal, T. DeMott, and J. P. Dewald, "Act 3d exercise targets gravity-induced discoordination and improves reaching work area in individuals with stroke," in *2007 IEEE 10th International Conference on Rehabilitation Robotics*, pp. 890–895, IEEE, 2007.

[45] J. S. Sulzer, M. A. Peshkin, and J. L. Patton, "Design of a mobile, inexpensive device for upper extremity rehabilitation at home," in *2007 IEEE 10th International Conference on Rehabilitation Robotics*, pp. 933–937, IEEE, 2007.

[46] M.-S. Ju, C.-C. Lin, D.-H. Lin, I.-S. Hwang, and S.-M. Chen, "A rehabilitation robot with force-position hybrid fuzzy controller: hybrid fuzzy control of rehabilitation robot," *IEEE Transactions on Neural Systems and Rehabilitation Engineering*, vol. 13, no. 3, pp. 349–358, 2005.

[47] I. Vanderniepen, R. Van Ham, M. Van Damme, R. Versluys, and D. Lefeber, "Orthopaedic rehabilitation: A powered elbow orthosis using compliant actuation," in *2009 IEEE International Conference on Rehabilitation Robotics*, pp. 172–177, IEEE, 2009.

[48] A. J. del Ama, Á. Gil-Agudo, J. L. Pons, and J. C. Moreno, "Hybrid fes-robot cooperative control of ambulatory gait rehabilitation exoskeleton," *Journal of neuroengineering and rehabilitation*, vol. 11, no. 1, p. 27, 2014.

[49] R. Ceres, J. Pons, L. Calderón, and J. Moreno, "La robótica en la discapacidad. desarrollo de la prótesis diestra de extremidad inferior manus-hand," *Revista Iberoamericana de Automática e Informática Industrial RIAI*, vol. 5, no. 2, pp. 60–68, 2008.

[50] E. Rocon, J. Belda-Lois, A. Ruiz, M. Manto, J. C. Moreno, and J. Pons, "Design and validation of a rehabilitation robotic exoskeleton for tremor assessment and suppression," *IEEE Transactions on Neural Systems and Rehabilitation Engineering*, vol. 15, no. 3, pp. 367–378, 2007.

[51] D. Mesonero Romanos, J. L. Pons Rovira, J. F. Fernández Lozano, M. Villegas, R. Ceres Ruíz, and E. Rocón, "Comparación entre sistemas electrocerámicos de desplazamiento mecánico. motores y actuadores piezoeléctricos," *Sociedad Española de Cerámica y Vidrio*, 2004.

[52] J. S. Schoenwald, P. M. Beckham, R. Rattner, B. Vanderlip, and B. E. Shi, "Exploiting solid state ultrasonic motors for robotics," in *Ultrasonics Symposium, 1988. Proceedings., IEEE 1988*, pp. 513–517, IEEE, 1988.

[53] K. Ito, H. Nagaoka, T. Tsuji, A. Kato, and M. Ito, "An emg controlled prosthetic forearm with three degrees of freedom using ultrasonic motors," *Transactions of the Society of Instrument and Control Engineers*, vol. 27, no. 11, pp. 1281–1289, 1991.

[54] J. Pons, H. Rodríguez, and R. Ceres, "High mobility hand prosthesis: A mechatronic approach," in *Proc. Of the 2nd International Conf. On Recent Advances in Mechatronics*, vol. 1, pp. 473–477, 1999.

[55] H. Das, X. Bao, Y. Bar-Cohen, R. Bonitz, R. Lindemann, M. Maimone, I. Nesnas, and C. Voorhees, "Robot manipulator technologies for planetary exploration," 1999.

[56] "Smartflex springs and wires." https://www.saesgetters.com/product-groups/shape-memory-alloys. Accessed: 2016-12-8.

[57] S. Kujala, A. Pajala, M. Kallioinen, A. Pramila, J. Tuukkanen, and J. Ryhänen, "Biocompatibility and strength properties of nitinol shape memory alloy suture in rabbit tendon," *Biomaterials*, vol. 25, no. 2, pp. 353–358, 2004.

[58] F. Butera, A. Coda, G. Vergani, and S. G. SpA, "Shape memory actuators for automotive applications," *Nanotec IT newsletter. Roma: AIRI/nanotec IT*, pp. 12–6, 2007.

[59] D. Stoeckel, "Shape memory actuators for automotive applications," *Materials & Design*, vol. 11, no. 6, pp. 302–307, 1990.

[60] F. Butera, "Shape memory actuators," *Advanced Materials & Processes*, vol. 166, no. 3, pp. 37–40, 2008.

[61] J. Van Humbeeck, "Non-medical applications of shape memory alloys," *Materials Science and Engineering: A*, vol. 273, pp. 134–148, 1999.

[62] L. M. Schetky, "Shape memory alloy applications in space systems," *Materials & Design*, vol. 12, no. 1, pp. 29–32, 1991.

[63] O. J. Godard, M. Z. Lagoudas, and D. C. Lagoudas, "Design of space systems using shape memory alloys," *Smart Structures and Materials 2003*, vol. 5056, pp. 545–558, 2003.

[64] H. Fujita, "Studies of micro actuators in japan," in *Robotics and Automation, 1989. Proceedings., 1989 IEEE International Conference on*, pp. 1559–1564, IEEE, 1989.

[65] K. Kuribayashi, "Millimeter-sized joint actuator using a shape memory alloy," *Sensors and actuators*, vol. 20, no. 1-2, pp. 57–64, 1989.

[66] K. Kuribayashi, "A new actuator of a joint mechanism using tini alloy wire," *the International journal of Robotics Research*, vol. 4, no. 4, pp. 47–58, 1986.

[67] G. B. Kauffman and I. Mayo, "The story of nitinol: the serendipitous discovery of the memory metal and its applications," *The chemical educator*, vol. 2, no. 2, pp. 1–21, 1997.

[68] G. F. Andreasen, "Method and system for orthodontic moving of teeth," July 26 1977. US Patent 4,037,324.

[69] D. S. Copaci, A. F. Caballero, A. M. Clemente, D. B. Rojas, and L. M. Lorente, "Ultrasonic motor based actuator for elbow joint functional compensation," in *ROBOT2013: First Iberian Robotics Conference*, pp. 181–194, Springer, 2014.

[70] D.-S. Copaci, A. Flores-Caballero, F. M. Monar, and D. Blanco, "Modelado de motores usm para la robotica de rehabilitacion," *XXXV Jornadas de Automática*, 2014.

[71] D. P. Greene and S. L. Roberts, "Kinesiology: movement in the context of activity," *Elsevier Health Sciences*, 2015.

[72] A. Gil-Agudo, A. Bernal-Sahún, A. De Los Reyes-guzmán, A. del Ama-Espinosa, and E. Rocón, "Applications of upper limb biomechanical models in spinal cord injury patients," *INTECH Open Access Publisher*, 2011.

[73] A. de los Reyes-Guzmán, A. Gil-Agudo, B. Peñasco-Martín, M. Solís-Mozos, A. del Ama-Espinosa, and E. Pérez-Rizo, "Kinematic analysis of the daily activity of drinking from a glass in a population with cervical spinal cord injury," *Journal of neuroengineering and rehabilitation*, vol. 7, no. 1, p. 1, 2010.

[74] H. Hongsheng, W. Juan, C. Liang, W. Jiong, and J. Xuezheng, "Design, control and test of a magnetorheological fluid fan clutch," in *Automation and Logistics, 2009. ICAL'09. IEEE International Conference on*, pp. 1248–1253, IEEE, 2009.

[75] "Hammerstein-wiener models." https://es.mathworks.com/help/ident/ug/identifying-hammerstein-wiener-models.html. Accessed: 2016-12-8.

[76] A. F. Caballero, D. S. Copaci, V. Peciña, D. B. Rojas, and L. M. Lorente, "Sistema avanzado de protipado rápido para control en la educación en ingeniería para grupos multidisciplinares," *Revista Iberoamericana de Automática e Informática Industrial RIAI*, vol. 13, no. 3, pp. 350–362, 2016.

[77] T. Senjyu, H. Miyazato, and K. Uezato, "Performance comparison of pi and adaptive controller for adjustable speed drives of ultrasonic motors," in *Industrial Technology, 1994., Proceedings of the IEEE International Conference on*, pp. 519–523, IEEE, 1994.

[78] H. Rodriguez, J. Pons, and R. Ceres, "A zpet-repetitive speed controller for ultrasonic motors," in *Robotics and Automation, 2000. Proceedings. ICRA'00. IEEE International Conference on*, vol. 4, pp. 3654–3659, IEEE, 2000.

[79] L. Huafeng, Z. Chunsheng, and G. Chenglin, "Precise position control of ultrasonic motor using fuzzy control," in *Ultrasonics Symposium, 2004 IEEE*, vol. 2, pp. 1177–1180, IEEE, 2004.

[80] Y. Izuno and M. Nakaoka, "High performance and high precision ultrasonic motor-actuated positioning servo drive system using improved fuzzy-reasoning controller," in *Power Electronics Specialists Conference, PESC'94 Record., 25th Annual IEEE*, pp. 1269–1274, IEEE, 1994.

[81] A. Villoslada, A. Flores, D. Copaci, D. Blanco, and L. Moreno, "High-displacement flexible shape memory alloy actuator for soft wearable robots," *Robotics and Autonomous Systems*, vol. 73, pp. 91–101, 2015.

[82] D. Copaci, A. Flores, A. Villoslada, and D. Blanco, "Modelado y simulación de actuadores sma con carga variable," *XXXVI Jornadas de Automática - 2015, Bilbao*, 2015.

[83] "Design time series narx feedback neural networks." https://es.mathworks.com/. Accessed: 2016-12-8.

[84] K. Andrianesis and A. Tzes, "Design of an innovative prosthetic hand with compact shape memory alloy actuators," in *Control & Automation (MED), 2013 21st Mediterranean Conference on*, pp. 697–702, IEEE, 2013.

[85] S.-H. Liu, T.-S. Huang, and J.-Y. Yen, "Tracking control of shape-memory-alloy actuators based on self-sensing feedback and inverse hysteresis compensation," *Sensors*, vol. 10, no. 1, pp. 112–127, 2009.

[86] G. Song, B. Kelly, and B. N. Agrawal, "Active position control of a shape memory alloy wire actuated composite beam," *Smart Materials and Structures*, vol. 9, no. 5, p. 711, 2000.

[87] N. Ma and G. Song, "Control of shape memory alloy actuator using pulse width (pw) modulation," *Proc. Soc. Photo-Opt. Ins.: Smart Structures and Materials*, pp. 348–359, 2002.

[88] J. Pons, D. Reynaerts, J. Peirs, R. Ceres, and H. VanBrussel, "Comparison of different control approaches to drive sma actuators," in *Advanced Robotics, 1997. ICAR'97. Proceedings., 8th International Conference on*, pp. 819–824, IEEE, 1997.

[89] M. Vasina, F. Solc, and K. Hoder, "Shape memory alloys-unconventional actuators," in *Industrial Technology, 2003 IEEE International Conference on*, vol. 1, pp. 190–193, IEEE, 2003.

[90] N. T. Tai and K. K. Ahn, "Apply adaptive fuzzy sliding mode control to sma actuator," in *Control Automation and Systems (ICCAS), 2010 International Conference on*, pp. 433–437, IEEE, 2010.

[91] A. Kilicarslan, G. Song, and K. Grigoriadis, "Anfis based modeling and inverse control of a thin sma wire," in *The 15th International Symposium on: Smart Structures and Materials & Nondestructive Evaluation and Health Monitoring*, pp. 69260H–69260H, International Society for Optics and Photonics, 2008.

[92] A. Kumagai, T.-I. Liu, and P. Hozian, "Control of shape memory alloy actuators with a neuro-fuzzy feedforward model element," *Journal of Intelligent Manufacturing*, vol. 17, no. 1, pp. 45–56, 2006.

[93] Á. Villoslada, N. Escudero, F. Martín, A. Flores, C. Rivera, M. Collado, and L. Moreno, "Position control of a shape memory alloy actuator using a four-term bilinear pid controller," *Sensors and Actuators A: Physical*, vol. 236, pp. 257–272, 2015.

[94] S. Martineau, K. Burnham, J. Minihan, S. Marcroft, G. Andrews, and A. Heeley, "Application of a bilinear pid compensator to an industrial furnace," *IFAC Proceedings Volumes*, vol. 35, no. 1, pp. 25–30, 2002.

[95] "Memry's nitinol alloys and superalloys." http://www.memry.com/products-services/melting/nitinol-alloys. Accessed: 2016-12-8.

[96] "Scapulohumeral/rhythm." https://www.physiopedia.com/Scapulohumeral/Rhythm. Accessed: 2016-12-8.

[97] S. Kumar, "Biomechanics in ergonomics," *CRC Press*, 1999.

[98] A. Favetto, *Glove Exoskeleton for Extra-Vehicular Activities: Analysis of Requirements and Prototype Design*. PhD thesis, Politecnico di Torino, 2014.

[99] M. Damsgaard, J. Rasmussen, S. T. Christensen, E. Surma, and M. De Zee, "Analysis of musculoskeletal systems in the anybody modeling system," *Simulation Modelling Practice and Theory*, vol. 14, no. 8, pp. 1100–1111, 2006.

[100] R. Davoodi, C. Urata, E. Todorov, and G. Loeb, "Development of clinician-friendly software for musculoskeletal modeling and control," in *Engineering in Medicine and Biology Society, 2004. IEMBS'04. 26th Annual International Conference of the IEEE*, vol. 2, pp. 4622–4625, IEEE, 2004.

[101] M. Khachani, R. Davoodi, and G. Loeb, "Musculo-skeletal modeling software (msms) for biomechanics and virtual rehabilitation," *IEEE Trans. Biomedical Eng*, 2000.

[102] J. M. Shippen and B. May, "Calculation of muscle loading and joint contact forces during the rock step in irish dance," *Journal of Dance Medicine & Science*, vol. 14, no. 1, pp. 11–18, 2010.

[103] S. L. Delp, F. C. Anderson, A. S. Arnold, P. Loan, A. Habib, C. T. John, E. Guendelman, and D. G. Thelen, "Opensim: open-source software to create and analyze dynamic simulations of movement," *IEEE transactions on biomedical engineering*, vol. 54, no. 11, pp. 1940–1950, 2007.

[104] S. L. Delp and J. P. Loan, "A graphics-based software system to develop and analyze models of musculoskeletal structures," *Computers in biology and medicine*, vol. 25, no. 1, pp. 21–34, 1995.

[105] D. W. Wagner, V. Stepanyan, J. M. Shippen, M. S. DeMers, R. S. Gibbons, B. J. Andrews, G. H. Creasey, and S. Beaupre, "Consistency among musculoskeletal models: caveat utilitor," *Annals of biomedical engineering*, vol. 41, no. 8, pp. 1787–1799, 2013.

[106] "Biomechanics of bodies." http://www.mathworks.es/videos/biomechanical-analysis-in-matlab-and-simulink-81831.html. Accessed: 2017-08-8.

[107] J. Shippen and B. May, "A kinematic approach to calculating ground reaction forces in dance," *Journal of Dance Medicine and Science*, vol. 16, no. 1, pp. 39–43, 2012.

[108] J. Shippen, "Biomechanical analysis of entry, egress and loading of a passenger vehicle with rear hinged rear doors," *International Journal for Traffic and Transport Engineering*, vol. 2, no. 2, 2012.

[109] B. Andrews, J. Shippen, M. Armengol, R. Gibbons, W. Holderbaum, and W. Harwin, "A design method for fes bone health therapy in sci," 2016.

[110] T. Lenzi, N. Vitiello, S. M. M. De Rossi, S. Roccella, F. Vecchi, and M. C. Carrozza, "Neuroexos: A variable impedance powered elbow exoskeleton," in *Robotics and Automation (ICRA), 2011 IEEE International Conference on*, pp. 1419–1426, IEEE, 2011.

[111] M. Esmaeili, K. Gamage, E. Tan, and D. Campolo, "Ergonomic considerations for anthropomorphic wrist exoskeletons: a simulation study on the effects of

joint misalignment," in *2011 IEEE/RSJ International Conference on Intelligent Robots and Systems*, pp. 4905–4910, IEEE, 2011.

[112] C. E. Clauser, J. T. McConville, and J. W. Young, "Weight, volume, and center of mass of segments of the human body," tech. rep., DTIC Document, 1969.

[113] R. S. Behnke, *Kinetic Anatomy With Web Resource*. Human Kinetics, 2012.

[114] D. Copaci, A. Flores, D. Blanco, and L. Moreno, "Shoulder exoskeleton for rehabilitation actuated with shape memory alloy," in *RoboCity16 Open Conference on Future Trends in Robotics*, pp. 283–292, Madrid, 2016.

[115] D. Copaci, E. Cano, L. Moreno, and D. Blanco, "New design of a soft-robotics wearable elbow exoskeleton based on shape memory alloy wires actuators," *Applied Bionics and Biomechanics*, vol. 2017, p. 11, 2017.

[116] B.-C. Kung, M.-S. Ju, C.-C. K. Lin, and S.-M. Chen, "Clinical assessment of forearm pronation/supination torque in stroke patients," *Journal of Medical and Biological Engineering*, vol. 25, no. 1, pp. 39–43, 2005.

[117] D. Copaci, D. Blanco, and M. L., "Wearable elbow exoskeleton actuated with shape memory alloy in antagonist movement. joint workshop on wearable robotics and assistive devices," *Joint Workshop on Wearable Robotics and Assistive Devices, International Conference on Intelligent Robots and Systems. IROS 2016, Daejeon, Korea.*, 2016.

[118] D. Copaci, A. Flores, F. Rueda, I. Alguacil, D. Blanco, and L. Moreno, "Wearable elbow exoskeleton actuated with shape memory alloy," in *Converging Clinical and Engineering Research on Neurorehabilitation II*, pp. 477–481, Springer International Publishing, 2017.

[119] I. Alguacil, E. Monge, D. Copaci, D. Blanco, M. Pérez De Heredia, and S. Collado, "Diseño de un exoesqueleto por segmentos para evaluación y tratamiento del miembro superior," in *54 Congreso Nacional de la Sociedad Española de Rehabilitación y Medicina Física (SERMEF)*, 2016.

[120] D. Copaci, D. Blanco, I. Guerra, S. Collado Vázquez, and P. de Heredia, "Exoesqueleto actuado por sma para movilizaciín de la muñeca," *XXXVI Jornadas de Automática*, 2016.

[121] D. B. Chaffin, G. Andersson, B. J. Martin, *et al.*, *Occupational biomechanics*. New York: Wiley New York, 1999.

[122] J. A. Diego-Mas, "Análisis biomecánico estático coplanar. ergonautas," *Universidad Politécnica de Valencia*, 2015.

[123] M. A. Oskoei and H. Hu, "Myoelectric control systems a survey," *Biomedical Signal Processing and Control*, vol. 2, no. 4, pp. 275–294, 2007.

[124] C. Battye, A. Nightingale, and J. Whillis, "The use of myo-electric currents in the operation of prostheses," *Bone & Joint Journal*, vol. 37, no. 3, pp. 506–510, 1955.

[125] R. Song, K.-y. Tong, X. Hu, and L. Li, "Assistive control system using continuous myoelectric signal in robot-aided arm training for patients after stroke," *IEEE Transactions on Neural Systems and Rehabilitation Engineering*, vol. 16, no. 4, pp. 371–379, 2008.

[126] A. Bottomley, "Myoelectric control of powered prostheses," *Bone & Joint Journal*, vol. 47, no. 3, pp. 411–415, 1965.

[127] K. Englehart, B. Hudgin, and P. A. Parker, "A wavelet-based continuous classification scheme for multifunction myoelectric control," *IEEE Transactions on Biomedical Engineering*, vol. 48, no. 3, pp. 302–311, 2001.

[128] B. Hudgins, P. Parker, and R. N. Scott, "A new strategy for multifunction myoelectric control," *IEEE Transactions on Biomedical Engineering*, vol. 40, no. 1, pp. 82–94, 1993.